Performance analysis of mobile relays for LTE

Yangyang Chen

▶ To cite this version:

uep

THÈSE / Télécom Bretagne
sous le sceau de l'Université européenne de Bretagne

pour obtenir le grade de Docteur de Télécom Bretagne
En accréditation conjointe avec l'Ecole Doctorale Matisse
Mention : Informatique

présentée par
Yangyang Chen
préparée dans le département Réseaux, Sécurité et Multimédia (RSM)
Laboratoire Irisa

Performance Analysis of Mobile Relays for LTE

Sous le sceau de l' Université européenne de Bretagne

Télécom Bretagne

En accréditation conjointe avec l'Ecole Doctorale Matisse

Ecole Doctorale – MATISSE

Performance Analysis of Mobile Relays for LTE

Thèse de Doctorat

Mention : Informatique

Présentée par **Yangyang Chen**

Département : Réseaux, Sécurité et Multimédia (RSM)

Laboratoire : IRISA

Directeur de thèse : Xavier Lagrange

Soutenue 17 Déc. 2015

Jury :

M. Bruno TUFFIN, Directeur de recherche, Inria/Irisa-Rennes (Président)
M. Jean-Marie GORCE, Professeur, INSA-Lyon (Rapporteur)
M. Tommy SVENSSON, Associate professor, Chalmers University of Technology (Rapporteur)
Mme. Marion BERBINEAU, Directrice de recherche, IFSTTAR (Examinateur)
M. Philippe MARTINS, Professeur, Télécom ParisTech (Examinateur)
M. Loïc BRUNEL, Responsable de recherche, Mitsubishi Electric R&D Centre (Examinateur)
M. Xavier LAGRANGE, Professeur, Télécom Bretagne (Directeur de thèse)

To my parents

Acknowledgements

On the way to this thesis I received lots of help from different people, I would like to take this opportunity to express my appreciations.

First of all, I would like to express my sincere gratitude to my supervisor, Prof. Xavier Lagrange. It is my great honor to work with Xavier during my Ph.D life. He gave me lots of insightful guides towards my research. The best thing is, whenever I met problems and difficulties, he was right there and ready to help me solve the problems. I could not have imagined having a better supervisor for my Ph.D study.

Besides my supervisor, I would like to thank Prof. Philippe Martins and Prof. Laurent Decreusefond. Thank you guys for bringing me into the gate of stochastic geometry, which becomes one of the most beautiful part in my thesis.

Furthermore, I would like to express my sincere gratitudes to the jury members. Their insightful questions and encouraging remarks on my work made my thesis defense a lifelong memory as well as a learning process. It is my utmost honor to have all these experts reviewing my work.

Moreover, my sincere thanks also goes to my colleagues in RSM department. Sara, Younes, Vladimir, I would never forget the days we worked together. A special thanks to Feng Yan for lots of discussions on both academic and daily life matters. Also, these years in Rennes, I made some very good friends like Yue Li, Yanhuang Li, Wenjing Shuai, Jialong Duan, Qipeng Song, Jie Zhu and Xiao Song. Because of you guys, I had a very colorful life, this would definitely be one of my best memories.

Last but not the least, I would like to thank my family, my parents Yungong Chen and Junhua Leng. No matter what decisions I have made, thank you for your endless love and support.

Abstract

Currently, the number of users using wireless broadband services is rising greatly with the introduction of smart phones, tablet computers and other new mobile devices. With this rapid popularity of mobile devices, people make intensive use of these devices to kill time when they are in public transportation vehicles such as buses, trams, or trains.

However, the service quality in public transportation vehicles is far from satisfactory. Public transportations are usually well shielded with coated windows, which leads to a rather high penetration loss between outdoor and in-vehicle. Traditionally, the UEs inside the public transportations connect to the macro base stations via wireless links, in which the penetration loss severely attenuates the signal quality and decreases the achievable data rate. Furthermore, during the handover procedure, a large group of UEs perform handover simultaneously, which causes signaling congestion.

To offer high-quality services to vehicular UEs, a relay is mounted in a vehicle with an external antenna to have a good link budget with the eNodeB and an antenna in the bus to provide an optimal link budget with vehicular UEs. This thesis investigates the deployment of mobile relay in LTE network from two aspects: mobility management and performance. We consider a scenario where mobile relays are deployed on public buses. We first study the different signaling procedures when a mobile relay is embedded in a public transport vehicle. We propose to keep the protocol stack that was defined for fixed relay and to extend it to mobile relays. The concept of global tunnel, which gathers several tunnels, is proposed to optimize the handover procedure of mobile relay nodes. Without adding any protocol in the stack, it is possible to group several handovers while keeping the possibility of managing the tunnel of each UE individually. The results show that the proposed solution dramatically reduces the number of signaling messages that each network node should process.

In the performance study, we analyze the different interference cases. Two new types of interferences, Relay-to-Relay interference and Relay-to-UE interference are identified. We study the data rate gain of a UE provided by a mobile relay deployed in a hexagonal network with Monte Carlo simulation and in a random network by using stochastic geometry. The results show that the data rate gain provided by a mobile relay is not guaranteed in all cases. Since vehicles are shielded with coated windows, the penetration loss is a key factor to decide whether mobile relay could bring data rate gain. We then investigate the capacity gain brought by mobile relays. We consider a network with multiple users and multiple relays. By using the stochastic geometry, a general analytical model for mobile relay scenario is proposed. The distribution of base stations, buses (mobile relays) are modeled by a Poisson Point Process. Important metrics like the CDF of the SINR and the CDF of the end-to-end rate are derived. The rate of the backhaul link and the rate of the access link are in general correlated when the same spectrum (or frequency) is used on both links, we take this fact into account when deriving the CDF of the end-to-end rate. Furthermore, we propose a TDD/FDD hybrid mobile relay mode, motivated by the fact that a vehicular UE is static relative to its serving mobile relay and close to it in this specific scenario, which leads to a relatively good channel condition on the access link. In addition, we evaluate and compare the performance of different modes using the proposed analytical model. Numerical results show that when the ratio of vehicular UEs in the cell is 0.4 and the penetration loss is 20 dB, FDD mobile relay mode and TDD/FDD hybrid mobile relay mode can achieve +16.3%, +29.1% cell rate gain respectively compared with the direct mode.

Keywords: 4th generation mobile network, Mobile Relay, Mobility Management, Stochastic Geometry, Performance Analysis

Résumé

Le nombre d'utilisateurs des services de haut débit sans fil est en forte augmentation au cours des années 2010 avec l'introduction des télé- phones intelligents, ordinateurs tablettes et autres nouveaux appareils mobiles.

Cependant, la qualité de service dans les transports publics est loin d'être satisfaisante. Traditionnellement, les terminaux à l'intérieur des transports publics se connectent à des stations de base macro-cellulaires via des liaisons sans fil, dans lesquelles la perte apportée par la traversée des ondes à travers les fenêtres atténue fortement le niveau du signal et diminue le débit de données réalisable. En outre, en cas de changement de cellule, plusieurs terminaux effectuent des transferts inter-cellulaires simultanément, ce qui provoque un accroissement brusque de signalisa- tion et peut conduire à un engorgement.

Pour offrir des services de haute qualité aux clients des transports, un relais est monté dans un véhicule avec une antenne externe pour avoir un bon bilan de liaison avec la station de base et une antenne dans le bus pour fournir un bilan de liaison optimal avec les terminaux. Cette thèse étudie le déploiement de relais mobile en réseau LTE à partir de deux aspects: gestion de la mobilité et analyse de performance. Nous étudions d'abord les différentes procédures de signalisation quand un relais mobile est intégré dans un véhicule de transport public. Nous proposons de garder la pile de protocole qui a été définie pour le relais fixe par les instances de normalisation et de l'étendre à des relais mobiles. Nous définissons le concept de tunnel global, qui regroupe plusieurs tunnels, pour réduire la signalisation en cas de transfert intercellulaire de noeuds relais mobiles.

Dans l'étude de performances, nous analysons les différents types d'interférences. Deux nouveaux types d'interférences (interférences re- lais à relais et relais à terminal) sont identifiés. Nous étudions le gain

de débit de données fourni par un relais mobile déployé dans un réseau hexagonal avec des simulations de Monte Carlo et dans un réseau aléatoire en utilisant la géométrie stochastique. Nous étudions alors le gain de capacité apporté par les relais mobiles avec plusieurs utilisateurs et plusieurs relais. Des indicateurs importants comme la répartition du rapport signal sur interférence et bruit et celle du débit de bout en bout sont calculés. En outre, nous proposons de combiner les modes duplex en temps et en fréquence, motivés par le fait qu'un terminal embarqué est statique par rapport à son relais mobile de service et proche de lui, ce qui conduit à un excellent bilan de liaison et rend intéressant un duplex-age temporel. En outre, nous évaluons et comparons les performances des différents modes de fonctionnement en utilisant le modèle analytique proposé.

Mots Clés: Réseaux mobiles de 4ème génération, Relais Mobile, Gestion de la Mobilité, Géométrie Stochastique, Analyse de performance

Contents

List of Figures

List of Abbreviations

3GPP	The Third Generation Partnership Project
AS	Access Stratum
AP	Application Protocol
AWGN	Additive white Gaussian noise
BS	Base Station
CCDF	Complementary Cumulative Distribution Function
CDF	Cumulative Distribution Function
CI	Connected state to Idle state
CN	Core Network
CSI	Channel State Information
DeNB	Donor eNodeB
DM	Direct Mode
eNodeB	Evolved NodeB
EPC	Evolved Packet Core
EPS	Evolved Packet System
E-UTRAN	Evolved Universal Terrestrial Radio Access Network
FDD	Frequency Division Duplexing
GPP	Ginibre Point Process
GSM	Global System for Mobile Communications
GPRS	General Packet Radio Service
GTP	GPRS Tunneling Protocol
GW	Gateway
HO	Handover
HSPA	High Speed Packet Access
HSS	Home Subscriber Server
LTE	Long Term Evolution
MBSFN	Multicast Broadcast Single Frequency Network
MCS	Modulation Coding Scheme
MME	Mobility Management Entity
MRC	Maximum Ratio Combining
NAS	Non-Access Stratum
NSR	Network triggered Service Request

OAM	Operation Administration Maintenance
OFDM	Orthogonal Frequency Division Multiplexing
OP	Outage Probability
PCRF	Policy Control and Charging Rules Function
PDCP	Packet Data Convergence Protocol
PDF	Probability Distribution Function
PDN	Packet Data Network
PDN-GW	Packet Data Network Gateway
PDCCH	Physical Downlink Control Channel
PDSCH	Physical Downlink Shared Channel
PPP	Poisson Point Process
QoS	Quality of Service
RAN	Radio Access Network
RAT	Radio Access Technologies
RB	Resource Block
RN	Relay Node
RNTI	Radio Network Temporary Identifier
R-PDCCH	Relay Physical Downlink Control Channel
RRC	Radio Resource Control
RRU	Remote Radio Units
SAE	System Architecture Evolution
SGW	Serving Gateway
SINR	Signal to Interference plus Noise Ratio
SYSTUF	SYSteme Telecom pour les Transports Urbains du Futur
TAI	Tracking Area Identity
TAL	Tracking Area List
TAU	Tracking Area Update
TDD	Time Division Duplexing
TEID	Tunnel Endpoint Identifier
TFT	Traffic Flow Templates
UE	User Equipment
UMTS	Universal Mobile Telecommunication System
USR	User triggered Service Request
vUE	Vehicular User Equipment

List of symbols

A	The area of the cell (km^2)
$\mathcal{A}$	Area of a single Voronoi cell
α	Frequency division parameter in TDD/FDD mode
$\mathcal{B}$	Range of the possible value of (χ, γ)
χ	Reference power defined as kP
ϵ	Average data rate
η	Cell energy efficiency
$f(S)$	Probability distribution function of SINR
h	Factor that takes the shadowing into account
H	A log-normal random variable
f_H	PDF (Probability Density Function) of H
F_H	Complimentary CDF (Cumulative Distribution Function) of H
I_{BS}	Interference from neighbor base stations
k	Propagation factor
κ	Average number of cell change
L	Penetration loss between outdoor and in-vehicle
$L_{in-vehicle}$	In-vehicle path loss
$L_{outdoor}$	Outdoor path loss
λ_o	Intensity of ordinary UEs
λ_r	Intensity of buses (mobile relays)
λ_s	Intensity of eNodeBs
λ_u	Intensity of UEs
M_y^x	Number of messages processed by entity x for procedure y
N_r	Noise power of relay node
N_u	Noise power of UE
n_u	Total number of UEs in the cell
n_o	Number of ordinary UEs in the cell
n_r	Number of buses (mobile relays) in the cell
n_v^i	Number of UEs inside a bus associated with the mobile relay i
$\overline{n}_v$	Average number of UEs in a bus
n_{tv}	Total number of vehicular UEs in a cell
ν	Average speed of a bus
p	Received power

p_0	Received useful signal on the access link when there is no fading
P	Transmitted power
P_R	Transmitted power of relay node
P_S	Transmitted power of eNodeB
P_{S_0}	Static power consumption for base stations
P_{R_0}	Static power consumption fo mobile relays
P_{S_ave}	Average power consumption for base station in the cell
P_{R_ave}	Average power consumption for mobile relays in the cell
$\mathbb{P}(n_u = i)$	Probability to have n_u UEs in area A
$\mathbb{P}(n_r = i)$	Probability to have n_r buses (mobile relays) in area A
Π	Generic realization of a Poisson Point Process of intensity $\lambda \mathrm{d}y$
Π_o	Poisson Point Process of ordinary UEs
Π_r	Poisson Point Process of eNodeBs
Π_s	Poisson Point Process of buses
Π^e	Marked PPP process whose atoms are (y, χ, γ, h)
$\psi_{\chi,\gamma}$	Probability to obtain $(\chi, \gamma) \in \mathcal{B}$
γ	Path loss exponent
r	A factor that takes the fading effect into account
R	Radius of the hexagonal cell
ρ	Parameter for downlink/uplink subframe configuration
ρ_r	Density of buses in the cell
ρ_u	Density of UEs per km^2 in the cell
$\mathcal{R}$	Achievable data rate
$\mathcal{R}_{max}$	Maximum data rate that LTE could support at a given bandwidth
σ_s	Standard deviation of shadowing
S or S	SINR on the considered link
$F_S(t)$	CDF of the SINR on the considered link
s_{eff}	SINR implementation efficiency of LTE
T	SINR threshold
$1/\tau_S$	Efficiency of the power amplifier for base stations
$1/\tau_R$	Efficiency of the power amplifier for mobile relays
$\overline{T}_D$	Average dwell time of a UE in a bus
$\overline{T}_C$	Average time in ECM_Connected state
$\overline{T}_I$	Average time in ECM_Idle state
ϱ	Probability of UE-triggered service request
ε	Probability that the UE is in CONNECTED state
W	System bandwidth
w_{eff}	System bandwidth efficiency of LTE
ξ	Power of the received signal when there is no fading
Ξ	Poisson point process of the inverse received power
Ξ^e	Marked Poisson Point Process $\Xi^e = \{(s, r), s \in \Xi, r \in \mathbb{R}^+\}$
y	Distance from a transceiver to a receiver (in km)
Y	Shannon capacity on the considered link

Chapter 1

Introduction

1.1 Motivations

Data traffic demand in cellular networks today is increasing at an exponential rate. According to a white paper by Cisco, the global mobile data traffic is expected to increase 11-fold between 2013 and 2018, reaching 15.9 exabytes per month [1]. This ever increasing mobile data traffic is creating challenges for cellular network operators. Existing cellular architectures are designed to cater large coverage areas, which often fail to achieve the expected throughput at cell edge or hot spot areas. To address this explosive growth in data demands driven by smart phones, tablets, and other media-hungry devices, heterogeneous networks have been introduced in the LTE-Advanced standardization [8, 9, 10]. Heterogeneous networks allow a mixed deployment of macro and micro base stations (BSs). Micro BSs can be classified as picocell BSs, femtocell BSs and Relay Nodes (RNs). In heterogeneous network deployments, the overlay macro BSs provide a wide area coverage while micro BSs are deployed in a selective area to fulfill specific capacity and coverage needs.

Micro BSs cover a small area using low transmit power, typically ranging from 100 mW to 2W. Picocell BSs are usually equipped with omni-directional antennas, and are deployed indoors or outdoors in a planned manner [8]. Femtocell BSs are consumer deployed in an unplanned manner for indoor use, and their transmit power is normally 100 mW or less [11]. Both picocell BSs and femtocell BSs connect to network via wired backhaul links. If a wired backhaul is not available, Relay Nodes (RN) can be deployed in a flexible manner where the air interface spectrum is used for backhaul connectivity and provide access to terminals. RNs are connected to network via wireless backhaul links. In this case, an RN appears as a User Equipment (UE) to the macro base station and as a regular base station to the UE it serves. In

the deployment of cellular networks, the cost of the backhaul to the various network nodes has been considered as an essential cost component, especially for the micro BSs. Because the site acquisition cost of micro BSs is expected to be lower than that of macro BSs. Therefore, the ability to deploy network nodes not relying on a wired backhaul is an appealing option to reduce total network deployment cost and operating costs [12].

Currently, the number of users using wireless broadband services is rising greatly with the introduction of smart phones, tablet computers and other new mobile devices, as shown in Figure 1.1. Cisco has predicted that the number of mobile devices is going to exceed the population on earth by the end of 2014, and by 2018, there will be nearly 1.5 mobile devices per capita [1]. With this rapid popularity of smart phones and tablets, people make intensive use of these devices to kill time when they are in public transportation vehicles such as buses, trams, or trains. However, the service quality in public transportation vehicles is far from satisfactory.
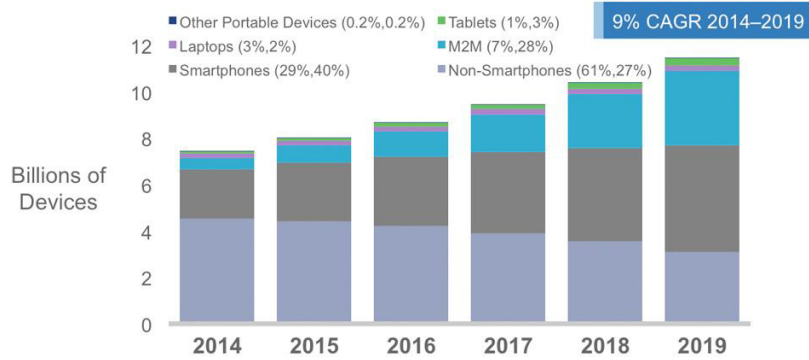
Figure 1.1: Global Mobile Devices and Connections Growth, source [1]

Public transportations are usually well shielded with coated windows, which leads to a rather high penetration loss between outdoor and in-vehicle [13]. For the 2 GHz band, penetration loss can be as high as 25 dB, and even goes up to 35 dB in Shanghai's high-speed magnetic levitation train [14]. Traditionally, the UEs inside the public transportations connect to the macro BSs via wireless links, in which the penetration loss severely attenuates the signal quality and decreases the achievable data rate. Also, due to the relative movement between the UE and the base station, the Doppler Frequency Shift might occur depending on the speed of the movement. The Doppler effect is particularly evident in a high-speed scenario, which can cause data symbol phase rotation and degrade the accuracy of data demodulation, thus leading to degraded performances [15].

Due to the penetration loss and the Doppler frequency shift, the link quality between a UE within a vehicle and the base station deteriorates, which generates relatively limited cell coverage and longer duration of cell selection, re-selection, paging, and handover procedure. During the handover procedure, a large group of UEs perform handover simultaneously. As predicted by the European Union project Mobile and wireless communications Enablers for the Twenty-twenty Information Society (METIS), by the year of 2020, it will be fairly common to have up to 50 active vehicular UEs per bus and up to 300 active vehicular UEs per train [16]. Such a large amount of simultaneous handovers would increase system signaling significantly, resulting in reduced handover successful rates because of channel congestion. Thus optimized mobility management schemes for vehicular UEs are needed.

Compared to typical wireless environments, offering high-quality services to the UEs in public transportations becomes an important and challenging issue [17, 18]. Several solutions have been discussed to address this issue, such as optimizing the deployment of macrocells, using layer 1 repeaters, or LTE backhaul plus on-board Wi-Fi access [19]. However, these solutions can only partially mitigate the problem. For example, deploying dedicated macrocells for vehicular UEs can not eliminate the signal loss caused by the penetration loss, which is one of the major challenges faced by vehicular UEs. Layer 1 repeaters can amplify and forward signals in a given frequency band, but the SINR (Signal-to-Interference-plus-Noise Ratio) can not be improved at layer 1 repeaters, so they can only by deployed at positions with good SINR. Using WiFi to provide Internet access to vehicular UEs is fairly common, but the QoS and security of the WiFi access are not guaranteed, and offering a seamless experience to vehicular UEs by WiFi technology is quite challenging. Besides, none of the above solutions can address the signaling issue during the simultaneous handovers of vehicular UEs.

Realizing the limitations of the above solutions, the Third Generation Partnership Project (3GPP) is investigating the deployment of mobile relays on public transportations such as buses, trams, or trains [20]. When the users are grouped on a bus or a tram, this can be seen as a mobile hot spot. With the aim of offering high-quality services to these users, deploying mobile relay node on public transportations is a natural idea. Therefore, we try to go deeper in the study of mobile relays in LTE network and address the relevant issues in this thesis.

1.2 Context of the thesis

Our work is performed within the project SYSTUF (SYSteme Telecom pour les Transports Urbains du Futur). The SYSTUF project is a response to the Intelligent Transportation Systems call of the French government program Investments for the Future National Fund for the digital society. This project deals with research and development in technologies, innovative products and services related to intelligent transportation systems and focuses on tramways and metro systems. Main partners of the project are Alcatel-Lucent, IFSTTAR, ALSTOM, Eurecom, RATP, Mitsubishi Electric R&D Centre Europe, Telecom Bretagne and SIMPLUSE. The duration of the project is from 2012 to 2015.

The project aims to demonstrate the feasibility of using a single communication technology based on LTE (Long term Evolution) both for the transport operators and for passengers in order to meet the Quality of Service requirements of both technical traffic (control, command, cctv, etc.) and user traffic (web, video, etc.) simultaneously. The technical traffic can be critical (control and command) or non vital while the user traffic is always non vital. The project also aims to enable the development of innovative services contributing to seamless mobility which meets the growing demand for "smart and environment-friendly mobility". Our work in the project is to investigate how to meet the requirements of user traffic for passengers. We thus concentrate our study on mobile relays.

1.3 The Contributions

Mobile relays are installed in public transportation vehicles. As the vehicle moves, the mobile relay moves along with the UEs in the vehicle. The vehicular UEs connect to the network by communicating with the in-vehicle antenna of mobile relay. On the other hand, the mobile relay communicates with the donor eNB (DeNB) via the outdoor antenna of mobile relay. By using two separate outdoor and in-vehicle antennas, mobile relay can eliminate the penetration loss between outdoor and in-vehicle. Moreover, mobile relay can create its own cell within a vehicle, group mobility management of vehicular UEs served by the same mobile relay can be performed.

However, there are also challenges in using mobile relays. How much gain can be attained through mobile relays in a LTE network? How to perform group handover using mobile relays under the current LTE system architecture? What's the funda-

mental benefits of deploying mobile relay on public transportation vehicles? These issues are still not fully investigated.

In this thesis we consider the scenario where mobile relays are deployed on public buses and investigate the fundamental benefits of deploying mobile relay in a LTE cellular network. In all the document, we take the example of buses for the sake of simplicity. However, the analysis can be extended to other transport systems: metros, tramways and trains. Most of the results have been reported (published or submitted) in different international conferences and journals. The contributions of our thesis work can be summarized in three parts.

1.3.1 Improvement of mobility procedures for mobile relays in LTE networks

We first study the different signaling procedures when the mobile relay is embedded in a public transport vehicle. We propose to keep the same protocol stack that was defined for fixed relay, and to extend it to mobile relays. The scheme of global tunnels is proposed to optimize the handover procedure of mobile relay nodes. Without adding any protocol in the stack, it's possible to group several handovers while keeping the possibility of managing the tunnel of each UE individually. This part of the work has been presented in PIMRC 2015 [21].

1.3.2 Impact of the interference on the data rate of one vehicular UE

We analyze and calculate the data rate gain of a UE provided by a mobile relay deployed in a hexagonal cellular network. We consider a network with one UE and one mobile relay. The analysis is based on the Shannon formula modified for LTE. We consider the case when a UE is directly connected to a base station and compare with the case when a UE is served by a mobile relay. Through Monte Carlo simulations, the data rate under different cases are obtained, and the effect of penetration loss on the data rate is studied. This part of the work has been published in WPMC 2013 [22].

Then, we extend the study to a random cellular network and compute some important metrics, such as the Cumulative Distribution Function (CDF) of the SINR and the average achievable rate on both the backhaul link and the access link. The computing is based on stochastic geometry approach, which can capture

the irregularity and randomness of a realistic network. Both log-normal shadowing and Rayleigh fading are considered. This part of the work has been published in Globecom 2014 [23].

1.3.3   Impact of mobile relays on the cell capacity

We investigate the capacity gain brought by mobile relays deployed in a hexagonal cellular network. We consider a network with multi-users and multi-relays. The distribution of terminals and mobile relays are modeled by spatial Poisson distribution. Equal bit rate scheduling is used. Two relay modes: pure-relay mode and femto-like mode are proposed and compared. The system performance is evaluated by Monte Carlo simulations. This part of the work has been published in CCNC 2014 [24].

Then, we extend the study to a random cellular network. A general analytical model for mobile relay scenario is proposed using stochastic geometry. Important metrics like the CDF of the SINR and the CDF of the end-to-end rate are derived. The rate of the backhaul link and the rate of the access link are in general correlated when the same spectrum (or frequency) is used on both links, we take this fact into account when deriving the CDF of the end-to-end rate. Furthermore, we propose a TDD/FDD (Time Division Duplexing/Frequency Division Duplexing) hybrid mobile relay mode, motivated by the fact that a vehicular UE is static relative to its serving mobile relay and close to it in this specific scenario, which leads to a relatively good channel condition on the access link. A small bandwidth is dedicated to the access link. The backhaul link and the access link can thus operate independently without additional complex mechanisms to avoid self-interference. In addition, we evaluate and compare the performance between two relay modes and direct mode using the proposed analytical model. The bandwidth is Round-Robin scheduled among users within a cell. The cell total average rate and the energy efficiency in different modes are evaluated.

1.4   The Structure of the Thesis

The rest of the thesis is organized as follows. Chapter 2 gives a survey about mobile relay study in cellular system and 4G network. Chapter 3 studies the different signaling procedures of mobile relay, an optimized mobility management scheme based on the idea of global tunnel is proposed and analyzed. Chapter 4 studies the impact of the interference on the data rate of one vehicular UE. It first evaluates the per-

formance in a hexagonal network based on simulations. Then the numerical results in a random networks are given based on stochastic geometry approach. Chapter 5 investigates the impact of mobile relays on the cell capacity. It first evaluates the performance in a hexagonal network based on Monte Carlo simulations. Then a general analytical model for mobile relay scenario is proposed using stochastic geometry. A TDD/FDD hybrid mobile relay mode suitable for this specific scenarios is proposed and analyzed. By using the proposed analytical model the performance of different modes are evaluated and compared. Finally, Chapter 6 provides concluding remarks and some possible future research directions.

Chapter 2

Functions of relays in cellular systems and 4G networks: an overview

In this chapter, we present the overall EPS network architecture and functions, including both the core network and the access network. The structure of LTE transmissions and the protocol architecture for the user plane as well as the control planes are discussed. We then give a general overview of relays. Some procedures related to relay, such as relay startup procedure, UE attach procedure, are addressed. Lastly, we present the related works on mobile relays.

2.1   Historical context for today's EPS network

Mobile communication systems are often divided into generations. The 'First Generation' system came out in the early 1980s. The 1G cellular systems comprised a number of independently developed systems worldwide (e.g. AMPS (Analogue Mobile Phone System), TACS (Total Access Communication System), NMT (Nordic Mobile Telephone)), using analogue technology. Then, in the mid 1980s, the 'Second Generation' system known as GSM (Global System for Mobile Communications) was developing using digital technology. The GSM system was designed as a circuit-switched network, at a modest peak data rate of 9.6 kbit/s. Higher data rates were introduced later in the GPRS (General Packet Radio Service) systems, also known as 2.5G, by enabling mobile users to access the Internet. Afterwards, in the early 2000s, the 'Third Generation' system, known as UMTS (Universal Mobile Telecom-

munications System), inherited the GPRS architecture and combined the properties of the circuit-switched voice network and the packet-switched data network, offering more possibilities compared to its predecessors. Later, the HSPA (High Speed Packet Access), also known as 3G+, extended and improved the performance of UMTS systems.

Driven by the creation and development of new services for mobile devices, the 3G evolution continued. The 3GPP Long Term Evolution (LTE) radio interface was initiated in 2004 with the objective of providing a new radio access technology focusing on packet-switched data. In parallel to the development of LTE, the overall system architecture of both the Radio Access Network (RAN) and the Core Network (CN) was re-designed, including the split of functionality between the two network parts. The LTE access network is also officially referred as Evolved Universal Terrestrial Radio Access Network (E-UTRAN). This evolution of the overall architecture was known as the System Architecture Evolution (SAE), and resulted in a new core network architecture referred to as the Evolved Packet Core (EPC) network. Together, the LTE and the EPC can be referred as the Evolved Packet System (EPS), where both the core network and the radio access network are fully packet-switched and all-IP network.

2.2 EPS architecture overview

EPS provides the users with IP connectivity to a PDN (Packet Data Network) for accessing the Internet. The concept of EPS bearers is used in EPS to route IP traffic from a gateway in the PDN to the UE. A bearer can be defined as an IP packet flow with a Quality of Service (QoS) between the gateway and the UE. Multiple bearers can be established for a user in order to provide different QoS services or connectivity to different PDNs. The overall EPS network architecture is comprised of the CN (EPC) and the access network (E-UTRAN), shown in Figure 2.1.

In the EPC network many network elements exist, but there is essentially only one element in the radio access network E-UTRAN, which is the evolved NodeB (eNodeB). Each element in EPS network is connected through standardized interfaces, which allows multivendor interoperability. The EPC and LTE network are described in more details below.
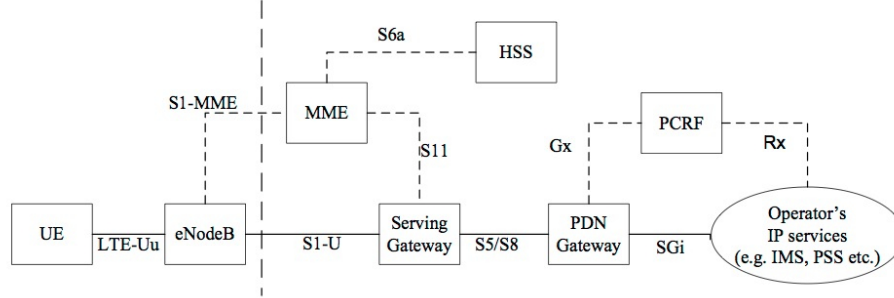
Figure 2.1: The EPS network architecture, source [2]

2.2.1 The Core Network

The EPC core network is very different from the GSM/GPRS core network used in GSM and WCDMA/HSPA. The EPC core network only supports the packet-switched domain rather than the support of the circuit-switched domain. Functionally, it's mainly responsible for the control of the UE and the establishment of bearers. The EPC consists of several different types of nodes, some of which are briefly described below:

The *Mobility Management Entity* is the control-plane node of the EPC. It's responsible for bearer management, connection management, and deals with security keys. In a word, MME processes the signaling between the UE and the EPC. The protocols running between the UE and the CN are referred as the Non-Access Stratum (NAS) protocols.

The *Serving Gateway* (S-GW) is the user-plane node connecting the EPC to the LTE RAN. All user IP packets are forwarded through the S-GW. It serves as a mobility anchor when UEs move between eNodeBs. It also has the information about the bearers when the UE is in idle state and temporarily buffers downlink data while the MME is paging the UE to re-establish the bearers. Besides, it also performs some administrative functions like collecting information for charging (e.g. the volume of data sent to or received from the user).

The *Packet Data Network Gateway* (PDN-GW) connects the EPC to the internet. It's responsible for IP address allocation for the UE and QoS enhancement according to the rules from the PCRF (see below). This is performed based on Traffic Flow Templates (TFTs).

The *Policy Control and Charging Rules Function* (PCRF) is responsible for policy control, QoS handling and controlling the charging functionalities in the Policy

11

Control Enforcement Function, which resides in the P-GW. It decides how a certain data flow will be treated.

The *Home Subscriber Service* (HSS) is a database containing subscriber information. It's in charge of generating security information and performing the authentication of the user.

2.2.2 The Access Network

The LTE radio access network uses a flat architecture and consists of a network of eNodeBs. There is no controller in LTE, which is a big different compared with the previous radio access network. LTE integrates the radio control function into the eNodeB, which allows tight interaction between the different protocol layers. The protocols that run between the eNodeBs and the UE are known as the Access Stratum (AS) protocols.

2.2.2.1 Interfaces and Functions

Normally the eNodeBs are connected to each other through the X2 interface, and to the EPC through the S1 interface, more specifically, to the MME through the S1-MME interface and to the S-GW through the S1-U interface. The interfaces of LTE radio access network are shown in Figure 2.2.
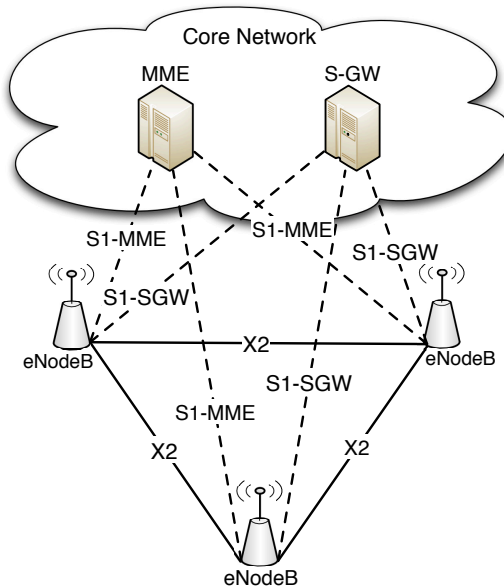
Figure 2.2: The overall E-UTRAN architecture

The E-UTRAN are responsible for all radio related functions, which can be summarized as follows:

- Radio Resource Management. It includes radio bearer control, radio admission control, radio mobility control, scheduling and resource allocation in uplink and downlink.

- Header Compression. It is done in *Packet Data Convergence Protocol* (PDCP) to compress IP packet header, which helps to efficiently utilize radio resource, especially for small packets like VoIP.

- Security. Encrypt the data sent over the radio interface.

- Connectivity to the EPC. This consists of the signaling towards the MME and the bearer path towards the S-GW.

2.2.2.2   Packet Access on LTE

In the above sections, the overall LTE architecture and functions were discussed, now we briefly introduce the structure of LTE transmissions.

As we know, OFDM (Orthogonal Frequency-Division Multiplexing) is used in LTE as the basic physical layer transmission scheme for both downlink and uplink. The OFDM subcarrier spacing equals 15 kHz. In the time domain, LTE transmissions are organized into radio frames with a length of 10 ms, each radio frame is divided into ten equal 1 ms subframes. Each subframe contains two time slots with a length of 0.5 ms, each slot contains certain number of OFDM symbols and cyclic prefix, the frame structure is shown in Figure 2.3.

As is illustrated in Figure 2.3, LTE defines two cyclic prefix length, the normal cyclic prefix and the extended cyclic prefix, corresponding to seven and six OFDM symbols per slot respectively. The reason for doing this is because the extended cyclic prefix is useful in specific environments with extensive delay spread, for example in very large radius cells. In LTE the smallest physical resource is a *resource element*, which contains one frequency symbol (on one subcarrier in the frequency domain and one OFDM symbol in the time domain). Multiple resource elements are grouped into *resource blocks* (RBs). Each resource block contains 12 consecutive subcarriers in the frequency domain and one slot in the time domain. Thus there are $7 \times 12 = 84$ resource elements in one resource block if normal cyclic prefix is configured, $6 \times 12 = 72$ resource elements in one resource block in the case of extended cyclic prefix. The
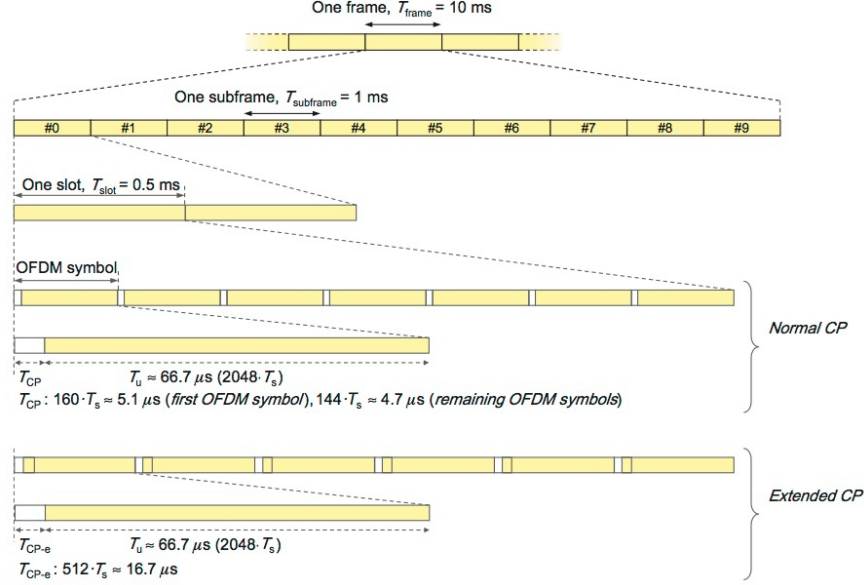
Figure 2.3: The LTE frame structure, source [3]

minimum scheduling unit can be defined as a resource-block pair which consists of two time-consecutive resource blocks within one subframe.

It's important to note that in LTE, each downlink subframe is divided into a control region and a data region, some resource elements are reserved for control data. The control region carries L1/L2 signaling to control uplink and downlink data transmissions. Normally L1/L2 control signaling contains downlink scheduling assignments, uplink scheduling grants and hybrid-ARQ acknowledgements. These control signalings are transmitted within the first part of each subframe. They allow terminals to decode downlink scheduling assignments as early as possible, which leads to a more efficient process. Basically the control region occupies one, two, or three OFDM symbols, shown in Figure 2.4.

As can be seen in Figure 2.4, the allocated RBs and the associated RNTIs are given in the first 1-3 symbols. RNTI is Radio Network Temporary Identifier, each terminal is identified by a RNTI. Normally the control region contains four different physical channel types.

- The *Physical Control Format Indicator Channel* (PCFICH), notifies the terminal about the size of the control region in terms of the number of OFDM symbols, one, two or three OFDM symbols. The PCFICH contains two bits of information and is coded into a 32-bit codeword. The codeword is mapped

14
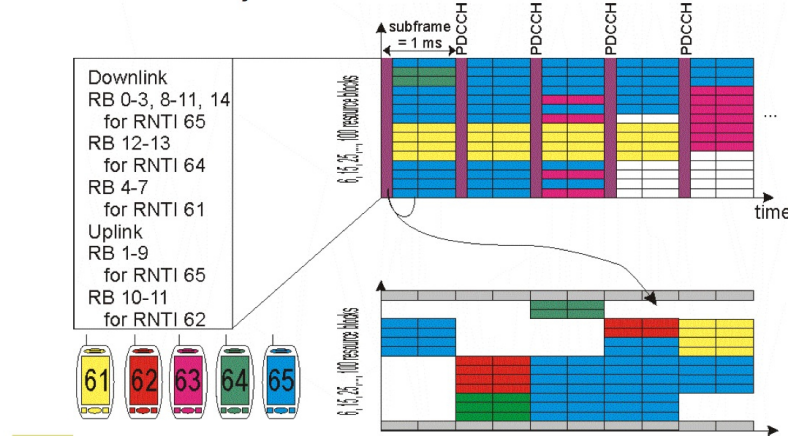
Figure 2.4: LTE control and data region, source [4]

to 16 resource elements.

- The *Physical Downlink Control Channel* (PDCCH) is used to carry downlink control information like downlink scheduling assignments and uplink scheduling grants. Downlink scheduling assignments include information that UE needs to properly receive, demodulate and decode the DLSCH. Uplink scheduling grants notify the UE about the resources and transport format used for uplink (ULSCH) transmissions. Hybrid-ARQ acknowledges are response to ULSCH transmissions. These information should be transmitted in every subframe. The terminal decodes them and knows whether there are some resource blocks for itself.

- The *Physical Hybrid-ARQ Indicator Channel* (PHICH) is used to transmit hybrid-ARQ acknowledgements for uplink PUSCH transmissions.

- The *Relay Physical Downlink Control Channel* (R-PDCCH) is a control channel used to transmit control information for relay nodes. It's not transmitted in the common control region. We'll discuss R-PDCCH in the relay section.

2.2.3 Protocol Architecture

The radio protocol architecture for LTE can be separated into control plane architecture and user plane architecture. The LTE protocol stack is shown in Figure 2.5.

15
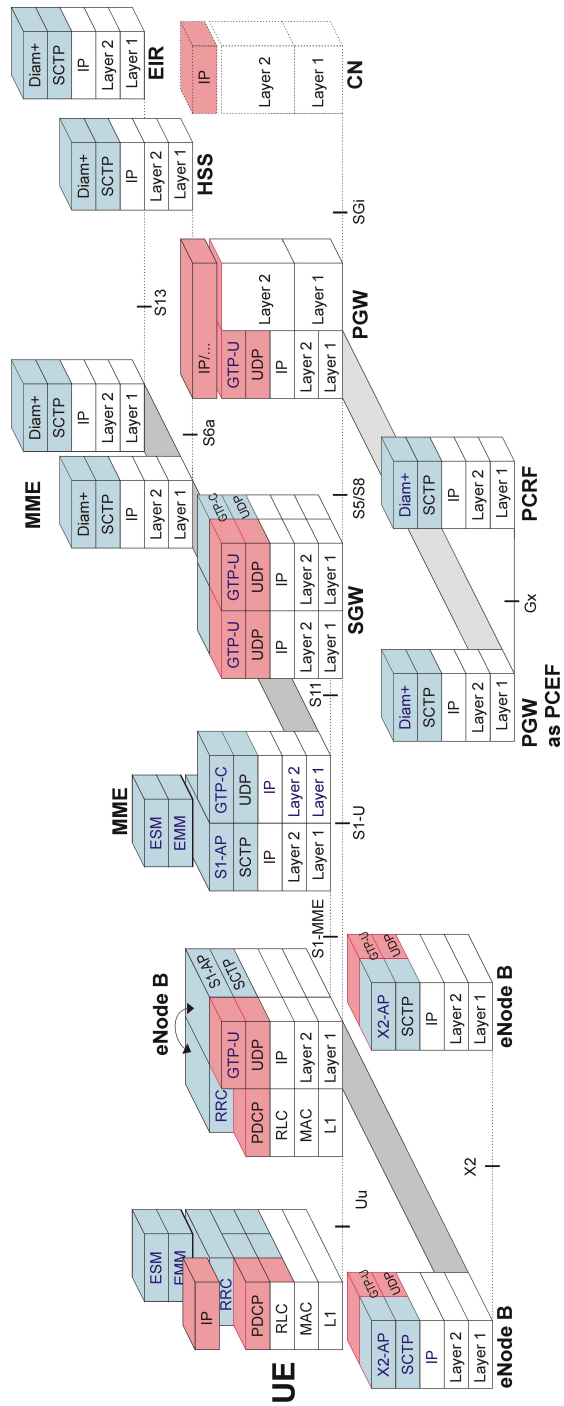
Figure 2.5: Global view of the LTE-EPC protocol stack

2.2.3.1 User Plane

On the user plane, packets in the core network are encapsulated in a specific EPC protocol and tunneled between the P-GW and eNodeB. Different tunneling protocols are used on different interfaces. A 3GPP-specific tunneling protocol called the GPRS Tunneling Protocol (GTP) [25] is used over the core network interfaces. This protocol tunnels user data between eNodeB and S-GW as well as between S-GW and P-GW, as shown in Figure 2.6. A tunnel that is used for user data is called a bearer. The endpoint of each tunnel is identified by a TEID (Tunnel Endpoint Identifier). Hence, each tunnel is associated to 2 TEID values. For example, an S1 tunnel has one TEID allocated by the eNodeB and another one allocated by the SGW. Each tunnel is identified by a TEID in the GTP-U messages, which should be a dynamically allocated random number. The GTP-U encapsulates all user IP packets.
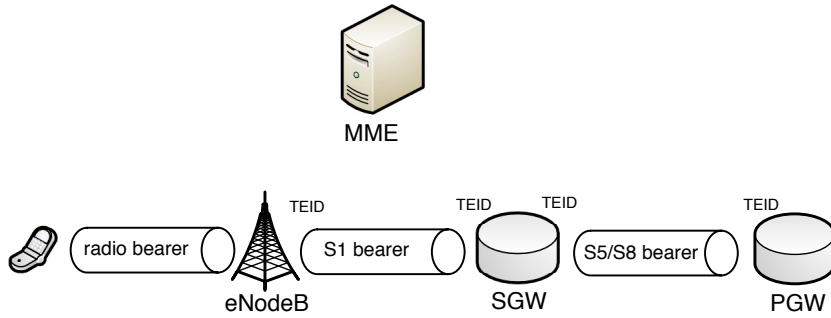
Figure 2.6: User plane tunnels

2.2.3.2 Control Plane

The control plane manages the signaling between E-UTRAN and EPC. More specifically, the control plane protocols are responsible for connection and bearer setup, mobility and security. The control plane of the access stratum handles radio-specific functionality. The access stratum interacts with the non-access stratum (NAS). Among other functions, the NAS control protocols handle tracking area update, paging, authentication and bearer establishment, modification and release. The S1-AP messages are sent between the MME and the eNB. Each S1-AP message contains two information elements: eNB UE S1AP ID and MME UE S1AP ID [26]. MME UE S1AP ID is one ID for the S1AP interface that is allocated on a per-UE bearer by the MME. The control plane connections and tunnels are shown in Figure 2.7.

17
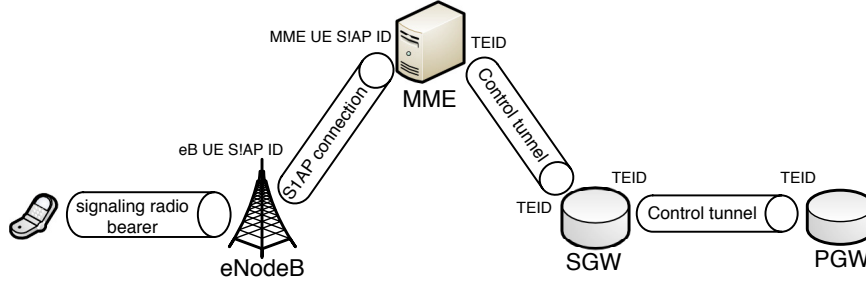
Figure 2.7: Control plane tunnels

2.3 An Overview of Relay Node

To extend coverage and improve capacity, 3GPP LTE-Advanced has introduced the concept of Relay Node. Relay Nodes, usually deployed at selective locations, aim to provide coverage in shaded areas or increase the capacity at hot spots [27]. 3GPP has specified relay node in release 10 of LTE standards [6]. Some details of the specified Relay Node are described in the following.

2.3.1 Vocabulary

The relay node is wirelessly connected to the radio access network via a donor eNodeB (DeNB). The relay node is connected to the DeNB via radio interface *Un*, a modified version of E-UTRAN air interface *Uu*. With the help of relay nodes, the radio link between the base station and the UE is divided into two hops. The link between the eNodeB and the relay node is referred to as the *backhaul link*, while the link between the relay node and the UE is referred to as the *access link*. Accordingly, the link between the eNodeB and the UE is referred to as the *direct link*. Both the backhaul link and the access link are expected to have better propagation conditions than the direct link. This is illustrated in Figure 2.8.
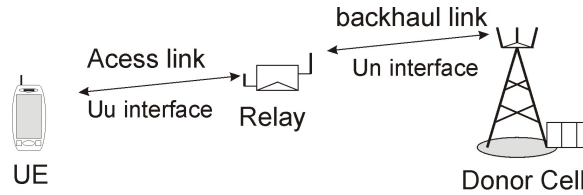
Figure 2.8: Access and backhaul links, source [5]

2.3.2 Types of Relay Nodes

Two types of RNs have been defined in 3GPP LTE-Advanced: type-1 relay and type-2 relay [28]. Specifically, from the UE viewpoint, type-1 relay appears as a regular eNodeB, it has its own cell ID, synchronization, broadcast, and control channels. Thus, type-1 relay is a layer-3 node. It can be used to either extend the coverage or improve the capacity.

In contrast, type-2 relay have not been standardized yet and only received a functional description from 3GPP technical reports. Type-2 relay can transmit data on PDSCH, but it does not have a separate physical cell ID. Terminals served by type-2 relay get control signaling of PDCCH from the eNodeB, which means terminals should be located within the coverage of an eNodeB. Type-2 relays are mainly designed to improve the capacity for certain hot spot areas.

2.3.2.1 Type-1 Relay Node

Since the relay communicates with both eNodeB and terminals, interference between the backhaul link and the access link must be avoided. Isolation between the access link and the backhaul link can be achieved within time, frequency or spatial domains. Depending on the spectrum used for the access link and backhaul link, type-1 relay can be further distinguished into inband relay and outband relay.

Inband relay implies that the backhaul link and the access link operate in the same spectrum, as shown in Figure 2.9. As the access link and the backhaul link share the same spectrum, some additional mechanisms are required to avoid interference between the access link and the backhaul link. A mechanism to separate transmissions on the access and backhaul links in the time domain is required. Such a mechanism was introduced as part of release 10 and will be detailed later.
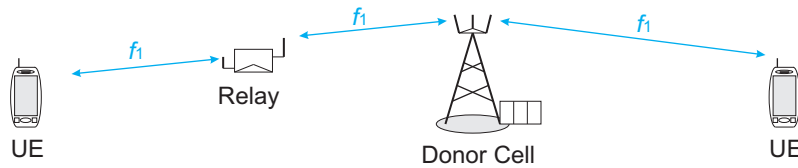
Figure 2.9: Inband Relay, source [5]

Outband relay implies that the backhaul link and the access link use different frequencies, as shown in Figure 2.10. Isolation between the backhaul link and the access link is obtained in the frequency domain. Relay can operate with full duplex in this case.
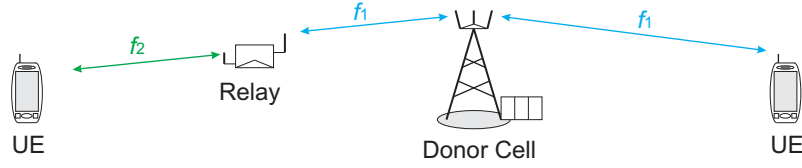
Figure 2.10: Outband Relay, source [5]

Compared with inband relays, outband relays can provide more capacity, because the access link can use the spectrum all by itself. But from Figure 2.9 and Figure 2.10 we can see, inband relays are more efficient from the spectrum usage point of view, because both access link and backhaul link share the same spectrum. From the technical point of view, inband operation is more complex, isolation in the time domain needs sophisticated configuration of the Un interface. Both inband relay and outband relay were discussed during the study of 3GPP, but only inband half duplex type-1 RNs are specified in 3GPP LTE release 10.

2.3.2.2   Type-2 Relay Node

As discussed above, type-2 relay nodes do not have separate physical cell ID, so they do not create any new cells and transmit cell-specific reference signals and PDCCH. In this case, type-2 relays are mainly used to enhance capacity instead of coverage extension. Since it has been agreed to standardize specifications for type-1 relay technology in 3GPP release 10, we focus on type-1 relay node in the thesis.

2.3.3   Subframe enhancements for inband Relay Node

In the case of inband relay node, the backhaul link and the access link operate on the same spectrum. A mechanism is required to ensure the relay is not transmitting on the access link while receiving on the backhaul link at the same time (and vice versa). One natural idea is to reserve some subframes for the backhaul link while blanking some subframes on the access link, so that the relay has the possibility to communicate with the DeNB. For the uplink transmission, the scheduler in the relay can block UE's uplink transmission through the uplink grant scheduling. However, for the downlink transmission, the served UEs are always expecting the control data on PDCCH in every subframe on the access link. Blanking subframes on the access link seems impossible.

Fortunately, a specific frame, which was originally defined for MBSFN (Multicast Broadcast Single Frequency Network), can be used. MBSFN subframe are

mainly targeted for multicast transmission. In a MBSFN subframe, UEs expect cell-specific reference signals and control signaling to be transmitted only in the first or two OFDM symbols, which means that the remain part of the subframe can be empty. By configuring some subframes as MBSFN subframes, the relay can stop transmitting on the data region of these subframes and receive from the donor eNodeB on the backhaul link. The number of MBSFN subframes in each radio frame depends on the current load on the backhaul link, which is configured either via RRC signaling from the donor eNodeB to the relay or via OAM.

It is important to note that since a relay needs to transmit some control information in the first two symbols of the MBSFN subframe, it can not listen the control part of the subframe sent from the donor eNodeB on the backhaul link. So control signaling for relay node can not be transmitted using the regular PDCCH. As a result, a new control channel called Relay PDCCH (R-PDCCH) is defined. R-PDCCH should start late enough so that the relay could finish transmitting its own control region and switch from transmit mode to receive mode. R-PDCCH is mainly used to dynamically assign resources to different relays and uplink grant scheduling. The mechanism of how relay works is illustrated in Figure 2.11 and Figure 2.12. The two figures have different options on whether the donor eNB keeps transmitting to served UEs when relay is transmitting on the access link. If the donor eNB transmits to other direct UEs when the relay is transmitting on the access link, there will be interference to vehicular UEs. However, the interference can be small enough to allow an acceptable bit rate.

2.4 Main procedures with a fixed relay node

In this section, we introduce LTE fixed relay architecture, protocol stack aspects and some signaling procedures that have already been standardized in LTE release 10.

2.4.1 Principles of the relay architecture

The architecture for supporting fixed RNs in release 10 is shown in Figure 2.13. The RN terminates the S1, X2 and Un interfaces. The DeNB provides S1 and X2 proxy functionality between the RN and other network nodes (other eNBs, MMEs and SGWs). The S1 and X2 proxy functionality includes passing UE-dedicated S1 and X2 signaling messages as well as GTP data packets between the S1 and X2 interfaces
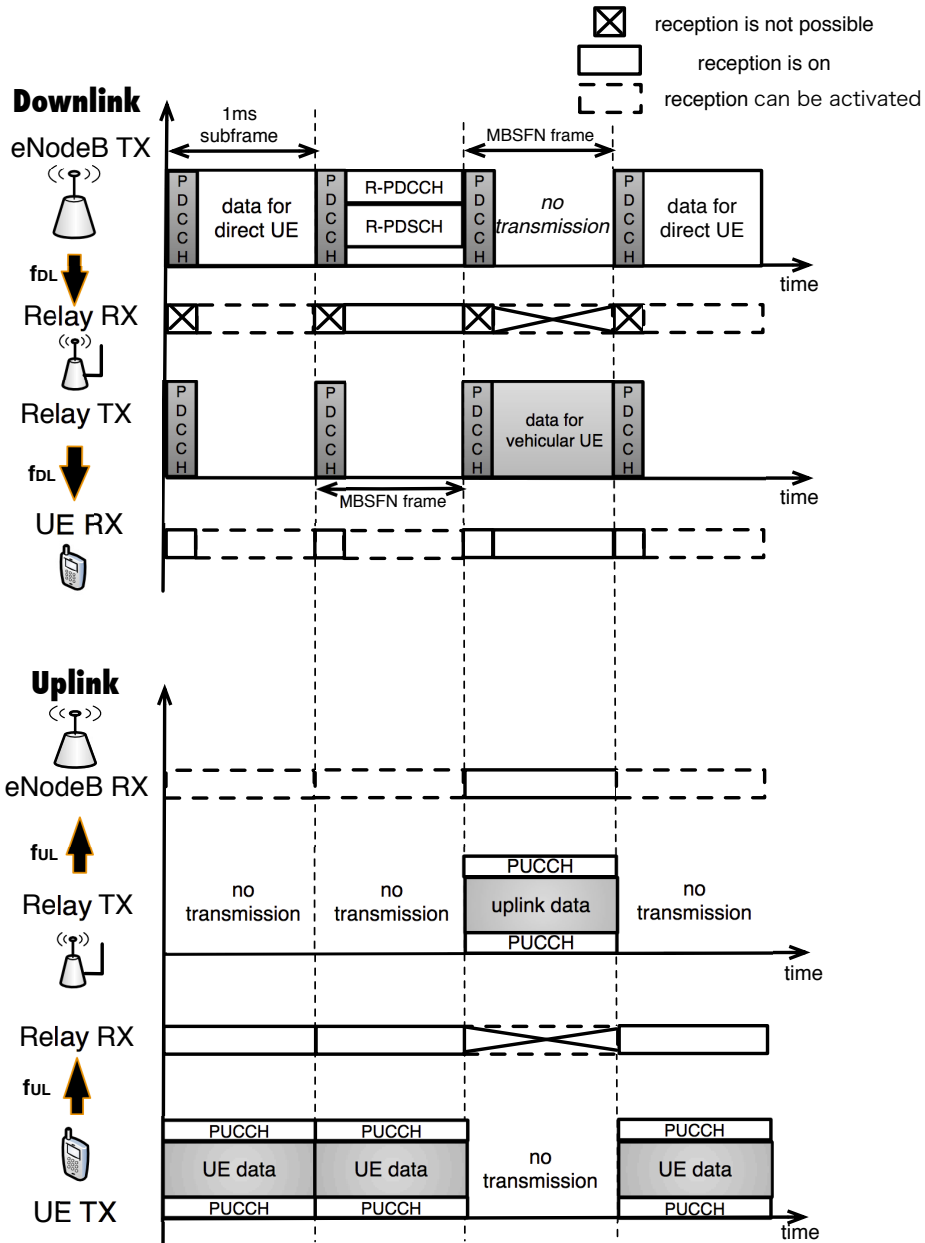
Figure 2.11: The mechanism of relay without donor eNodeB transmission when there is a transmission on the access link

Figure 2.12: The mechanism of relay with donor eNodeB transmission to a direct UE when there is a transmission on the access link
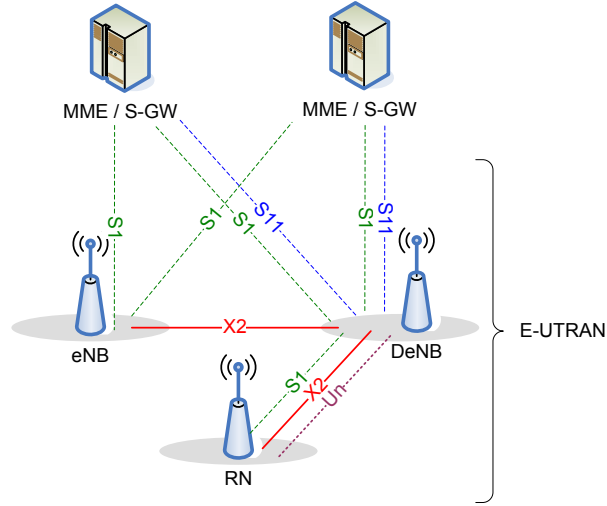
Figure 2.13: The architecture for supporting RNs, source [6]

associated with the RN and the S1 and X2 interfaces associated with other network nodes. Due to the proxy functionality, the DeNB appears as an MME (for S1-MME), an eNB (for X2) and an S-GW (for S1-U) to the Relay Node. Thus, S11 interface is used between the donor eNodeB and the MME.

With this architecture, the donor eNodeB can execute call admission control on a per-UE flow basis. In this architecture, the relay maintains one S1 interface (to the donor eNodeB), while the donor eNodeB maintains one S1 interface to each MME in the respective MME pool.

2.4.2 User plane aspects

The user plane protocol architecture for RN is shown in Figure 2.14. In relay case "home eNodeB GW" function is added into the donor eNodeB. The GTP protocol is used to transfer user data from the donor eNodeB to relay station. There is a GTP tunnel per-UE bearer spanning from the S-GW/P-GW of the UE to the donor eNodeB, then this GTP tunnel switches to another GTP tunnel at the donor eNB through one-to-one mapping and transfers user data from the donor eNB to the relay station. The donor eNB classifies the incoming packets into RN radio bearers based on the QCI of the UE bearer.

24
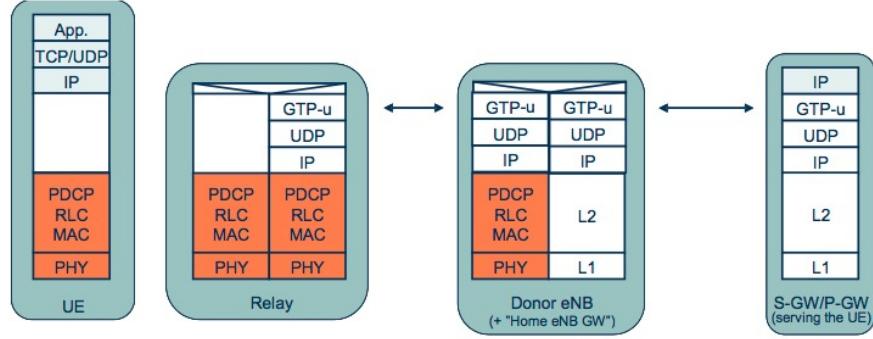
Figure 2.14: The user plane protocol architecture for relay node, source [7]

2.4.3 Control plane aspects

The control plane protocol architecture for RN is shown in Figure 2.15. The S1-AP messages are sent between the MME and the donor eNB, and between the donor eNB and the relay. There is a S1-AP proxy mechanism at the donor eNB which is similar to the home eNB GW function. S1 signaling connections are processed by the donor eNB. For all UE-dedicated procedures the donor eNB processes and forwards all S1 messages between the relay node and the MMEs. When donor eNB receives the S1-AP messages, it modifies S1-AP UE IDs, transport layer address and GTP TEIDs but leaves other parts of the message unchanged. In this case, there is a mapping relationship about S1-AP UE IDs at the donor eNB. For non-UE-dedicated S1-AP procedures, they are terminated at the donor eNB and handled locally between the relay and the donor eNB, between the donor eNB and the MME(s). This operation is transparent for the MME and the relay. From the view of the relay, it looks like it connects to the MME directly, as it's shown in Figure 2.16. The S1-AP messages are encapsulated by SCTP/IP. In this case, no new functionality is required in the S1-AP (and X2-AP) protocols [6].

2.4.4 Relay Startup Procedure

When a new relay is installed in the network, it would attach itself to the network automatically. The procedure is based on the normal UE attach procedure. There are two phases during the relay startup procedure. The RN startup procedure is illustrated in Figure 2.17.

In the first phase, the relay node creates RRC (Radio Resource Control) con-
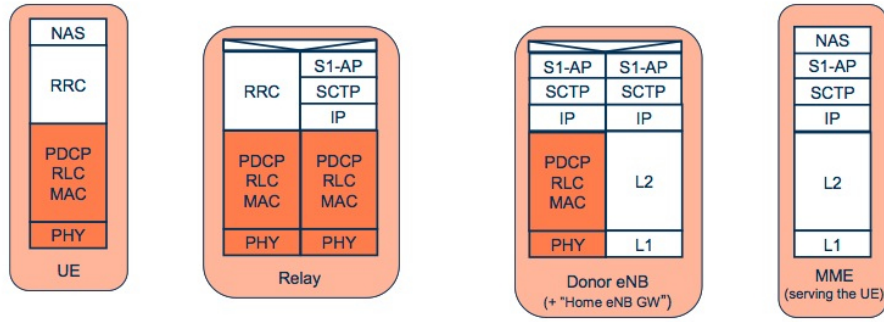
Figure 2.15: The control plane protocol architecture for relay node, source[7]
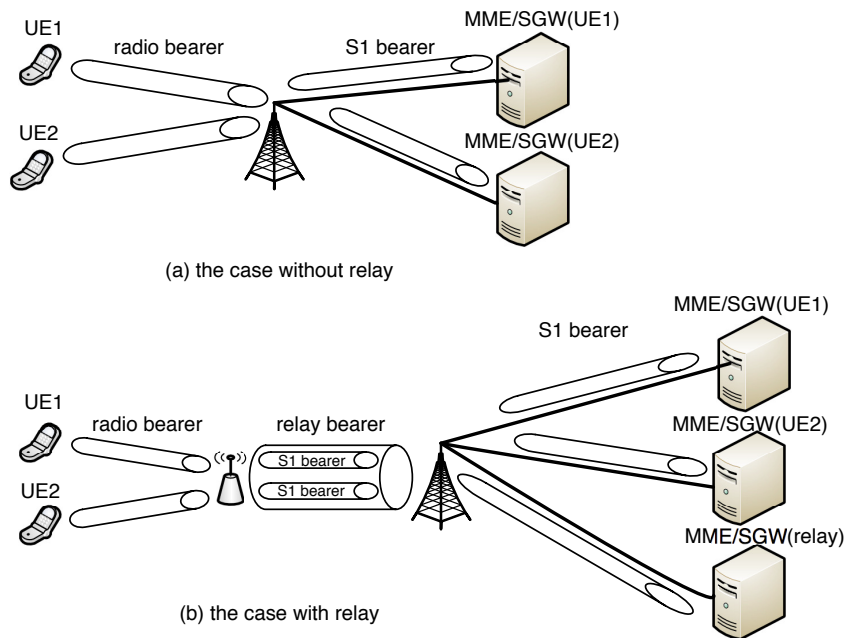
Figure 2.16: Tunnels and connections
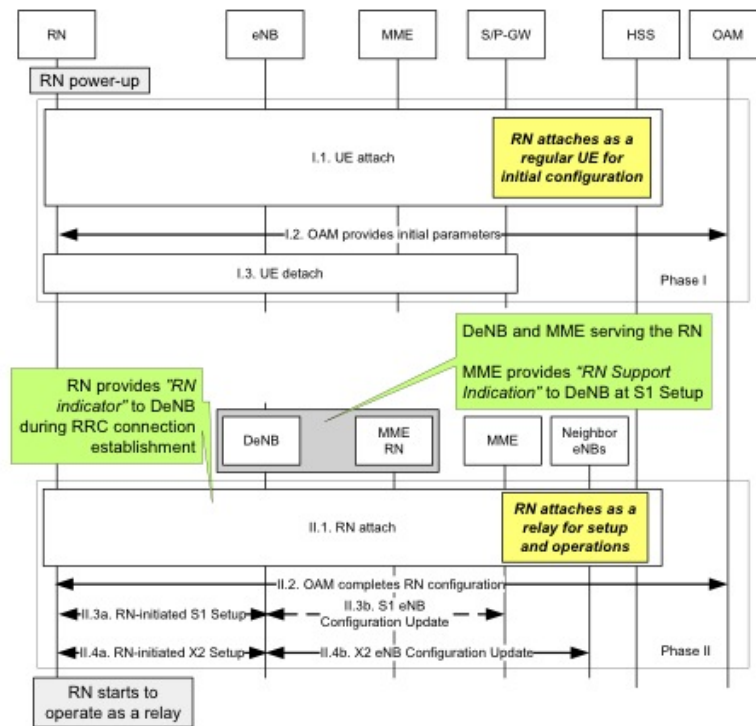
Figure 2.17: Relay Startup Procedure, source [6]

nection to the eNodeB and attaches itself as a regular UE for initial configuration. The MME (RN) creates a "UE" context which holds relay subscription information downloaded form the HSS. During this phase the relay node obtains the list of all possible donor eNodeBs which it can connect to from OAM (Operation Administration Maintenance), then the relay node detaches from the network as a UE and triggers the second phase. The MME performs the S-GW and P-GW selection for the RN as a normal UE. Note that the eNodeB that relay is associated to retrieves initial configuration in the first phase may not be the donor eNodeB of the relay. The details of RN attach as a regular UE are shown in Figure 2.18.
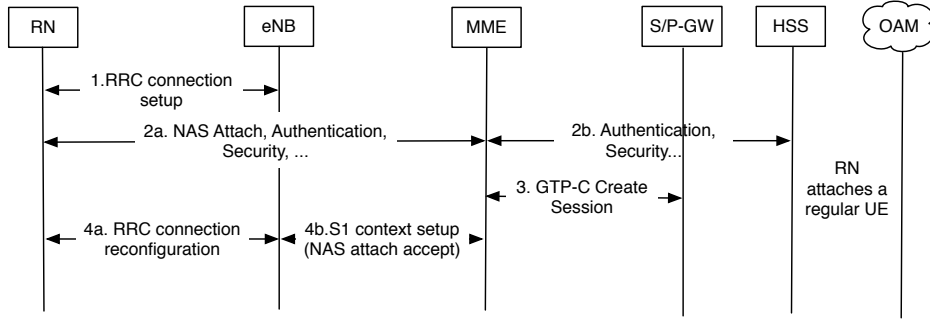
Figure 2.18: Relay Attaches as a regular UE

In the second phase, the relay node connects to the donor eNodeB selected from the list obtained in the first phase. The relay node sends a RN indication to the donor eNodeB during RRC connection establishment. After knowing this, the donor node can select a MME which is supporting RN functionality. The DeNB sends the RN indicator and the IP address of the S-GW/P-GW function embedded in the DeNB, within the Initial UE Message, to an MME supporting RN functionality. The MME obtains the subscription data from the HSS (Home Subscriber Server) to verify whether the relay node is allowed to join in the network. If not, the RRC connection is released. After the DeNB initiates setup of bearer for S1/X2, the RN initiates the setup of S1 and X2 associations with the DeNB. After the S1 setup, the DeNB performs the S1 eNB Configuration Update procedure. After the X2 setup, the DeNB performs the X2 eNB Configuration Update procedure to update the cell information. The details of RN attach as a relay node are shown in Figure 2.19. The MME in Figure 2.19 refers to the MME supporting RN. The DeNB appears as an MME, an eNB and an S-GW to the relay.
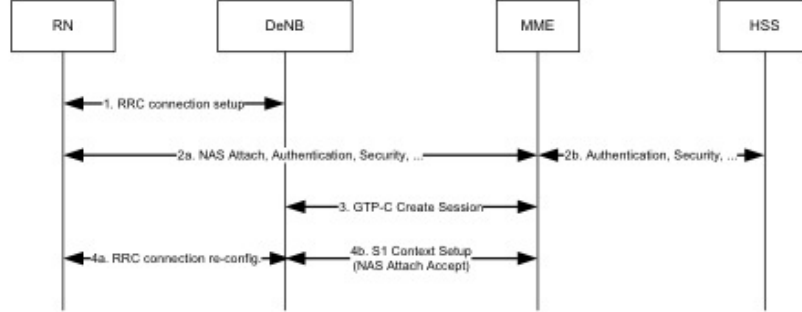
Figure 2.19: Relay Attaches as a relay node, source [6]

2.4.5 UE Attach Procedure

The initial attach of a UE connecting via a relay node is shown in Figure 2.20. The procedure corresponds to the legacy attach mechanism. The UE first initiates the attach process after cell selection and random access by transmitting an Attach Request message with RRC parameters to the relay. The relay sends the Attach Request message to the MME (UE) via the donor eNB. The MME (UE) then selects the S-GW and sends Create Bearer Request message to the S-GW/P-GW. After the bearer is established, the MME (UE) sends an Attach Accept message to the RN. This message is contained in S1 message Initial Context setup request. After the UE completes the RRC configuration, the relay sends the Attach Complete message to the MME (UE). As we can see, the DeNB is involved in the procedure by forwarding the corresponding S1 signalling between the RN and the MME (UE). As the S1 signaling always goes via the proxy functionality of the DeNB, the DeNB is explicitly aware of a UE attaching via the RN [7].

2.4.6 Mobility to or from RN

In case of the mobility for a UE moving between RN and neighbor eNB, there are generally two cases depending on the state the UE is in. If the UE is in RRC_IDLE state, all the LTE mobility procedures are performed autonomously within the UE. In IDLE state, the location of the UE is only known by the network at the Tracking Area List (TAL) level. When a UE in IDLE state arrives in the coverage of a relay, depending on whether the relay node has a specific TAI (Tracking Area Identity) or not, the UE may trigger a tracking area update. If the UE is in RRC_CONNECTED state, handover from RN to eNodeB or from eNodeB to RN would be triggered.
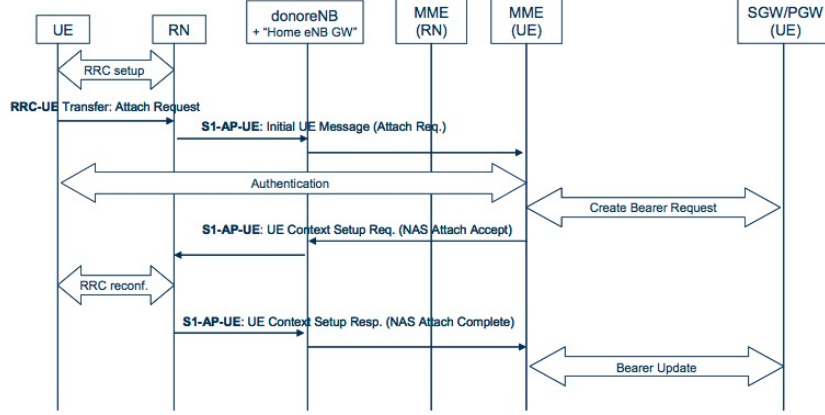
Figure 2.20: UE attach procedure via a fixed relay node, source [7]

The handover procedure with relay nodes is similar to the handover between two sectors (intra donor eNodeB case) or the handover between two eNodeBs (inter donor eNodeB case).

In 3GPP release 10, the mobility of relay node is not supported. Regarding the mobility issues of the UEs and the RN, we will detail them in Chapter 3.

2.5 Related work on mobile relays

2.5.1 Review of Existing Solutions

In order to provide high-quality services to vehicular UEs in public transportations, several solutions have been discussed in 3GPP technical report [19], such as dedicated deployment of macro eNBs, Layer 1 repeaters or LTE backhaul plus on-board Wi-Fi access. In this section, we briefly review the advantages and disadvantages of these solutions.

2.5.1.1 Dedicated Deployment of Macro eNBs

The route of a public transportation vehicle is usually known, especially the route of high-speed train. To optimize the coverage along the route line operators can deploy dedicated base stations using directive antennas. UEs in the public transportations are directly served by these dedicated bases stations. More specifically, a mixed deployment with high-power cells and low-power cells, i.e. HetNet deployment, can be used. The high-power cells can be configured as the serving node with the aim

of extending coverage, while the low-power cells can be added to improve capacity. For instance, with Carrier Aggregation, the Primary Component Carrier can be transmitted by the high-power cell, while the Secondary Component Carrier can be transmitted by the low-power cell. By using cross-carrier scheduling, most of the control signaling can be sent by the high-power cells, the data can be sent by the low-power cells. Without Carrier Aggregation, the use of RRUs (Remote Radio Units) can be considered. The RRUs share the same cell ID, therefore the closest RRU can serve the vehicular UEs in the vehicle without triggering handovers between RRUs belonging to the same macro cell.

However, dedicated deployment of macro eNBs can not eliminate the impact of penetration loss, which is one of the major challenges faced by vehicular UEs. Also, operators still face the challenges of site acquisition, deployment, and maintenance. Moreover, this solution can not be easily extended to urban scenarios [18].

2.5.1.2   Layer 1 Repeaters

Layer 1 repeaters are low-cost electronic devices that can amplify and forward signals in a certain frequency band [29]. Since repeaters do not re-generate the received signal, they are particularly useful in high SINR environments. Moreover, if the transmitter and the receiver antennas are sufficiently isolated, for example, inside and outside the vehicle respectively, the repeaters then can possibly work in full-duplex mode. By deploying layer 1 repeaters on the public transportation, the penetration loss through walls and windows can be overcome. Also, though a layer 1 repeater, the UEs can reduce their transmit power and extend battery life.

However, a major disadvantage of layer 1 repeater is that not only the desired signal is amplified and forwarded, but also unwanted interference such as inter-cell interference and noise. Thus layer 1 repeaters can not improve the SINR and have to be deployed at positions with advantageous SINR gain.

2.5.1.3   LTE backhaul plus on-board Wi-Fi access

Since most smart phones and laptops support WiFi technology, the idea of using WiFi to provide Internet access to vehicular UEs is straightforward. Several railway companies (i.e. Virgin, Bahn) have already provided this kind of on-board service. The wireless node can be placed on the roof of a public transportation vehicle and connect as an LTE UE to the eNB through the backhaul link, while providing Internet access to vehicular UEs with WiFi Access Points. Penetration loss can thus

be eliminated. An optimized outdoor antenna (e.g. a smart antenna mounted on the train roof) can also be envisaged to enhance the performance of the backhaul link. Moreover, all UEs on board can use this wireless node for data connections or VoIP calls, while continuing to use the existing 2G RAT (Radio Access Technologies) for voice. This solution can be built with currently available technology and requires no changes to specifications, so it is likely to be less complex and to cost less than a mobile relay. Furthermore, this solution enables Wi-Fi-only devices to use the LTE network as backhaul for their data connections, which may bring extra income.

However, it's still difficult to offer a seamless experience to vehicular UEs by WiFi technology. For instance, WiFi technology can not guarantee the QoS of the WiFi access. In the WiFi standard 802.11e, Quality of Service enhancements for wireless LAN applications are defined, but it requires that all the APs are controlled by the same central unit [30]. Also, the WiFi technology is affordable for everyone in the open ISM (Industrial-Science-Medical) frequency band, the interference in these radio bands can not be coordinated as the dedicated frequency bands owned by cellular operators. Besides, the security of WiFi network is a big concern [31]. WiFi was excluded by the partners. Hence, we do not consider them in the thesis.

2.5.2 A brief state of the art of fixed relay

Realizing the limitations of the above existing solutions, the 3GPP has launched the study on mobile relay in [19]. The 3GPP study mainly focuses on the high speed train scenario under the context of the worldwide deployment of high speed railway. As a fast, reliable, comfortable, green mode of transportation, high speed trains have been built or under construction in many countries currently [15]. High speed train scenario is characterized as follows: the trains operated with high speed, e.g. 350 km/h, the trains move along a known trajectory, and high penetration loss of the radio signal through the well shield carriages. However, as a promising solution, deploying mobile relay is not limited to the high speed train scenario, but can also be used to improve the user experience in other public transportations, such as buses, trams.

According to the mobility behavior of Relay Node, relays can be characterized into two categories: fixed relays and mobile relays. To increase coverage and enhance capacity, fixed relay are proposed and studied before mobile relay. Extensive works have been done various aspects of fixed relay network, including downlink performance [32], uplink performance [33], coverage [34], codes design [35], resource

allocation [36, 37, 38, 39], optimal relay placement [27], mobile association [40]. However, the studies on fixed relay can not be directly applied into the mobile relay scenario. First of all, fixed relay can not compensate the signal loss caused by penetration loss, which is a major concern for vehicular UEs. Besides, the doppler effect might occur in fast moving environments. Second, what's the impact of deploying mobile relay in LTE network is unknown. For instance, how to guarantee the fair scheduling between UEs and mobile relays. Furthermore, RN mobility is not considered in fixed relay network, group mobility is thus not supported. To support group mobility, existing architecture or protocols need to be further designed or optimized.

Chapter 3

Mobility Optimization for mobile relays in LTE networks

3.1 Introduction

In this chapter, we focus on the mobility management aspects of deploying mobile relays in the network. The mobility procedures comprise cell selection, cell reselection and paging in RRC_IDLE state and handover in RRC_CONNECTED state. When people are moving within a vehicle simultaneously, there is a lot of signaling that are exchanged between the UEs within the same vehicle and the core network. Such a large amount of signaling would improve the system signaling cost, result in channel congestion and reduce handover successful rate. Thus optimized mobility management schemes for vehicular UEs are needed.

In the following sections, we first give a state of the art about mobility management study of mobile relays. Then we study different signaling procedures when the relay is embedded in a public transport vehicle and when the architecture for fixed relays is kept. We first describe the main procedures with a fixed relay node. Then we propose the concept of global tunnel and analyze the processing cost on different network nodes in different modes.

3.2 State of the Art

In 3GPP release 10, an architecture based on proxy S1/X2 was selected as the baseline architecture to support a fixed relay node. But the mobility of relay node is not considered and supported [6]. When RN mobility is considered, several han-

dovers are made at the same time if there is no enhancement of the procedures. Due to the mobility of mobile relay, further enhancements or new procedures may be required in order to support all existing network functionalities. Some studies have been done on two aspects: architecture [17, 41] and handover optimization [42, 43, 44, 45, 46, 47, 48].

In [17], the authors presented an optimized architecture for mobile relay. The initial GW (Gateway) architecture where the SGW/PGW of mobile relay and relay GW are always located in the initial DeNB and the GW relocation architecture where the relocation of mobile relay's SGW/PGW and relay GW is performed were introduced. The solution was to combine these two architectures, the GW relocation is performed only when necessary, i.e. the mobile relay is far away from the initial DeNB and the routing path is quite long. In [41], the authors compared the pros and cons of two architectures. They concluded that the architecture based on full L3 relay (refer to [7]) has more benefits for mobile relay since the handover procedures is more simplified in this case.

In the previous works related to the handover of mobile relay, the authors in [42] proposed an enhanced handover scheme by using mobile relays to predict the movement of high speed train, which can accelerate the measurement procedure when the path is known in advance. In [43], the authors designed a quick handover scheme for high speed rail. When a mobile relay is approaching to a predefined location, the handover is triggered directly without following the LTE-A specification. In [44], the authors proposed a handover scheme based on the relative velocities between trains and UEs, so that a UE can avoid accessing/connecting to the neighbor mobile relay passing by with high relative velocity in order to reduce ping-pong effect. In [45], the authors proposed an enhanced handover mechanism by extending the IEEE 802.16m specification on relay. In [46, 47], the authors formulated an optimization problem and optimized the handover parameters by minimizing the outage probabilities. In [48], the authors discussed several architecture alternatives for mobile relays and proposed optimized mobile relay handover procedures based on mobility area. Mobility area is a set of eNodeBs. Path switches for vehicular UEs are only performed when mobility area changes. Handover latencies of the procedures are analyzed. However, this proposal requires extra planning effort on the operator side and some upgrades of the standard 3GPP based protocols.

Most of related works focused on optimizing the handover procedure of mobile relay node deployed on high speed trains and required some upgrades or modifications of the standard 3GPP based protocols. Until now, no specification is defined for

relay node mobility. Several proposals are studied by 3GPP in [19]. Some consider restrictive assumptions (SGW collocated with eNodeB).

3.3 Main signaling procedures with a fixed relay node

3.3.1 Methodology of the study

In this section and the following ones, we conduct our study based on the flow chart in Figure 3.1. First we consider a typical scenario and describe the signaling procedures with a fixed relay in this scenario. We consider the following scenarios: a user goes under the coverage of a relay, then connects his/her terminal through the relay to the network, uses his/her terminal (data exchange) and finally leaves the relay coverage. We assume the relay is already attached to the eNodeB (see section 2.4.4 for more details on the attachment). Next we compute the processing cost in different scenarios. The processing cost is defined as the number of requests received and processed by an entity per unit time. We give an example in Figure 3.2. In Figure 3.2 and following ones, we show the number of messages processed by each network entity, which is denoted by M_y^x for procedure y (e.g. $y = \text{TAU}$) and entity x (e.g. $x = \text{MME}$). This is used latter for the analytical evaluation. Then we compute the total processing cost in different modes (direct mode and relay modes) in section 3.5.

3.3.2 Principles of the relay architecture

Here we recall the architecture "Proxy S1/X2" that is defined for fixed relay node, as shown in Figure 3.3. The basic idea is to add "home eNB GW" functions into the DeNB in order to provide the SGW/PGW-like functions needed for RN (Relay Node). The DeNB appears as a MME (for S1), an eNB (for X2) and a SGW to the relay node. Both U-plane and C-plane of the S1 interface is terminated at the RN. There is only one radio connection between each RN and the DeNB, but there are as many connections as the number of UEs between the DeNB and the MME(UE), and between the DeNB and SGW(UE), as shown in Figure 3.4.

37
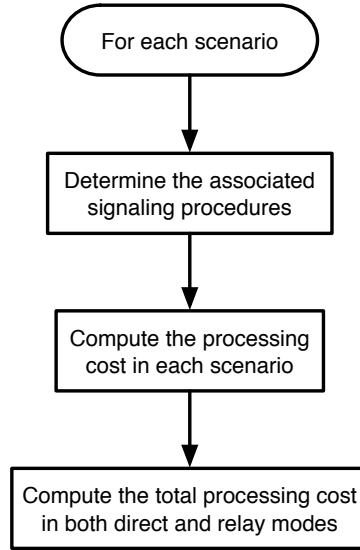
Figure 3.1: The flow chart for the study
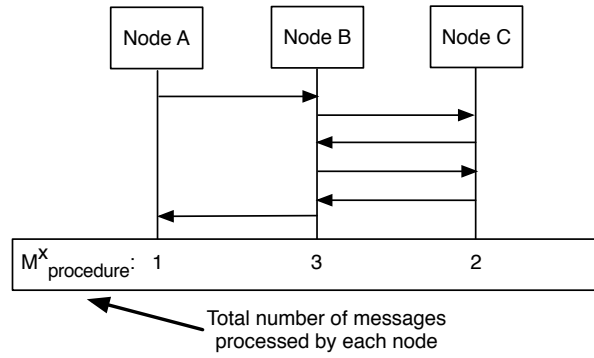
Figure 3.2: An example for the processing cost
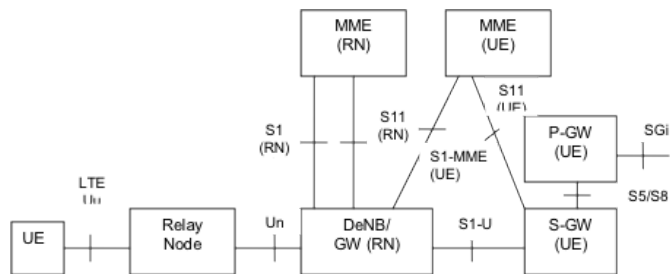
Figure 3.3: Relay Architecture (source [6])

38
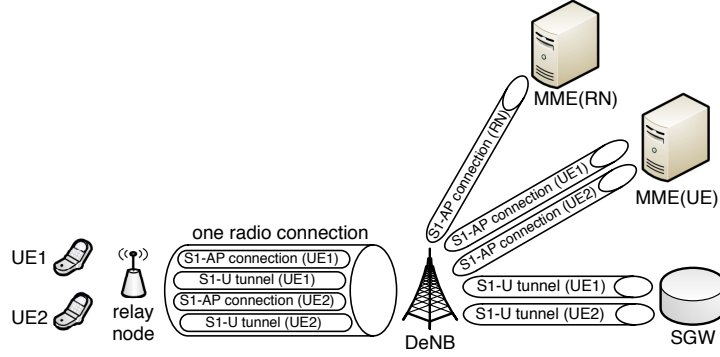
Figure 3.4: Tunnels and connections with fixed relays

3.3.3 Arrival of an inactive UE in the coverage of a relay

We consider a UE in IDLE state when no NAS signaling connection between UE and network exists. In IDLE state, the location of the UE is only known by the network at the Tracking Area List (TAL) level. In this state, the UE can receive broadcast or multicast data, it will monitor a paging channel in order to detect incoming calls, perform neighbor cell measurements and cell selection as well as re-selection also. When an inactive UE arrives in the coverage of a relay, depending on whether the relay node has a specific TAI (Tracking Area Identity) or not, the UE may trigger a tracking area update.

3.3.3.1 The relay node has the same TAI as the DeNB

If the same TAI is allocated to the relay and to the DeNB, then the UE does not send any signaling when it enters the area covered by the relay. In this case, the network is not aware that the UE moves into the coverage of a relay. A UE in IDLE state is restricted to periodic paging reception and serving cell monitoring. On receipt of a paging message, the UE performs a service request procedure and moves into CONNECTED state.

3.3.3.2 The relay node has a different TAI from the DeNB

When a UE moves to the coverage of a relay, it detects that it has entered a new TA that is not in the list of TAIs. The Tracking Area Update (TAU) procedure is thus initiated by the UE. The TAU procedure is shown in Figure 3.5.
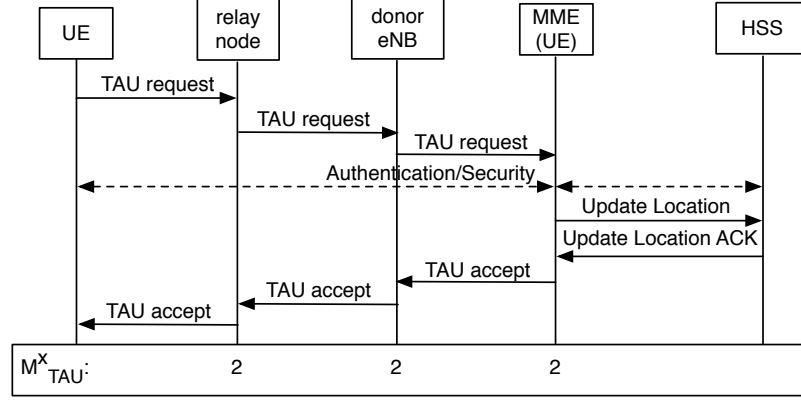
Figure 3.5: Tracking Area Update Procedure (In this figure and all the next ones, index x is used for a node. In this figure for instance, $M_{\text{TAU}}^{\text{RN}} = 2, M_{\text{TAU}}^{\text{DeNB}} = 2, M_{\text{TAU}}^{\text{MME}} = 2$)

3.3.4 Arrival of an active UE in the coverage of a relay

We consider a UE in CONNECTED state when the UE is actively communicating with the network by transmitting and receiving user data. In this state, the location of UE is known at the cell level. When an active UE arrives in the coverage of a relay, the handover between the serving eNB and the relay node is triggered. Depending on whether the relay node has a specific TAI or not, the UE may trigger a tracking area update. Assume that the UE is served by an eNB and goes in the coverage of a relay node managed also by this eNB.

3.3.4.1 The relay node has the same TAI as the DeNB

When the relay node has the same TAI as the DeNB, the handover without TAU is triggered, as shown in Figure 3.6. In the handover preparation phase, the DeNB establishes the proxy relationship with the relay node. In the handover completion phase, the relay node sends a PATH SWITCH REQUEST message to MME (UE) to inform that the UE has changed cell. A new GTP tunnel is established between the SGW (UE) and the DeNB. The DeNB is explicitly aware of a UE attached to the RN due to the S1 proxy and X2 proxy functionality. In the case when the source eNB is not the DeNB, similar procedures are performed except the DeNB forwards the messages between the relay node and the source eNB.
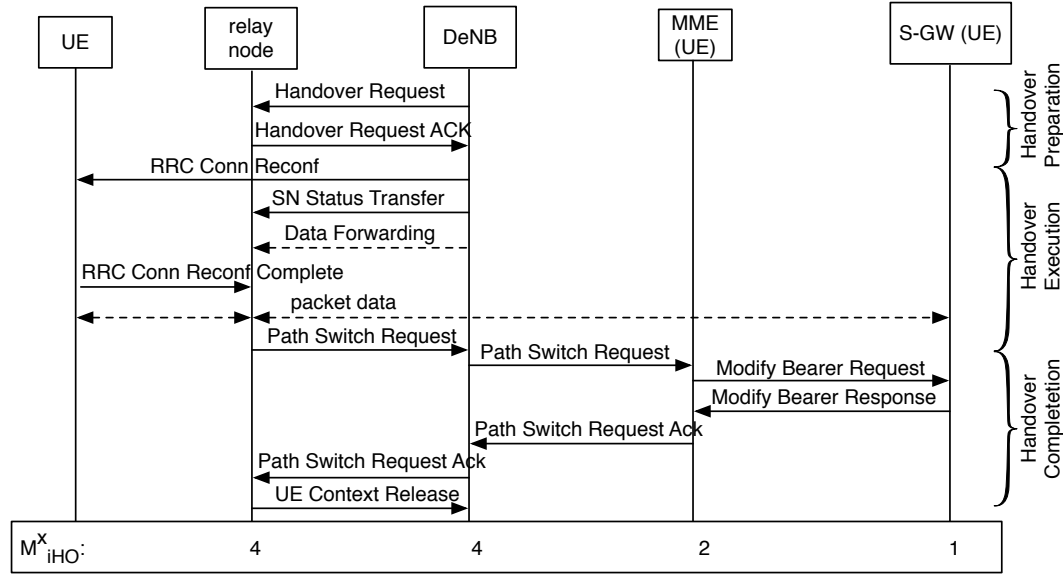
Figure 3.6: X2-Handover from the serving eNB to relay node without TAU

3.3.4.2   The relay node has a different TAI from the DeNB

When the relay node has a different TAI from the DeNB, the handover with TAU is performed, as shown in Figure 3.7. Since the relay node has a different TAI from the DeNB, after handover, TAU procedure is performed so that the MME (UE) is aware that the UE is served by a relay node.

3.3.5   Switch from CONNECTED state to IDLE state

A UE can be either in CONNECTED state or in IDLE state. If a UE does not transmit or receive any data for a while, the eNB releases the RRC (Radio Resource Control) connection and asks the MME to release the S1 tunnel and the S1-AP connection. That event is triggered by the eNB, which manages a RRC inactivity timer. The UE then switches from CONNECTED state to IDLE state, as shown in Figure 3.8. Typically, the RRC inactivity timer is in the range of a few seconds to a few tens of seconds.

3.3.6   UE triggered Service Request procedure

When there is uplink data to be sent from a UE in IDLE state to the network, the UE performs Service Request procedure illustrated in Figure 3.9. An connection is
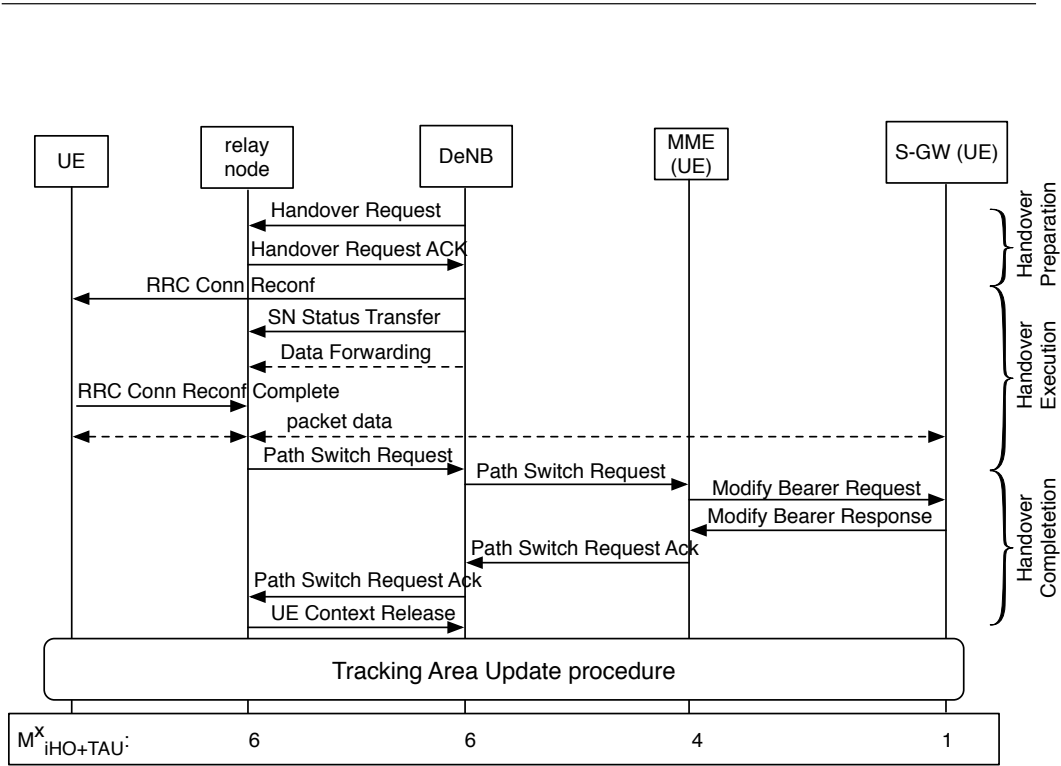
Figure 3.7: X2-Handover from the serving eNB to relay node with TAU
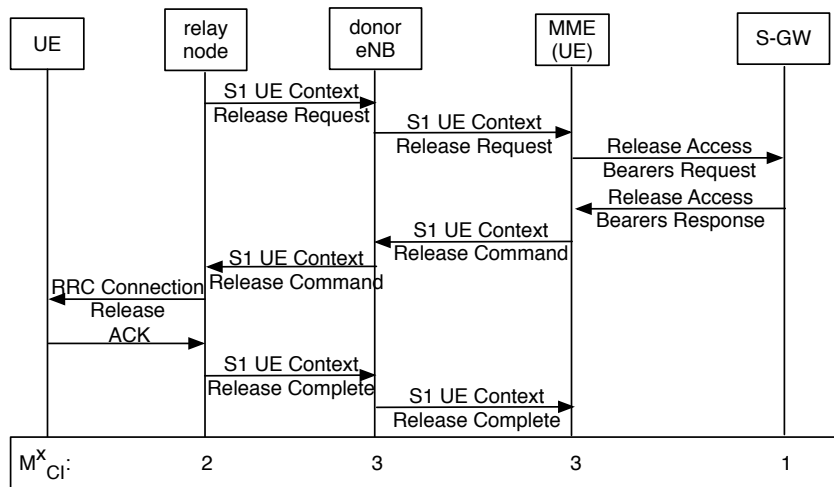
Figure 3.8: Switch from CONNECTED state to IDLE state (CI)

setup in the control plane and user plane, allowing the UE to receive and send data traffic.
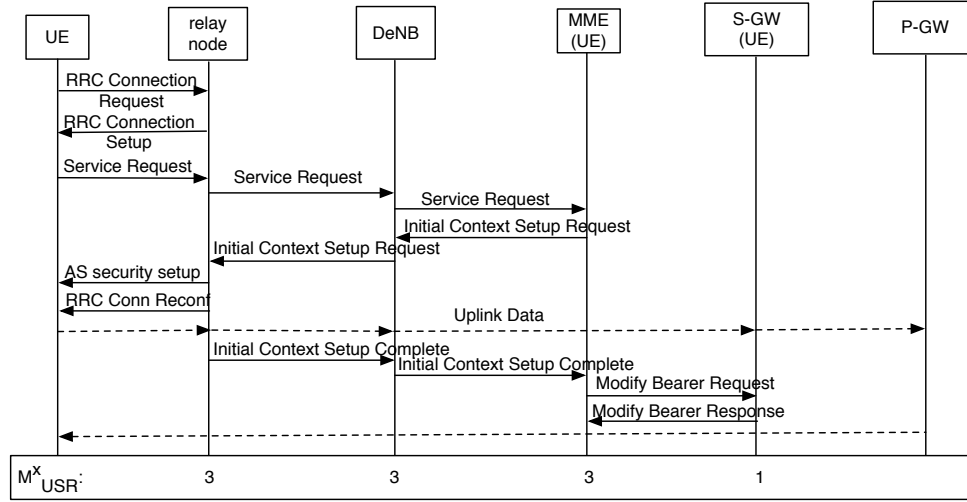
Figure 3.9: UE triggered Service Request procedure (USR)

3.3.7 Network triggered Service Request procedure

When the network has downlink traffic to deliver to a UE in IDLE state, the Network triggered Service Request procedure is performed, as shown in Figure 3.10. First the SGW buffers the downlink data and identifies which MME is serving the UE, then the SGW informs the MME to trigger the paging procedure in order to find and activate the UE. If the relay node has a same TAI as the DeNB, the UE is paged in all eNBs belonging to the TAL (Tracking Area List). If the relay node has a specific TAI, the paging message is only sent to the relay node. Once the UE is located, it triggers the Service Request procedure described above.

3.3.8 Departure of an inactive UE from a relay node

When an inactive UE leaves the coverage of a relay, depending on whether the relay node has a specific TAI (Tracking Area Identity), the UE may trigger a tracking area update.
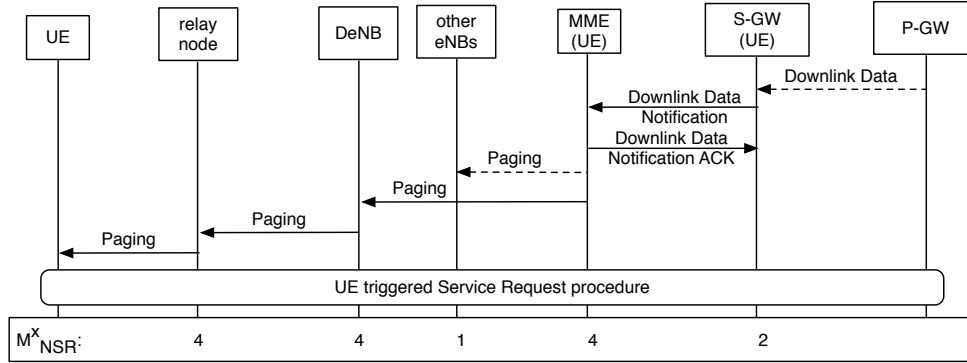
Figure 3.10: Network triggered Service Request procedure (NSR)

3.3.8.1 Relay node has a same TAI with the DeNB

When the relay node has a same TAI with the DeNB, the network is not aware that the UE leaves the coverage of a relay.

3.3.8.2 Relay node has a different TAI with the DeNB

When the UE leaves the coverage of a relay, it detects that it has entered a new TA. The Tracking Area Update (TAU) procedure is thus initiated, the procedure is basically the same the procedure described in Figure 3.5, except the UE now directly exchanges the messages with the eNB.

3.3.9 Departure of an active UE from a relay node

When an active UE leaves the coverage of a relay, the handover from relay node to the eNB is performed. Depending on whether the relay node has a specific TAI, the UE may trigger a tracking area update. Assume the target eNB is the donor eNB of relay node.

3.3.9.1 Relay node has a same TAI with the DeNB

When the relay node has a same TAI with the DeNB, the handover is performed as shown in Figure 3.11. In the case when the target eNB is not the DeNB, the DeNB forwards the signaling messages between the relay node and the target eNB.
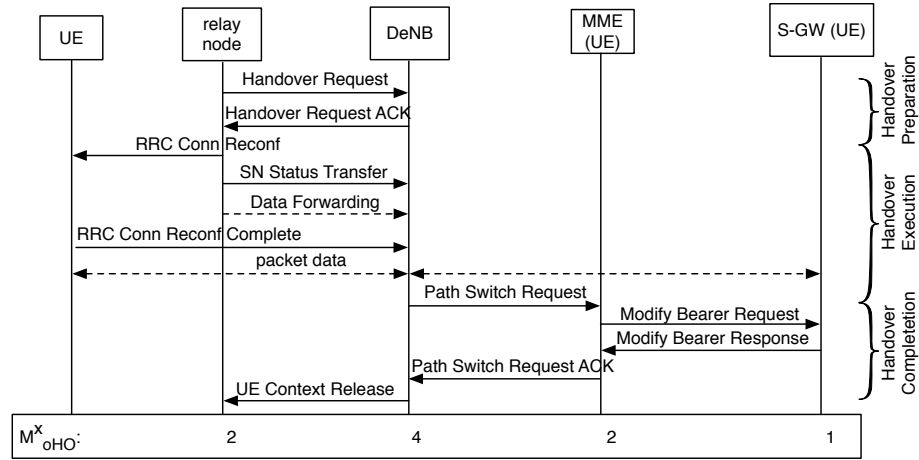
Figure 3.11: Handover from RN to eNB without TAU

3.3.9.2 Relay node has a different TAI with the DeNB

When the relay node has a different TAI with the DeNB, the Tracking Area Update (TAU) procedure is triggered between the target eNB and the MME (UE) after the handover procedures, as shown in Figure 3.12.
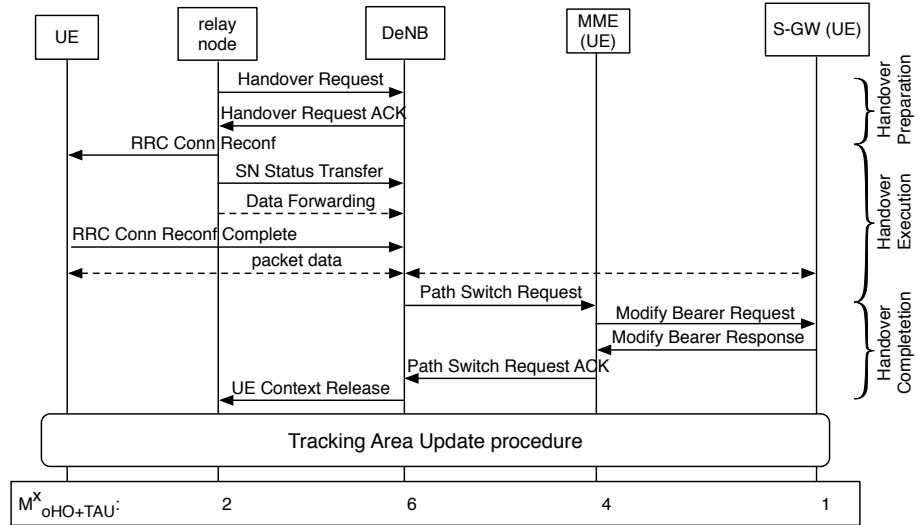
Figure 3.12: Handover from RN to eNB with TAU

3.4 Global Tunnel

In this section, we first give a brief introduction on GTP-U protocol, then we propose the concept of global tunnel, next we explain how it can be used for mobile relays. We introduce two options: X2 global tunnel and S1 global tunnel.

3.4.1 Reminder of GTP-U protocol

The GTP-U header is a variable length header whose minimum length is 8 bytes. The outline of the GTP-U header is shown in Figure 3.13. As we can see, there is a field named Extension Header Flag (E). This flag indicates the presence of a meaningful value of the Next Extension Header field. When it is set to '1', the Next Extension Header field is present and shall be interpreted. The field of Next Extension Header Type defines the type of Extension Header that follows this field in the GTP-PDU. The general format of the GTP-U Extension Header is shown in Figure 3.14. The Extension Header Length field specifies the length of the particular Extension header in 4 bytes unit. The length of the Extension header shall be defined in a variable length of 4 bytes, i.e. $m + 1 = n * 4\ bytes$, where n is a positive integer.
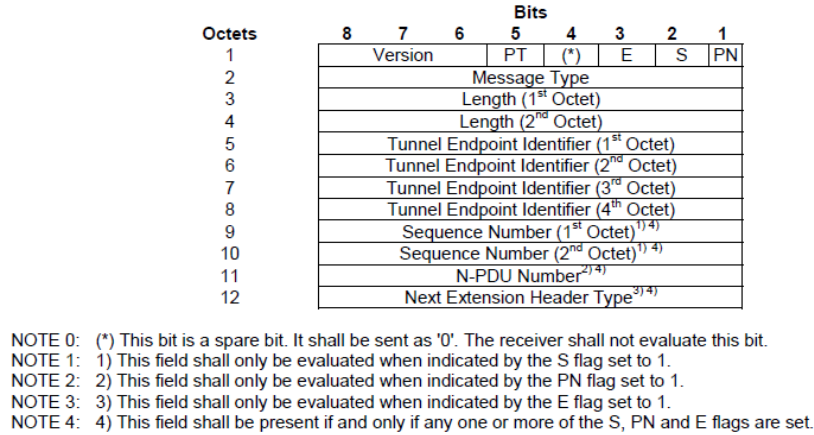
Figure 3.13: The outline of the GTP-U header
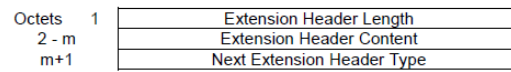
Figure 3.14: The outline of the GTP-U Extension Header

Bits 7 and 8 of the Next Extension Header Type define how the recipient shall

handle unknown Extension Types. The meaning of bits 7 and 8 of the Next Extension Header Type is shown in Figure 3.15. And the definition of Extension Header Type is shown in Figure 3.16.

Bits		Meaning
8	7	
0	0	Comprehension of this extension header is not required. An Intermediate Node shall forward it to any Receiver Endpoint
0	1	Comprehension of this extension header is not required. An Intermediate Node shall discard the Extension Header Content and not forward it to any Receiver Endpoint. Other extension headers shall be treated independently of this extension header.
1	0	Comprehension of this extension header is required by the Endpoint Receiver but not by an Intermediate Node. An Intermediate Node shall forward the whole field to the Endpoint Receiver.
1	1	Comprehension of this header type is required by recipient (either Endpoint Receiver or Intermediate Node)

Figure 3.15: Definition of bits 7 and 8 of the Extension Header Type

Next Extension Header Field Value	Type of Extension Header
0000 0000	No more extension headers
0000 0001	Reserved - Control Plane only.
0000 0010	Reserved - Control Plane only.
0010 0000	Service Class Indicator
0100 0000	UDP Port. Provides the UDP Source Port of the triggering message.
1000 0001	RAN Container
1100 0000	PDCP PDU Number [4]-[5].
1100 0001	Reserved - Control Plane only.
1100 0010	Reserved - Control Plane only.

Figure 3.16: Definition of Extension Header Type

3.4.2 Implementation of Global Tunnel

The scenario we consider is the deployment of mobile relay on buses. The UEs inside the bus are served by the mobile relay mounted on the bus. With the movement of the bus, some users get on the bus while some other users get off the bus. There is one radio connection between the mobile relay and DeNB but as many tunnels as the number of vehicular UEs between the DeNB and the SGW (UE). It's possible that different vehicular UEs have different SGW.

In order to reduce the number of signaling messages in mobile relay scenario, we propose the concept of global tunnel. The idea is to gather several tunnels in the same global tunnel and use this global tunnel to transmit the data traffic for vehicular UEs served by the same mobile relay. The global tunnel uses the GTP-U protocol. According to the specification [49], the GTP-U header includes an extension field named Extension Header Flag (E). We propose to use this option to transport a second TEID in the extension header that identifies the tunnel that is specific to

a UE. The TEID that is in the standard header identifies the global tunnel. The extended GTP-U header is shown in Figure A.1. Note that intermediate nodes do not need to be modified to transport global tunnels.
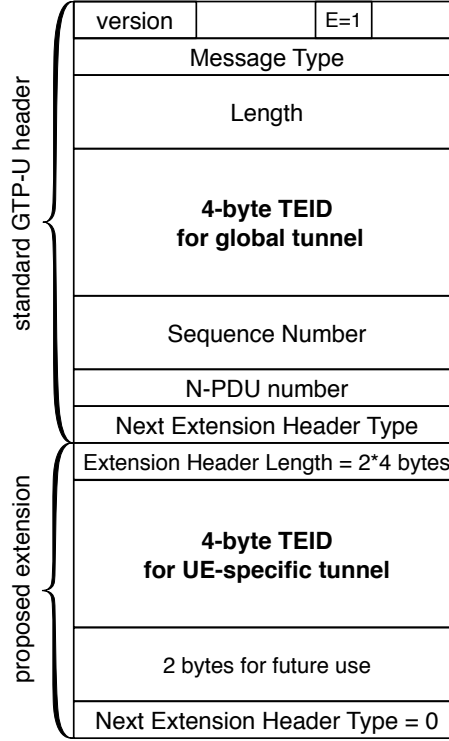
Figure 3.17: Extended GTP-U header

Implementing global tunnel would increase the cost on the user plane, it brings extra 8 bytes for each GTP-U header. But considering the data packet can be often as large as 1500 bytes, the ratio of the extra cost in a packet is very small, it can be seen to be negligible.

3.4.3 Global X2 Tunnel

During the handover of mobile relay, we propose to set up a global tunnel between the source DeNB and the target DeNB for the data forwarding of vehicular UEs, as shown in Figure 3.18. All vehicular UEs that are connected to the mobile relay before the handover have their data transmitted on the following path: mobile relay-target DeNB-source DeNB-SGW (UE). But for UEs that connects through the mobile relay after the handover, a direct path is established between the target DeNB and SGW(UE). For a given UE, its mobility anchor is the serving DeNB when

it attaches to the mobile relay. Global X2 tunnel is kept as long as it's necessary. It is released as soon as all UEs that use it leave the bus.
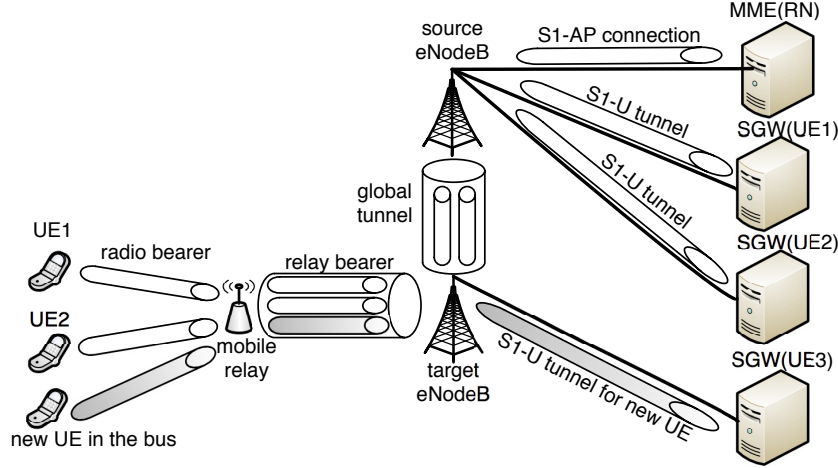
Figure 3.18: The global X2 tunnel during the handover of mobile relay

With the global X2 tunnel, mobile relay handover procedure is shown in Figure 3.19. Handover preparation and execution phases are basically the same as specified in [19], except the source DeNB includes the global tunnel information within the Handover Request message. The target DeNB establishes the global tunnel and includes the information within the Handover Request Acknowledge message to indicate that it accepts the proposed forwarding of downlink data for this bearer. The global tunnel between source DeNB and target DeNB is established in handover preparation phase. Forwarding is used for both uplink and downlink as opposed to standard procedure.

In the handover completion phase, path switch is triggered by the target DeNB. The target DeNB sends the Path Switch Request message to the MME (RN) to inform it that new tunnels and connections for vehicular UEs should be set through the target DeNB. Data on all existing connections are routed through the X2 interfaces. When all UEs have left the bus, a Context Release message is then sent to the source DeNB by the target DeNB. The source DeNB releases data and control plane related resources.

3.4.4 Global S1 Tunnel

Instead of having as many S1-U tunnels as the number of vehicular UEs between the DeNB and the SGW (UE), a global S1 tunnel can be established between the
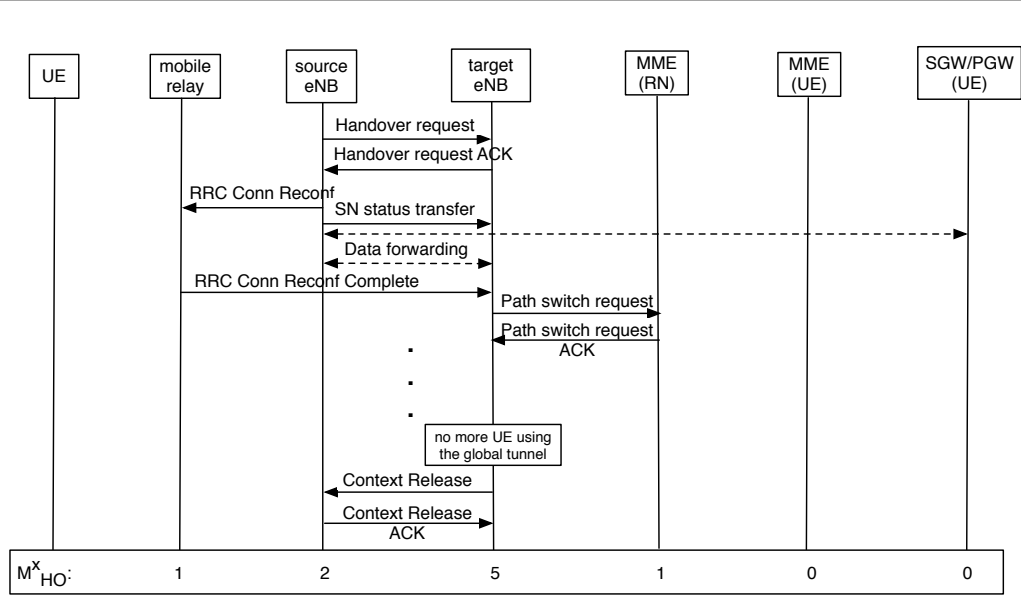
Figure 3.19: Mobile relay handover procedure based on global X2 tunnel (HO)

DeNB and the SGW (UE), illustrated in Figure 3.20.
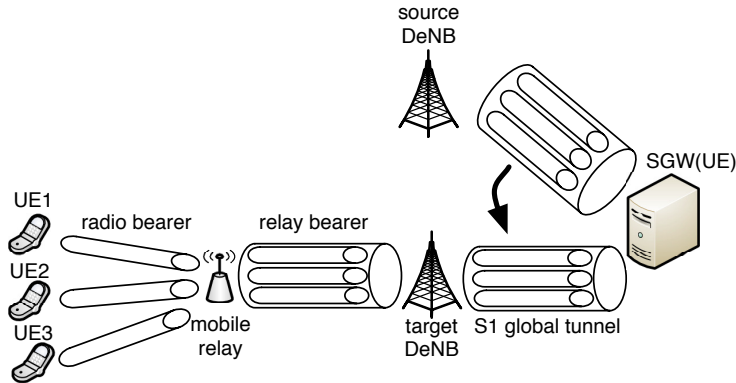
Figure 3.20: The global S1 tunnel during the handover of mobile relay

Mobile relay handover procedure based on global S1 tunnel is shown in Figure 3.21, which is basically the same as the standard handover procedure. Assume that mobile relay and vehicular UEs are served by the same MME. In the handover completion phase, the target DeNB sends a Path Switch Request message to the MME (RN&UE) to inform that the mobile relay has changed the cell, the global tunnel information are included in this message. After receiving this message, the MME (RN&UE) informs the SGW (UE) to switch the downlink data path. Then the MME confirms the target DeNB with the Path Switch Request Acknowledge

50

message. The global S1 tunnel is thus established between the target DeNB and the SGW (UE) in this phrase.
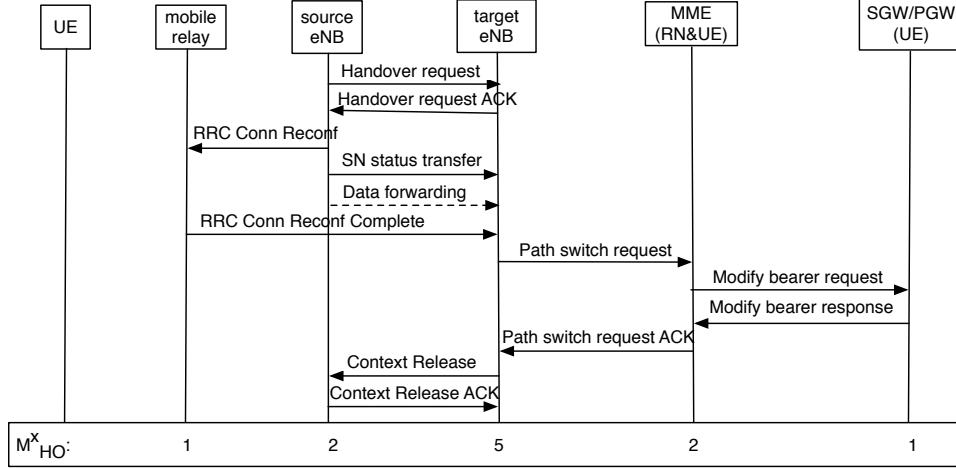
Figure 3.21: Mobile relay handover procedure based on global S1 tunnel (HO)

3.4.5 Discussions on the RRC inactivity timer

The interactivity of applications in smart phones generates frequent switching of UEs between IDLE and CONNECTED states in the standard case. A lot of signaling messages (i.e. service request procedures and resource release procedure) are thus exchanged between the network entities (DeNB, MME, SGW). In mobile relay scenario the mobility of users is constrained by the public transport (buses in our case): when a UE is connected to a RN, this is valid for typically ten minutes or more. Based on this characteristic, when a vehicular UE is inactive, it's interesting to keep its S1 tunnels active in order to have a very fast Service Request procedure, so that the related signaling messages can be reduced. This is possible if the network is aware of the location of the vehicular UE, or in other words, if a specific TAI is defined for each mobile relay.

Therefore, we propose to keep the RRC inactivity timer on the radio interface in order to spare radio resource, but to deactivate it for the tunnels between the RN and the DeNB, and between the DeNB and both the MME and the SGW. Note that this requires maintaining the RRC connection between the RN and the DeNB. If there is absolutely no traffic in the bus, some "keep alive" messages should be transmitted by the RN. However, if there are some vehicular UEs, the probability

of such an event is low. Defining a specific TAI for a mobile relay is thus very interesting.

3.4.6 S1-AP control connections

In the control plane, the S1-AP messages are sent between the relay node and the DeNB, and between the DeNB and the MME (UE). There is a S1-AP proxy mechanism at the DeNB, so each vehicular UE has two pairs of S1AP IDs, as shown in Figure 3.22. The pair of S1AP IDs between the RN and the DeNB are defined as RN vUE S1UnAP ID and DeNB vUE S1UnAP ID. The pair of S1AP IDs between the DeNB and the MME (UE) are defined as DeNB vUE S1AP ID and MME vUE S1AP ID. The relay node is seen as an ordinary UE by the DeNB, its S1AP IDs between the DeNB and MME (RN) are defined as eNB RN S1AP ID and MME RN S1AP ID. To maintain the mapping relationship during the handover of relay node, we need to specify the handover procedures.
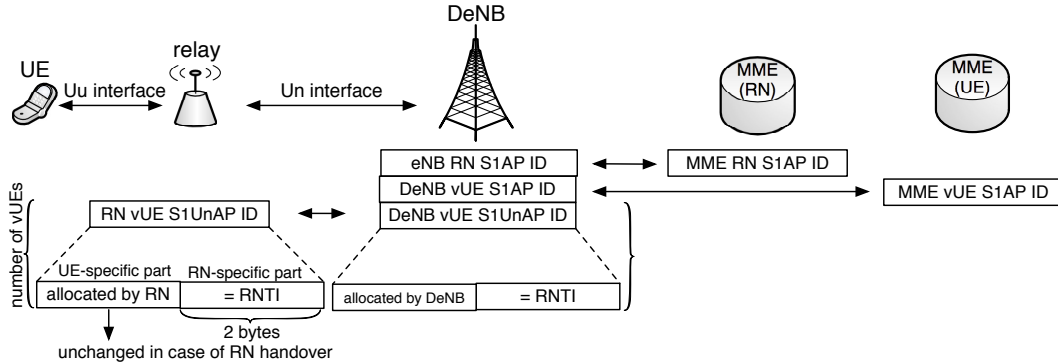
Figure 3.22: The S1-AP mapping relationship

When the handover of relay node happens, the source DeNB sends the Handover Request message to the target DeNB. The relay node is considered as an ordinary UE from the view of DeNB, so MME RN S1AP ID is included in this message as the normal handover procedure. Besides the S1AP ID of relay node, the list of S1AP IDs of vehicular UEs are also included in the message, in order to help the target DeNB execute admission control and establish the mapping relationship. Vehicular UEs are handover with the relay node, RN vUE S1AP-Un IDs at the relay side are unchanged, so we keep the pair of S1AP IDs between the RN and the DeNB unchanged, which means RN vUE S1UnAP ID and DeNB vUE S1UnAP ID are sent to the target DeNB through the Handover Request message. If no further

enhancement is proposed, the size of a pair of RN vUE S1UnAP ID and DeNB vUE S1UnAP ID is 7 bytes.

Here we propose a concept of global S1AP ID, which complies with the concept of global tunnel. Considering one DeNB can serve several mobile relays simultaneously, for a certain vehicular UE, we split its pair of S1UnAP ID between the RN and the DeNB into relay-specific part (e.g. 2 bytes) and UE-specific part (e.g. 1-2 bytes). Relay-specific part is filled with the RNTI of relay node, while UE-specific part is filled with a counted number. In the Handover Request message, all vehicular UEs under the same relay node have the same relay-specific part of S1AP ID, besides this relay-specific ID, we only need to include the UE-specific part of S1AP IDs, which could save some packet sizes. Also, the list of MME vUE S1AP ID allocated by the MME (UE) should be included in the Handover Request message, no need to include DeNB vUE S1AP ID allocated by the source DeNB, leave the target DeNB allocate its own DeNB vUE S1AP ID.

When the target DeNB receives the Handover Request message, by using the included S1AP IDs, the target DeNB builds the same mapping table between the RN and the MME as the mapping table at the source DeNB. The target DeNB allocates new DeNB vUE S1AP ID and establishes the mapping between the DeNB and the MME (UE). Until now, the MME (relay) and the MME (UE) are not aware of the handover.

Then the target DeNB sends the Path Switch Request message to the MME (RN) to inform it that the relay has changed the cell. The E-RAB field in the message are left blank or a pre-defined value, so that when the MME (RN) receives the message, it would not send any modify bearer request but record the target eNB now is the the donor eNB, and reply with a Path Switch Response message. When a Path Switch Response message from the MME (RN) is received at the target DeNB, the target DeNB sends a grouped Path Switch message to the MME (UE), inform it that the UE has changed the cell. The list of new DeNB vUE S1AP IDs are grouped and included in the message. The optimized procedure of relay handover is shown in Figure 3.23.

3.5 Processing Cost Evaluation

In this section, we provide a simple analysis based on the computation of the average processing cost of signaling messages. We consider a hexagonal network with cell radius R and all cells in the same tracking area. There are on average $\overline{n}_v$ users in a
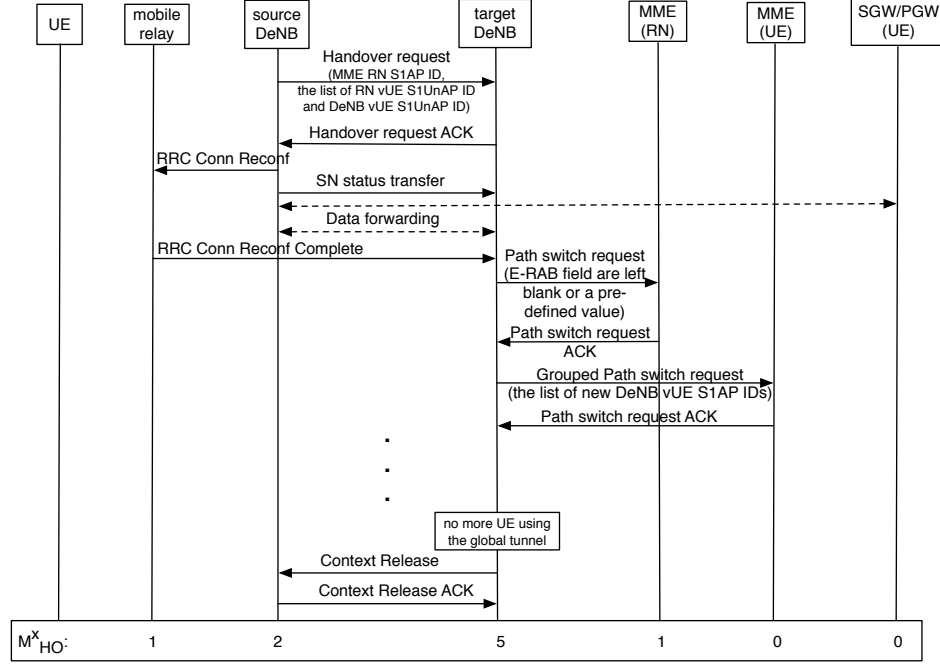
Figure 3.23: The optimized relay node handover procedures based on global X2 tunnel

bus. Users get in the bus and stay in it for $\overline{T}_D$ on average. They use applications that generate sporadic traffic. Hence, the UE switches between ECM_Idle and ECM_Connected states. Let $\overline{T}_C$ and $\overline{T}_I$ be the average duration of CONNECTED and IDLE states respectively. The activity of the application is triggered by the terminal with probability ϱ (and by the network with probability $1 - \varrho$). Assume that all UEs are in IDLE state when they get on the bus. The parameters are listed in the Table 3.1. For more details about the values of parameters, please refer to **Appendix A**.

Table 3.1: Definition and default values for the Parameters

Definition	Variables	Default value
Average number of UEs in a bus	$\overline{n}_v$	10
Average dwell time of a UE in a bus	$\overline{T}_D$	600 s
Probability of UE-triggered service request	ϱ	50%
Average time in ECM_Connected state	$\overline{T}_C$	10 s
Average time in ECM_Idle state	$\overline{T}_I$	80 s
Average speed of a bus	ν	4 m/s
Radius of the hexagonal cell	R	700 m

The probability that the UE is in CONNECTED state is $\varepsilon = \frac{\overline{T}_C}{\overline{T}_I + \overline{T}_C}$. The average

54

number of transitions from CONNECTED state to IDLE state or from IDLE state to CONNECTED state per unit time is $\frac{1}{\overline{T}_I + \overline{T}_C}$. In order to compute the number of messages due to handover events, we use the fluid-flow model [50][51] to obtain the average number of cell change with perimeter length ϑ. Let ν and A be the average speed of a bus and the area of the region respectively. So the average number of cell change $\kappa = \frac{\nu\vartheta}{\pi A} = \frac{4\sqrt{3}}{3\pi}\frac{\nu}{\iota}$ for an hexagonal network. The average number of handover per UE per unit time is $\kappa\varepsilon$, the average number of cell change in IDLE state is $\kappa(1 - \varepsilon)$.

Next we compute the processing cost and compare the total processing cost in direct mode where UEs in a bus directly connect to eNodeB and the processing cost in mobile relay mode. In mobile relay mode, we consider two cases: mobile relay with the same TAI as the DeNB and mobile relay with a specific TAI.

3.5.1   Direct Mode

There is no tracking area update procedure in direct mode, but there are service request procedure, resource release procedure and as many handovers as the number of UEs in CONNECTED state during each cell change. The total number of incoming messages C_{DM}^x processed by entity x per bus per unit time in direct mode is:

$$C_{\mathrm{DM}}^x = \overline{n}_v \big[\frac{\varrho M_{\mathrm{USR}}^x + (1 - \varrho)M_{\mathrm{NSR}}^x + M_{\mathrm{CI}}^x}{\overline{T}_I + \overline{T}_C} + \kappa\varepsilon M_{\mathrm{HO}}^x \big] \tag{3.1}$$

where x is the entity on which the cost is computed (e.g. $x = $ eNB, MME or SGW).

3.5.2   Mobile Relay Mode

3.5.2.1   same TAI (mode R1)

There is no tracking area update procedure in this relay mode, but there are service request procedure, resource release procedure and one grouped handover of relay node during each cell change. The total number of incoming messages C_{R1}^x processed by entity x per bus per unit time in this mode is:

$$C_{\mathrm{R1}}^x = \overline{n}_v \frac{\varrho M_{\mathrm{USR}}^x + (1 - \varrho)M_{\mathrm{NSR}}^x + M_{\mathrm{CI}}^x}{\overline{T}_I + \overline{T}_C} + \kappa M_{\mathrm{HO}}^x \tag{3.2}$$

3.5.2.2 specific TAI (mode R2)

In order to keep the S1 tunnels active and have a very fast Service Request procedure, a specific TAI is defined for mobile relay. So in this case, there are no service request procedure and resource release procedure, but tracking area procedure is triggered when a UE gets in the bus and gets off the bus. The total number of incoming messages C_{R2}^x processed by entity x per bus per unit time in this mode is:

$$C_{R2}^x = \overline{n}_v \frac{2}{\overline{T}_D} M_{TAU}^x + \kappa M_{HO}^x \tag{3.3}$$

3.6 Numerical Results and Analysis

In this section, we compute the processing cost based on real statistics in Rennes, France (the average dwell time of a UE in a bus and the average speed of a bus). The statistics are presented in Table I. We mainly consider the processing cost on the core network side (eNodeB, MME, SGW), as RN operates on radio interface and appears as a UE for DeNB, the processing cost on RN is not included.

3.6.1 Impact of the average number of UEs in a bus

First we evaluate the processing cost against the average number of UEs, as shown in Figure A.3. Different modes (direct mode, mobile relay mode R1 with the same TAI and mobile relay mode R2 with a specific TAI) are presented from left to right in the figure. As the number of UEs in a bus increases, the number of signaling messages also increases in all modes. Mode R1 does not reduce any signaling messages compared with direct mode. This is because the handover is not frequent as the bus moves relatively slowly, the advantage of grouped handover in relay mode is not obvious.

However, in mobile relay mode R2 the number of signaling messages is dramatically reduced about 85% compared with direct mode when there are 20 UEs on average in a bus. This is due to the combination of global tunnels with a specific tracking area and the maintenance of S1 tunnels for inactive vehicular UEs, the signaling messages for service request procedure and resource release procedure are saved.
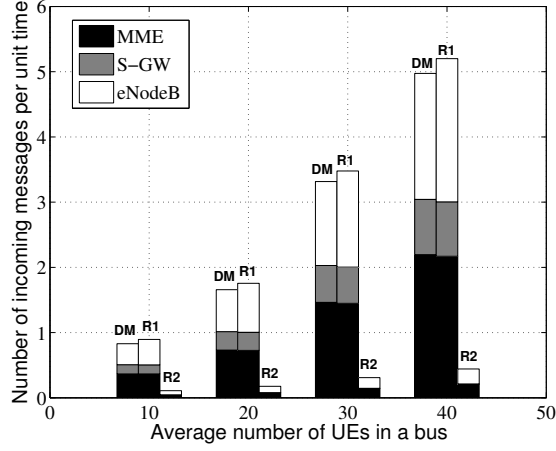
Figure 3.24: Processing cost in terms of the average number of UEs in a bus (DM: Direct Mode, R1: relay mode with the same TAI, R2: relay mode with a specific TAI)

3.6.2 Impact of the average time in ECM_Connected state and ECM_Idle state

Then we study the impact of the average time in ECM_Connected state and ECM_Idle state, as shown in Figure 3.25. We consider different applications, such as web browsing, social networks (i.e. Facebook, twitter). The average time in CONNECTED state is set to $[10, 30, 60]$, the average time in IDLE state is set to $[80, 160]$. The average number of UEs in a bus is set to 10.

As we can see, the number of signaling messages in mobile relay mode R2 is dramatically reduced and is independent of the type of applications. This is because no matter whatever the application behavior is, the S1 tunnels are kept alive between the RN and the DeNB, and between the DeNB and both the MME and the SGW.

3.6.3 Impact of the probability of UE-triggered service request

Then we study the impact of the probability of UE-triggered service request, as shown in Figure 3.26. The probability of UE-triggered service request increases from 10% to 90%.

As we can see, with the increase of the probability of UE-triggered service request, the trend of the number of signaling messages is decreasing. This is because compared with network-triggered service request, UE-triggered service request pro-
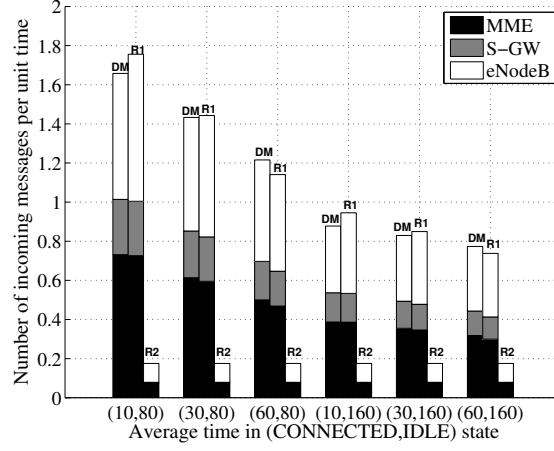
Figure 3.25: Impact of the average time in ECM_Connected state and ECM_Idle state

cedure have less signaling overhead, which can be referred to the discussions in Section 3.3.
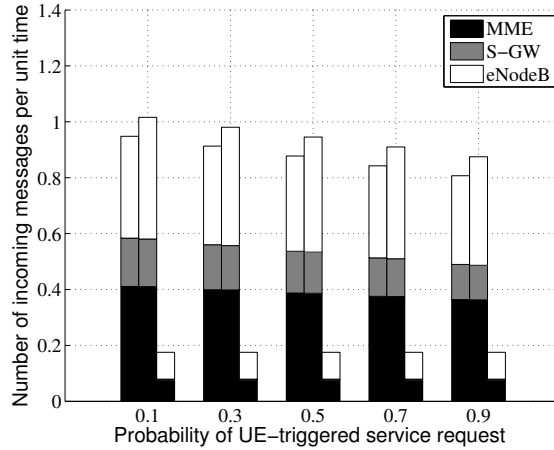
Figure 3.26: Impact of the probability of UE-triggered service request

3.7   Summary

In this chapter, we have studied the mobility aspects of mobile relays. We propose to keep the same protocol stack that was defined for fixed relay, and to extend it to mobile relays. The concept of global tunnels is proposed which is compatible with

the GTP protocol. Without adding any protocol in the stack, it's possible to group several handovers while keeping the possibility of managing the tunnel of each UE individually. It's shown that the number of signaling messages that each network node should process can be dramatically reduced when global tunnels are combined with a specific tracking area and when S1 tunnels are kept alive for inactive vehicular UEs. The solution introduced in this chapter can be easily applied to any transport systems: metros, tramways and trains.

Chapter 4

Impact of the interference on the data rate of a vehicular UE

4.1 Introduction

As previously discussed, relay transmission is a two-step transmission. Both the backhaul link and the access link can have a higher bit rate than the direct link. Does a two-step transmission always achieve better data rate than the direct transmission? To answer this question, in this chapter we study the impact of the interference on the data rate of a vehicular UE and investigate how much data rate gain can be attained through a mobile relay.

We first consider a mobile relay deployed on a bus in a regular hexagonal network and compute the average data rate provided by this mobile relay based on Monte Carlo simulations. All parameters are chosen to be as close as possible to LTE. The analysis is mainly based on an adjusted Shannon formula for LTE [52]. Then considering the limitations of hexagonal networks, we extend our study and present an analytical model in random networks based on the stochastic approach. By applying different parameters into this analytical model, we derive the CDF (Cumulative Distribution Function) of the SINR and the average achievable rate on different links.

4.2 State of the Art

The performance studies on mobile relays can be generally classified into two categories: deploy mobile relay on high speed train [53, 54, 55, 56, 57, 58] and deploy mo-

bile relay on vehicular case, i.e. public buses or trams [46, 59, 60, 61, 62, 63, 64, 65]. Previous studies show that both the QoS of vehicular UEs and the system capacity can be significantly improved with the assistance of mobile relays.

Most of preliminary studies [53, 54, 55, 56, 57, 58, 66] focused on high speed train scenario and showed the capacity and coverage improvement through the deployment of mobile relays. In [53], the author investigated the capacity gain for high speed railway with and without relay assistance based on a simple system model without fast fading. In [55, 56], the authors presented the throughput gain using coordinated and cooperative mobile relays on top of trains. The study in [67] discussed the resource allocation problem for high-speed railway communication. The authors formulated an optimization resource allocation problem and tried to maximize the number of served vehicular UEs. An algorithm based on Hungarian method was proposed. In high-speed environment, the doppler frequency shift has serious effects. The authors in [57, 58] addressed this issue. In [66, 68, 69], it was shown that by using the predictor antennas mounted on top of vehicles, the reliability of the backhaul links can be enhanced.

In previous works related deploying mobile relays on buses, the authors in [59] presented a very simplified system model without shadowing fading and fast fading. The capacity of fixed relay and mobile relay was analyzed based on simulations. It was found that both fixed relay and mobile relay can bring capacity gain to vehicular UEs, but the capacity gain of fixed relay is rather small. In [60], the authors studied the performance of mobile relay assisted transmission and compared with the transmission assisted by fixed relay. For an accurate comparison, the fixed relay position was optimized in terms of outage probability (OP). It's shown that when the penetration loss is moderate to high, mobile relay had a better performance than fixed. Then in [61], the authors continued to study the benefits of mobile relay from an energy efficiency point of view. The impact of the interferences from neighbor eNBs and other mobile relays was not investigated. In [62], the authors considered a two cells system and studied the outage probability of a vehicular user served by mobile relay and compared with optimized fixed relay assisted transmission. But the systems considered in the above mentioned studies [60, 60, 61] were either a noise limited system with one vehicular UE or a system with two-cell and one vehicular UEs, which were quite simple and not realistic. In [65], the authors evaluated different inter-cell interference coordination and multi-antenna interference suppression techniques for mobile relays. In [63], the authors considered a scenario where the WiFi or Bluetooth was used on the access link, and evaluated the performance of

mobile relay under different transmitters and receivers schemes. In [64], the authors did some field trial tests on uplink joint detection for mobile relays and compared the performance of different detections schemes. Most of the related works focused on regular network deployment (i.e., the hexagonal grid model) and evaluated the performance of mobile relay by system-level simulations. However, this approach has its limitations and is not able to accurately capture the spatial irregularity and randomness of a real cellular network with mobile relays.

Recently, stochastic geometry has been widely used as a tractable approach to model and quantify the key metrics (outage probability and rate) in wireless networks [10, 70, 71, 72]. This approach has the advantages of being scalable to multiple layers of base stations and accurate to model location randomness. Additionally, powerful tools from stochastic geometry can be used to derive performance results in closed form. Soon, extensive studies have been on various wireless networks using stochastic geometry approach: cellular networks [10, 73], Device-to-Device (D2D) networks [74], heterogeneous networks [75, 76], vehicular ad hoc networks [77], sensor networks [78], cognitive networks [79].

In the previous related works, the authors in [75] developed a tractable and accurate model for a downlink heterogeneous cellular network consisting of K tiers of randomly located BSs and derived the average rate of the link between UE and the associated BS. In this model the authors considered wired backhaul link which is connected to core network through fiber or cable line. But in relay network, the backhaul link is wireless and usually the bottleneck. In [80], the authors proposed an analytical model to evaluate the energy efficiency of cooperative relay network. Based on the spatial PPP (Poisson Point Process) the distribution of SINRs and mean achievable rates of both non-cooperative users and cooperative users were derived. In [80] cooperative relaying technique was used as a complementary transmission for the UEs close to relay stations. In [81, 82], the authors studied the energy efficiency of a relay-assisted network with the assumption that eNodeB only serves at most one UE or relay at any time. How the bandwidth was shared among users within a cell was not considered. In [83], the energy efficiency of cooperative networks aided by the energy harvest technique was investigated through stochastic analysis. To the best of our knowledge, none of the aforementioned studies used the stochastic geometry approach to investigate the benefits of mobile relays.

4.3 System Model

4.3.1 Propagation Model

The propagation loss can be divided into three parts: outdoor path loss, penetration loss and in-vehicle path loss. Outdoor path loss is modeled by Okumura-Hata formula [84]. The penetration loss between outdoor and in-vehicle is denoted by L, which is set within a certain range. Inside the vehicle it's assumed to be free space propagation. Let y (in km) be the distance from a transmitter to a receiver. Path loss model is summarized in Table 4.1.

Table 4.1: Propagation Loss

outdoor path loss	$L_{outdoor} = 141.78 + 35\log_{10}(y)$
penetration loss	[10, 30] dB
in-vehicle path loss	$L_{in-vehicle} = 98.4 + 20\log_{10}(y)$

Denote the received power as p, the received signal power can thus be written with a general formula as follows:

$$p = rhky^{-\gamma}P \tag{4.1}$$

where r is a factor that takes the fading effect into account, h is a factor that takes shadowing into account, k is a propagation factor, γ is the path loss exponent, and P is the transmitted power. The shadowing effect is modeled by a log-normal random variable H. In other words, $10\log H$ is a Gaussian r.v. with standard deviation σ_s.

Different links suffer different propagation loss (k, γ), as shown in Figure 5.9. The backhaul link mainly suffers outdoor path loss. The direct link mainly suffers outdoor path loss and the penetration loss. We assume free space propagation without shadowing on the access link. The received useful signal on the access link when there is no fading is thus constant and denoted by p_0.

4.3.2 Interference

We consider only co-channel interference. All other interferences (e.g. adjacent frequency) are assumed to be negligible. The co-channel interference is assumed to be equivalent to Additive white Gaussian noise (AWGN). According to the transmission policy of the BS in the access time slot, we consider two relay modes: pure-relay
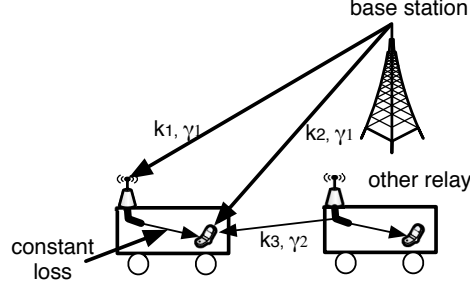
Figure 4.1: Illustration of propagation loss on different links

mode and femto-like mode.

4.3.2.1 Pure-Relay Mode

In the pure-relay mode, BSs stop transmitting to ordinary UEs when mobile relays transmit to vehicular UEs in the access time slot. This mode requires the coordination between BSs. For vehicular UEs, interference only comes from neighbor relays in this mode in the access time slot, shown as dotted line in Figure 4.2.

(a)backhaul link transmission
first phrase

(b)access link transmission
second phrase
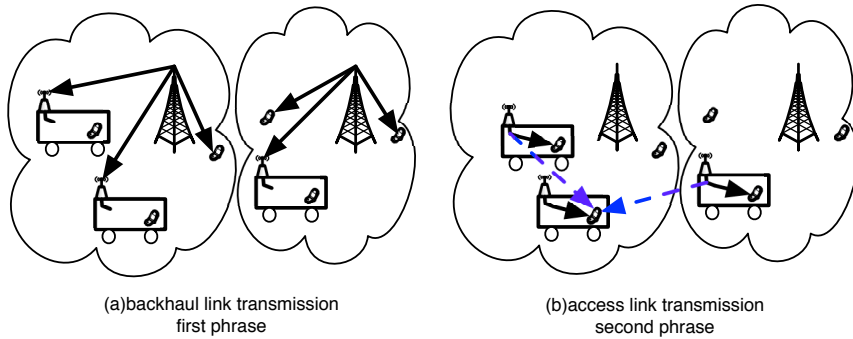
Figure 4.2: Illustration of Pure-relay mode

4.3.2.2 Femto-Like Mode

In the femto-like mode, during the access time slots BSs and mobile relays transmit to ordinary UEs and vehicular UEs respectively at the same time. Like the femtocells that generally use the same frequency band on the access link as macrocell in an OFDMA system, we name this mode femto-like mode [85]. So for vehicular UEs, interference comes from both neighbor relays and all BSs on the access time slot, shown as dotted line in Figure 4.3. The difference of these two modes in the time

domain is shown in Figure 4.4. For a more detailed illustration, please refer to Figure 2.11 and Figure 2.12.

(a)backhaul link transmission
first phrase

(b)access link transmission
second phrase
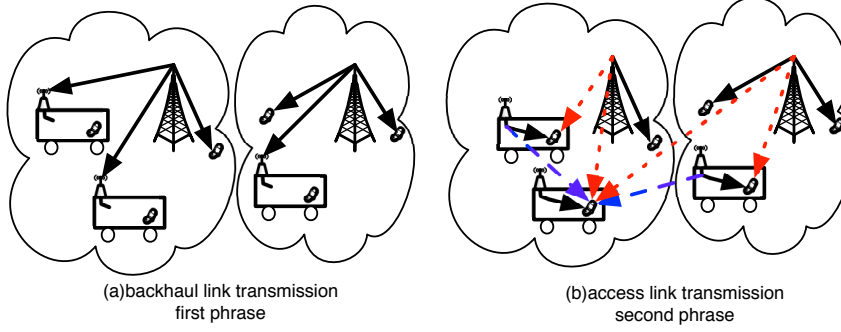
Figure 4.3: Illustration of Femto-like mode
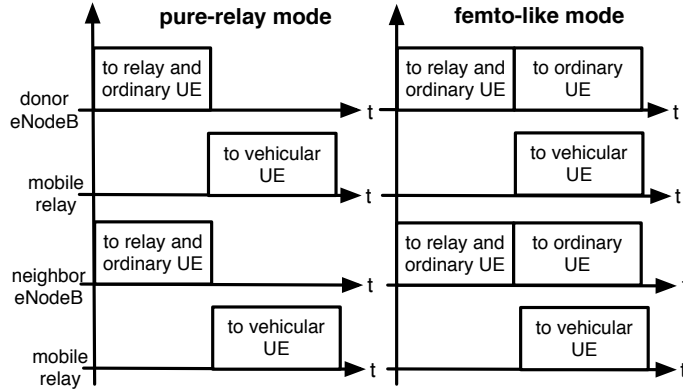
Figure 4.4: Pure-relay mode vs Femto-like mode

4.4 Hexagonal Network

We first consider a regular hexagonal network and focus on the scenario of deploying a mobile relay on a public transportation vehicle (i.e., buses) and compute the data rate gain provided by this mobile relay. The considered scenario is shown in Figure 4.5. The analysis is mainly based on the Shannon formula adjusted for LTE [52], expressed as follows:

$$\mathcal{R} = \mathrm{W} w_{eff} \log(1 + \frac{\mathrm{S}}{s_{eff}}) \tag{4.2}$$
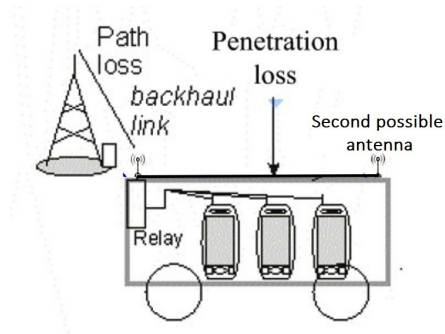
Figure 4.5: Mobile relay deployed on a public transportation vehicle

where $\mathcal{R}$ is the achievable data rate, W is the system bandwidth, S is the SINR (Signal to Interference plus Noise Ratio) on the considered link, w_{eff} is the system bandwidth efficiency of LTE, and s_{eff} is the SINR implementation efficiency of LTE.

4.4.1   Direct Transmission in LTE

We consider a direct mode where the UE connects directly to the eNodeB through the direct link. Considering the fact that the data rate in LTE is limited by the MCS (Modulation Coding Scheme), the maximum transport size is included when calculating the data rate. The data rate in the direct mode is thus given by:

$$\mathcal{R} = \min\{Ww_{eff} \log(1 + \frac{S}{s_{eff}}), \mathcal{R}_{max}\} \qquad (4.3)$$

where $\mathcal{R}_{max}$ is the maximum data rate that LTE could support at a given bandwidth. According to the transport block size table [86], the maximum data rate $\mathcal{R}_{max}$ is 36690 kbit/s when the system bandwidth is 10 MHz.

4.4.2   Relay Transmission in LTE

In the relay case, the backhaul link and the access link are separated in the time domain. The DeNB transmits the data to mobile relay in the first time slot, then mobile relay transmits the data to vehicular UE in the second time slot. We assume time is equally splitted between the first and the second time slot, as shown in Figure 4.6. The maximum data rate $\mathcal{R}_{max}$ should then be divided by two.

In the relay case, we also assume that there is no synchronization between eN-odeBs. When the relay transmits to a UE, the donor eNodeB does not transmit, but other neighbor eNodeBs can still transmit. And the mobile relay is randomly
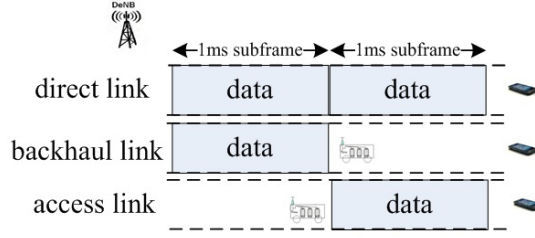
Figure 4.6: Timing relations between the backhaul link and the access link

distributed in the cell, it can be at any location within a cell, the mobility of RN is not especially modeled.

4.4.3 The calculation of SINR

In this section, we compute the SINR in the direct mode and in the relay mode. Fading effect is not considered in this analysis. The values of parameters for each type of link are summarized in Table 4.2.

Table 4.2: The table of the variables for each type of link

Description	Value
The penetration loss	L dB
Propagation factor on the backhaul link k_1	$10^{-14.178}$
Propagation factor on the direct link k_2	$10^{-14.178} \times 10^{-L/10}$
Propagation factor on the link from other relays k_3	$10^{-14.178} \times 10^{-2L/10}$
Propagation factor on the access link k_4	$10^{-9.84}$
Path loss exponent γ_1	3.5
Path loss exponent on the access link γ_2	2

4.4.3.1 SINR in the direct mode

In the direct mode, the UE in the bus communicates with the eNodeB directly, there is only one direct link. The direct link only suffers the outdoor path loss and penetration loss. So the SINR of the UE is expressed as follows:

$$S_t = \frac{k_2 h y^{-\gamma_1} P_S}{\sum_j k_2 h y_j^{-\gamma_1} P_S + N_u} \tag{4.4}$$

where P_S is the transmitted power of the serving eNodeB, $\sum_j k_2 h y_j^{-\gamma_1} P_S$ is the cumulative interference from neighbor base stations j, y is the distance between UE

68

and donor eNodeB, $k_2 = 10^{-14.178} \times 10^{-\text{L}/10}$, $\gamma_1 = 3.5$, h is the shadowing and N_u is the noise power of UE.

4.4.3.2 SINR in the relay mode

In the relay case, there are two separate links, the backhaul link and the access link. The signal that mobile relay receives from the donor eNodeB mainly suffers outdoor path loss. Thus the SINR at relay's receiver is expressed as follows:

$$S_r = \frac{k_1 h y^{-\gamma_1} P_S}{\sum_j k_1 h y_j^{-\gamma_1} P_S + N_r} \tag{4.5}$$

where P_S is the transmitted power of the DeNB, $\sum_j k_1 h y_j^{-\gamma_1} P_S$ is the cumulative interference from neighbor base stations j, y is the distance between mobile relay and the donor eNodeB, $k_1 = 10^{-14.178}$, $\gamma_1 = 3.5$, h is the shadowing and N_r is the thermal noise of relay node.

Then mobile relay transmits the data to vehicular UE in the vehicle. The signal on the access link mainly suffers in-vehicle path loss. We consider two relay modes: pure-relay mode and femto-like mode. The SINR at UE's receiver in the pure-relay mode is expressed as follows:

$$S_u = \frac{k_4 h y^{-\gamma_2} P_R}{\sum_j k_3 h y_j^{-\gamma_2} P_R + N_u} \tag{4.6}$$

where P_R is the transmitted power of relay node, $\sum_j k_3 h y_j^{-\gamma_2} P_R$ is the cumulative interference from neighbor mobile relay j, y is the distance between the indoor antenna of mobile relay and the receiver of vehicular UE, $k_4 = 10^{-9.84}$, $k_3 = 10^{-9.84} \times 10^{-2\text{L}/10}$, $\gamma_2 = 2$, h is the shadowing and N_u is UE's thermal noise. In the femto-like mode, the interference should also include the received power from the DeNB.

Besides we consider the possibility of installing two antennas at very different positions on the bus in the relay case, as shown in Figure 4.5. One antenna is installed in the front of the bus, antenna A, while the other one is installed in the back of the bus, antenna B. When two antennas are far away, for example 20 meters, the shadowing between two antennas can be seen uncorrelated [87]. Considering the bus is usually 20 meters or even longer, we consider these two antennas suffer independent random shadowing. Then we could attain two SINRs, S_A and S_B, and use MRC (maximum ratio combining) to get diversity gain. Note that S_A and S_B are both computed with (5) but for different values of shadowing h. Thus the total SINR on the backhaul link in this case can be written as:

$$S_r = S_A + S_B \tag{4.7}$$

4.4.4 The Calculation of Average Data Rate

Based on the above computing we can calculate the achievable data rate at a given distance either in the traditional case or the relay case. We assume that Channel State Information (CSI) is known, link adaptation is perfect. In the traditional case, the data rate is computed direct by the formula 4.3. However, in the relay case the achievable data rate of a vehicular UE is the end-to-end rate limited by the backhaul link and the access link. The achievable data rate in the relay case can be written as follows:

$$\mathcal{R}_u = \min\{\frac{1}{2}W w_{eff} \log(1 + \frac{S_u}{s_{eff}}), \mathcal{R}_r\} \tag{4.8}$$

where $\mathcal{R}_u$ is the achievable end-to-end data rate of a vehicular UE, $\mathcal{R}_r$ is the data rate on the backhaul link.

To map the results to system level performance, we need to consider SINR's distribution, the *probabilty distribution function* $f(S)$, over the cell area. Besides, SINR S is a function of user's location x. So theoretically the average data rate over the cell can be written as:

$$\epsilon = \int_0^{+\infty} S_u(g(x))f(g(x))p(x)\mathrm{d}x \tag{4.9}$$

where ϵ is the average data rate, $g(x)$ represents SINR S as a function of user's location x and $p(x)$ is the probability distribution function of user's location.

4.4.5 Performance Evaluation

We use Monte Carlo simulations to evaluate the data rate gain that deploying a mobile relay to serve a UE in the bus. The simulated network includes a hexagonal cellular layout with 19 base stations. Each base station employs omni directional antenna. There is only one UE randomly distributed in the network. At each location the UE takes the whole bandwidth. In the direct mode, the UE is directly served by the base station, while in the relay modes the UE in the vehicle is attached to the mobile relay with a fixed distance (i.e., 20 meters). Considering the public bus is usually 40 meters long at most, the transmitted power of mobile relay for the

70

access link is carefully set as -10 dBm [88]. Some main system parameters related to our LTE system are summarized in Table 4.3.

Table 4.3: System Parameters

Parameter	Value
System parameters	
Carrier Frequency	2 GHz
System Bandwidth	10 MHz
Bandwidth Efficiency	0.65
SNR Efficiency	0.95
Penetration loss	[10, 30] dB
Outdoor Shadowing	8 dB standard deviation
In-vehicle Shadowing	4 dB standard deviation
eNodeB parameters	
Transmit power	46 dBm
Antenna Gain	14 dBi
Mobile Relay parameters	
Transmit power	-10 dBm
Noise Figure	5 dB
User Equipment parameters	
Noise Figure	9 dB

4.4.5.1   Achievable data rate at different distances

First of all, we compare the achievable data rate of UE at different distances in the direct mode and relay modes. The results are shown in Figure 4.7.

From Figure 4.7 we can see, when the UE is located close to the donor eNodeB, the direct mode performs better. This is because there are two separate transmission links in the relay modes, the transmission in this case is not efficient compared with the direct transmission. Then with the increase of the distance, the data rate begins to decrease. Due to the penetration loss, the signal in the direct mode deteriorates more severe than that in the relay modes. Also we notice that when the UE is close to the donor eNodeB, the interference from donor eNodeB decreases the data rate significantly. After the distance is larger than about 500m, the transmitted power of mobile relay could dominate the SINR of the vehicular UE, the interference from the donor eNodeB can be ignored.
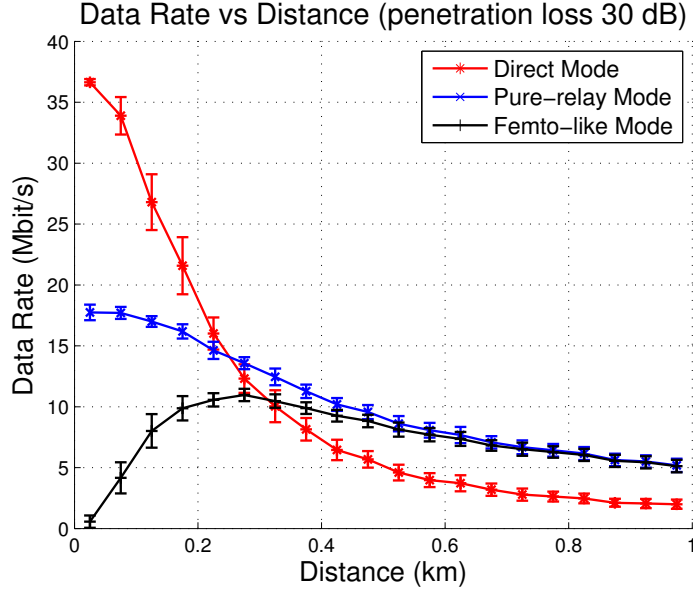
Figure 4.7: Achievable Data Rate (with 95% confidence interval)

4.4.5.2 The performance of the relay case with two antennas

We evaluate the performance of installing two antennas on a bus. The results are shown in Figure 4.8. We can see the performance of the relay case with two antennas performs better than the pure-relay mode with one antenna, the performance is improved due to diversity gain. Thus it's possible to install two antennas at different positions on the bus.

4.4.5.3 Data Rate Gain

In the simulated scenario, the distribution of the UE is discrete. Thus the formula 4.9 can be simplified to:

$$\epsilon = \frac{\sum_{i=1}^{n} \mathcal{R}_i}{n} \tag{4.10}$$

where ϵ is the average data rate, $\mathcal{R}_i$ is the UE's achievable data rate at a given distance, n is the number of UEs that randomly distributed in the network. We compute the average data rate gain under different penetration loss and make a comparison. The results are shown in Table 4.4. We consider the pure-relay mode with one antenna and with two antennas. The direct mode is considered as a baseline. We can see that the larger the penetration loss is, the more considerable data rate gain that mobile relay could bring. Since the penetration loss in vehicles

72
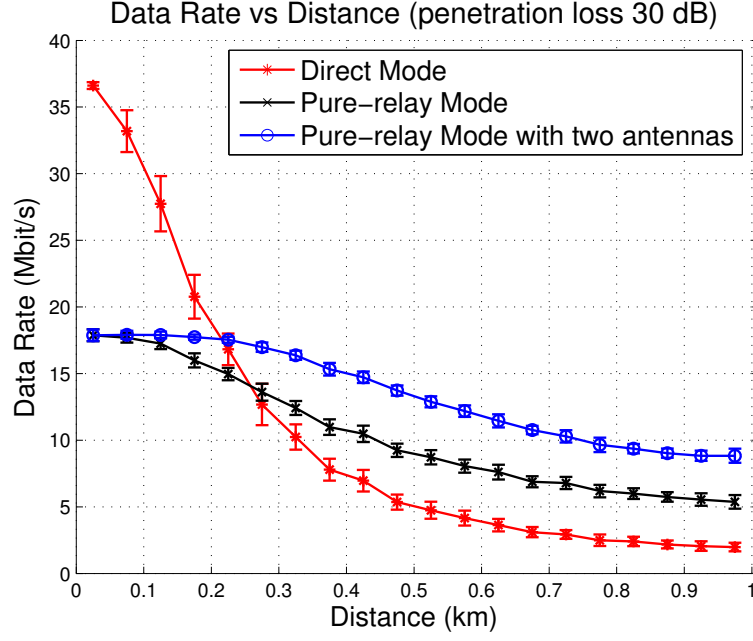
Figure 4.8: Achievable Data Rate with two antennas case (with 95% confidence interval)

is normally between 20 to 30 dB [89], considerable data rate gain can be attained in the mobile relay scenario. Besides, the performance can be further improved by using more sophisticated receiver at relay's receiver.

Table 4.4: Data Rate Gain

Penetration Loss	Pure-relay mode with one antenna	Pure-relay mode with two antennas
10 dB	-55%	-20%
15 dB	-46%	-13%
20 dB	-32%	+5%
25 dB	-5%	+45%
30 dB	+49%	+126%

4.5   Random Network

In this section, we extend our analysis to a more realistic random network and propose an analytical model using the stochastic geometry approach.

4.5.1 Network Model

We consider that both eNodeBs and buses are spatially distributed as a Poisson Point Process (PPP) Π_s and Π_r of respective intensity λ_s and λ_r (see Figure 4.9). The two processes are independent. Each bus is installed with one mobile relay. All eNodeBs have the same transmitted power P_S, and all mobile relays have the same fixed transmitted power P_R. There are several vehicular UEs in each bus. Each vehicular UE is always attached to the same mobile relay, which is assumed to be known. That relay is called the serving mobile relay. In the following, we consider a vehicular UE, we compute the distribution function of its SINR and the average achievable data rate of this vehicular, then we analyze the data rate gain that mobile relay might bring.
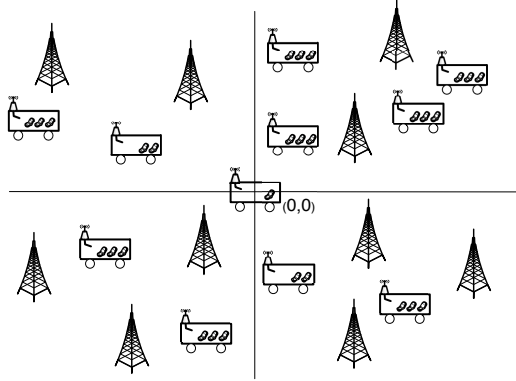
Figure 4.9: Illustration of spatial poisson distribution

The distance between a vehicular UE and the mobile relay is very small compared to the distance to the eNodeBs and between the relays. In other words, a bus and all UEs within the bus can be seen as at the same location. We analyze the SINR of an vehicular UE. Without loss of generality, we assume that the vehicular UE and the serving mobile relay under consideration are located at the origin. The other relays are distributed as a PPP.

4.5.2 Propagation Model

The shadowing effect is modeled by a log-normal random variable H. In other words, $10 \log H$ is a Gaussian r.v. with standard deviation σ_s. Let f_H be the PDF (Probability Density Function) of H, and F_H be the complimentary CDF

(Cumulative Distribution Function) of H.

$$F_H(\beta) = \int_\beta^\infty f_H(t)dt = Q(\frac{10\ln\beta}{\sigma_s\ln 10}) \tag{4.11}$$

where $Q(x) = \frac{1}{\sqrt{2\pi}}\int_x^\infty \exp(-\frac{u^2}{2})du$.

The fading effect is modeled by an exponential r.v. of mean 1.

In the following we first analyze the power of the received signal ξ when there is no fading and then we include the fading phenomenon. The objective is to re-write equation 4.1 with a reduced number of random variables. Hence, we have:

$$\xi(Y,\chi,\gamma,h) = hy^{-\gamma}\chi \tag{4.12}$$

where χ is a reference power defined as kP. Note that χ is the power received at distance 1 ($y = 1$) when there is no shadowing ($h = 1$). Variable χ takes both the transmitted power and the specific propagation factor on the considered link into account. The received power when fading is considered is then:

$$p = r\xi(Y,\chi,\gamma,h) \tag{4.13}$$

For notation simplicity, we denote by $\mathcal{B}$ the range of the possible value of (χ,γ). Let $\psi_{\chi,\gamma}$ for $(\chi,\gamma) \in \mathcal{B}$ be the probability to obtain (χ,γ). For instance, $\psi_{\chi_1,\gamma_1} = \frac{\lambda_1}{\lambda_1+\lambda_2}$ with $\chi_1 = P_1k_1$, $\psi_{\chi_2,\gamma_2} = \frac{\lambda_2}{\lambda_1+\lambda_2}$ with $\chi_2 = P_2k_2$. Note that $\mathcal{B}$ does not include (χ_1,γ_2) and (χ_2,γ_1).

4.5.3 Distribution Function of the Received Signal

The network includes nodes that can be eNodeBs and relays. EnodeBs (respectively relays) are distributed according to a Poisson Point Process of intensity λ_s (respectively λ_r). All nodes are distributed according to a PPP of intensity $\lambda = \lambda_s + \lambda_r$. Let Π be the generic realization of a Poisson Point Process of intensity λdY over $\mathbb{R}^2$. Let Π^e (e stands for enriched) be the marked PPP process whose atoms are (Y,χ,γ,h) with Y refers to the position of BS or relay, χ is the referenced power, γ is the path loss exponent, and h is the shadowing. The distance between a random point Y and the origin is denoted by y ($y = ||Y||$).

4.5.3.1 Poisson Point Process of Path Loss Shadowing

Proposition 1: The process of the inverse received power $\Xi = \{\xi^{-1}(Y, \chi, \gamma, h), (Y, \chi, \gamma, h) \in \Pi^e\}$ is a Poisson point process on $\mathbb{R}^+$ with intensity measure given by $\Lambda([0, t]) = \lambda \sum_{(\chi, \gamma) \in \mathcal{B}} \psi_{\chi, \gamma} \int_{\mathbb{R}^2} F_H(\frac{y^\gamma}{t\chi}) \mathrm{d}Y$.

Proof: The marks of the marked PPP $\Pi^e = (Y, \chi, \gamma, h)$ are i.i.d, so Π^e is a PPP of intensity $\lambda \mathrm{d}Y \otimes \sum_{(\chi, \gamma) \in \mathcal{B}} \psi_{\chi, \gamma} \delta_{\chi, \gamma} \otimes f_H(h) \mathrm{d}h$.

We consider the probability kernel $p((Y, \chi, \gamma, h), A) = 1_{\{\xi^{-1}(Y, \chi, \gamma, h) \in A\}}$ for all Borel $A \subset \mathbb{R}^+$ and apply the displacement theorem.

For any t on the $\mathbb{R}^+$, Ξ is a Poisson Point Process on $\mathbb{R}^+$ with intensity measure given by:

$$
\begin{aligned}
\Lambda([0, t]) &= \lambda \sum_{(\chi, \gamma) \in \mathcal{B}} \psi_{\chi, \gamma} \int_{\mathbb{R}^2} \int_{\mathbb{R}} 1_{\{\xi^{-1}(Y, \chi, \gamma, h) \leq t\}} f_H(h) \mathrm{d}h \mathrm{d}Y \\
&= \lambda \sum_{(\chi, \gamma) \in \mathcal{B}} \psi_{\chi, \gamma} \int_{\mathbb{R}^2} F_H(\frac{y^\gamma}{t\chi}) \mathrm{d}Y
\end{aligned}
\tag{4.14}
$$

This concludes the proof. $\qquad\square$

Let $B(t, \chi, \gamma) = \int_{\mathbb{R}^2} F_H(\frac{y^\gamma}{t\chi}) \mathrm{d}Y$, $\Lambda'(t)$ admits a derivative:

$$
\begin{aligned}
\Lambda'(t) &= \lambda \sum_{(\chi, \gamma) \in \mathcal{B}} \psi_{\chi, \gamma} B'(t, \chi, \gamma) \\
&= 2\pi \lambda \sum_{(\chi, \gamma) \in \mathcal{B}} \psi_{\chi, \gamma} \int_{\mathbb{R}} \frac{z^\gamma}{t^2 \chi} f_H(\frac{z^\gamma}{t\chi}) z \mathrm{d}z
\end{aligned}
\tag{4.15}
$$

Let "$\xi_0^{-1} > t$" be the event "The realization of process Ξ has no point in the interval [0,t]". Let $f_{\xi_0^{-1}}$ be the PDF of ξ_0^{-1}. The CDF and PDF of ξ_0^{-1} can be easily derived according to the property of Poisson point process.

Lemma 1: The PDF of ξ_0^{-1} is given by:

$$
f_{\xi_0^{-1}}(t) = \lambda \sum_{(\chi, \gamma) \in \mathcal{B}} \psi_{\chi, \gamma} B'(t, \chi, \gamma) e^{-\lambda \sum_{(\chi, \gamma) \in \mathcal{R}} \psi_{\chi, \gamma} B(t, \chi, \gamma)}
\tag{4.16}
$$

Proof: The number of points in the interval [0,t] follows a Poisson random variable of mean $\lambda \sum_{(\chi, \gamma) \in \mathcal{B}} \psi_{\chi, \gamma} B(t, \chi, \gamma)$, so:

$$
\mathbb{P}(\xi_0^{-1} > t) = e^{-\lambda \sum_{(\chi, \gamma) \in \mathcal{B}} \psi_{\chi, \gamma} B(t, \chi, \gamma)}
\tag{4.17}
$$

The PDF thus can be deduced by $f_{\xi_0^{-1}}(t) = -\frac{\mathrm{d}}{\mathrm{d}t} \mathbb{P}(\xi_0^{-1} > t)$. $\qquad\square$

4.5.3.2 Interference

Based on process Ξ, we compute the interference from the points in PPP Π. Define a marked Poisson Point Process $\Xi^e = \{(s,r), s \in \Xi, r \in \mathbb{R}^+\}$ where the mark r is the fading effect modeled by an exponential r.v. of mean 1. The intensity is thus $\Lambda'(s)\mathrm{d}s \otimes e^{-r}\mathrm{d}r$. The interference can be written as:

$$I = \sum rs^{-1} \tag{4.18}$$

According to the definition of Laplace transform:

$$\mathcal{L}_I(u) = \mathbb{E}[e^{-uI}] \tag{4.19}$$

Then according to Corollary 2.1.2 of [71]:

$$
\begin{aligned}
\mathcal{L}_I(u) &= \mathbb{E}[e^{-u\int s^{-1}r\mathrm{d}\Xi_e(s,r)}] \\
&= \exp(-\int_{\mathbb{R}}(1 - \int_{\mathbb{R}^+} e^{-us^{-1}r}e^{-r}\mathrm{d}r)\Lambda'(s)\mathrm{d}s) \\
&= \exp(-\lambda \sum_{(\chi,\gamma)\in\mathcal{R}} \psi_{\chi,\gamma} \int_{\mathbb{R}} B'(s,\chi,\gamma)\frac{1}{1+su^{-1}}\mathrm{d}s)
\end{aligned}
\tag{4.20}
$$

In the following, we use (4.20) to compute the CDF of the SINR on different links.

4.5.3.3 The CDF of the SINR on the backhaul link

The considered mobile relay is attached to the DeNB that provides the best average signal strength. Then the DeNB transmits to mobile relay on the backhaul link. For mobile relay, the interference comes from other BSs. Based on process Ξ, reorder $\xi^{-1}(Y, \chi_1, \gamma_1, h)$ where $\chi_1 = k_1 P_1$, mobile relay attaches to the DeNB Y_0 with the smallest $\xi^{-1}(Y_0, \chi_1, \gamma_1, h)$. Let S_r be the SINR of mobile relay on the backhaul link, therefore:

$$S_r = \frac{r_{Y_0}\xi(Y_0, \chi_1, \gamma_1, h)}{N_r + \sum_{Y \neq Y_0} r\xi(Y, \chi_1, \gamma_1, h)} \tag{4.21}$$

where Y is the position of neighbor BSs, N_r is the noise power of mobile relay.

The CDF of the SINR on the backhaul link is:

$$\mathbb{P}(S_r < T) = 1 - \sum_\beta \mathbb{P}(S_r \geq T|\xi^{-1}(Y_0, \chi_1, \gamma_1, h){=}\beta)\mathbb{P}(\xi^{-1}(Y_0, \chi_1, \gamma_1, h){=}\beta) \tag{4.22}$$

where $\mathbb{P}(\xi^{-1}(Y_0, \chi_1, \gamma_1, h) = \beta)$ is the event that the considered mobile relay is attached to a donor eNodeB that provides the maximum received power.

$$
\begin{aligned}
&\mathbb{P}(S_r \geq T|\xi^{-1}(Y_0, \chi_1, \gamma_1, h) = \beta) \\
&= \mathbb{P}(r_{Y_0} \geq T\beta(N_r + I)|\xi^{-1}(Y_0, \chi_1, \gamma_1, h) = \beta) \\
&= \mathbb{E}(e^{-T\beta(N_r+I)}|\xi^{-1}(Y_0, \chi_1, \gamma_1, h) = \beta) \\
&= e^{-TN_r\beta}\mathcal{L}_I(T\beta)
\end{aligned} \tag{4.23}
$$

On the backhaul link, the interference comes from other BSs, which is a PPP of intensity λ_s. By averaging all $\xi^{-1}(Y_0, \chi_1, \gamma_1, h) = \beta$, from (4.15), (4.20) and (4.23) we obtain:

$$\mathbb{P}(S_r < T) = 1 - \int_{\mathbb{R}^+} \lambda_s B'(\beta, \chi_1, \gamma_1)e^{-\lambda_s B(\beta,\chi_1,\gamma_1)-TN_r\beta-\lambda_s D(\chi_1,\gamma_1,\beta)}\mathrm{d}\beta \tag{4.24}$$

where $B(\beta, \chi_1, \gamma_1) = \int_{\mathbb{R}^2} F_H(\frac{y^{\gamma_1}}{t\chi_1})\mathrm{d}y$, $D(\chi_1, \gamma_1, \beta) = \int_\beta^{+\infty} B'(s, \chi_1, \gamma_1)\frac{1}{1+s(\beta T)^{-1}}\mathrm{d}s$.

4.5.3.4   The CDF of the SINR on the direct link

We also consider the case without mobile relay, to make a comparison. In this case, BS transmits to the UE inside the bus on the direct link. The interference comes from neighbor BSs. The CDF of the SINR on the direct link can be obtained by applying (χ_3, γ_1) into (4.24).

4.5.3.5   The CDF of the SINR on the access link

Femto-like mode

We assume that the distance between the mobile relay and vehicular UEs is fixed in relay case. In femto-like mode, BSs and mobile relays transmit to their served UEs simultaneously. For vehicular UE inside the bus, the interference comes from all BSs and other mobile relays. Let S_v be the SINR on the access link, therefore:

$$S_v = \frac{r_0 P_0}{N_u + \sum r\xi(Y, \chi, \gamma, h)} \tag{4.25}$$

where r_0 is the fading on the access link, P_0 is the constant received power from the serving mobile relay, Y is the position of BSs and other relays, N_u is the noise power of UE.

The CDF of the SINR on the access link is:

$$\mathbb{P}(S_v \geq T) = \mathbb{P}(r_0 \geq \frac{T(N_u + I)}{P_0})$$
$$= e^{-\frac{TN_u}{P_0}} \mathcal{L}_I(\frac{T}{P_0}) \tag{4.26}$$

In femto-like mode, the interference is from all points in the PPP Π of intensity λ. From (4.15), (4.20) and (4.26) we obtain:

$$\mathbb{P}(S_v < T) = 1 - \exp\left(-\frac{TN_u}{P_0} - \lambda \sum_{(\chi,\gamma)\in\mathcal{B}} \psi_{\chi,\gamma} \int_0^\infty B'(s,\chi,\gamma) \frac{1}{1+s(\frac{T}{P_0})^{-1}} \mathrm{d}s\right) \tag{4.27}$$

where in this case $\mathcal{B} = \{(\chi_3, \gamma_1), (\chi_2, \gamma_2)\}$ with $\psi_{\chi_3,\gamma_1} = \frac{\lambda_s}{\lambda}$, $\psi_{\chi_2,\gamma_2} = \frac{\lambda_r}{\lambda}$, $\chi_2 = P_R k_2$ and $\chi_3 = P_S k_3$.

Pure-relay mode

In pure-relay mode, at a given time only mobile relays transmit to their served UEs. For vehicular UE inside the bus, the interference only comes from other relays, which is a PPP of intensity λ_r. The CDF of the SINR on the access link in pure-relay mode can be thus obtained by applying (χ_2, γ_2) with $\chi_2 = P_R k_2$ and $\psi_{\chi_2,\gamma_2} = \frac{\lambda_r}{\lambda}$ into (4.27).

4.5.3.6 Special Case

Significant simplification is possible when the path loss exponent $\gamma = 4$, as already proposed in [10]. The CDF of the SINR on the backhaul link for this case is given as Proposition 2.

Proposition 2:

$$\mathbb{P}(S_r < T) = 1 - \int_0^\infty \exp(-K(T)u - \frac{TN_r}{\lambda_r^2 C_1^2} u^{\frac{\gamma_1}{2}}) \mathrm{d}u \tag{4.28}$$

where $C_1 = \pi \chi_1^{\frac{2}{\gamma_1}} e^{\frac{2\sigma_s^2}{\gamma_1^2}}$ with $\chi_1 = k_1 P_S$, and $K(T) = 1 + \sqrt{T}(\frac{\pi}{2} - \arctan \frac{1}{\sqrt{T}})$.

Proof:

$$B(t, \chi_1, \gamma_1) = \pi \chi_1^{\frac{2}{\gamma_1}} e^{\frac{2\sigma_s^2}{\gamma_1^2}} t^{\frac{2}{\gamma_1}} = C_1 t^{\frac{2}{\gamma_1}} \tag{4.29}$$

Accordingly, the derivative of $B(t, \chi_1, \gamma_1)$ is:

$$B'(t, \chi_1, \gamma_1) = \frac{2C_1}{\gamma_1} t^{\frac{2}{\gamma_1} - 1} \tag{4.30}$$

Therefore:

$$\mathbb{P}(S_r < T) = 1 - \frac{2C_1 \lambda_r}{\gamma_1} \int_0^\infty \beta^{\frac{2}{\gamma_1} - 1} \times \exp(-\lambda_r C_1 \beta^{\frac{2}{\gamma_1}} (1 + T^{\frac{2}{\gamma_1}} \int_{T^{-\frac{2}{\gamma_1}}}^{+\infty} \frac{1}{1 + v^{\frac{\gamma_1}{2}}} \mathrm{d}v) - T N_r \beta) \mathrm{d}\beta$$

$$= 1 - \int_0^\infty \exp(-K(T)u - \frac{T N_r}{\lambda_1^2 C_1^2} u^{\frac{\gamma_1}{2}}) \mathrm{d}u$$

$$\tag{4.31}$$

where $C_1 = \pi \chi_1^{\frac{2}{\gamma_1}} e^{\frac{2\sigma_s^2}{\gamma_1^2}}$ with $\chi_1 = k_1 P_S$, and $K(T) = 1 + \sqrt{T}(\frac{\pi}{2} - \arctan \frac{1}{\sqrt{T}})$. $\qquad \square$

4.5.4 Average Data Rate

4.5.4.1 Link Capacity

Let S be the SINR on the considered link. Let $F_S(t)$ be the CDF of the SINR on the considered link, which can be computed according to the discussions above. Let $\mathcal{R}_l$ be the Shannon capacity on the link l. The average data rate on the considered link is thus:

$$\mathbb{E}[\mathcal{R}_l] = \int_0^{+\infty} \mathbb{P}(\mathcal{R}_l > x) \mathrm{d}x$$

$$= \int_0^{+\infty} (1 - F_S(2^x - 1)) \mathrm{d}x \tag{4.32}$$

4.5.4.2 Direct Mode

In direct mode, there are no mobile relays. The UE connects directly to the serving eNodeB. The average achievable data rate in direct mode can be directly calculated by (4.32).

4.5.4.3 Relay Mode

In relay mode, there are two links between eNodeB and UE, the backhaul link and the access link. The achievable date rate of a vehicular UE is limited by these two links. We consider that a given amount of data is transmitted and that enough

resource is allocated to the backhaul link and the access link. Let $\mathcal{R}_b$ be the average achievable rate on the backhaul link, let $\mathcal{R}_a$ be the average achievable rate on the access link. Denote the average achievable rate of a vehicular UE in relay mode as follows:

$$\mathcal{R} = \frac{1}{\frac{1}{\mathcal{R}_1} + \frac{1}{\mathcal{R}_2}} \tag{4.33}$$

where $\mathcal{R}_1$ and $\mathcal{R}_2$ are computed respectively. For instance, the average achievable rate on the backhaul link is:

$$
\begin{aligned}
\mathcal{R}_1 &= \mathbb{E}[\log_2(1 + S_r)] \\
&= \int_{\mathbb{R}^+} \int_{\mathbb{R}^+} \lambda_s B'(\beta, \chi_1, \gamma_1) e^{-\lambda_s B(\beta, \chi_1, \gamma_1) - (2^y - 1) N_r \beta - \lambda_s D(\chi_1, \gamma_1, \beta, 2^y - 1)} \mathrm{d}\beta \mathrm{d}y
\end{aligned}
\tag{4.34}
$$

where $D(\chi_1, \gamma_1, \beta, 2^y - 1) = \int_\beta^{+\infty} B'(s, \chi_1, \gamma_1) \frac{1}{1 + s(\beta(2^y - 1))^{-1}} \mathrm{d}s$.

4.5.5 Numerical Results

In this section, we first present the comparison of the Monte Carlo simulations and the analytical results in terms of the CDF of the SINR. Then we compare the average achievable rate in the direct mode and in two relay modes. In direct mode, UEs inside the bus connect directly to BS. Mobility and handover are not taken into account. The configurations of the system are shown in Table 4.5.

Table 4.5: The table of the variables for system model

Description	Value
Density of BSs	$2 \times 10^{-6}\ m^{-2}$
Density of mobile relays	$7 \times 10^{-6}\ m^{-2}$
Shadowing	6 dB
Propagation factor on the backhaul link	$10^{-14.2}$
Propagation factor on the link from other relays	$10^{-18.2}$
Propagation factor on the direct link	$10^{-16.2}$
Path loss exponent on the backhaul link	4
Path loss exponent on the link from other relays	4
The transmitted power of BS	36 dBm
The transmitted power of relay	-10 dBm
Mobile relay noise figure	5 dB
UE noise figure	9 dB
Distance between mobile relay and vehicular UE	20 m

4.5.5.1   The CDF of the SINR

Figure 4.10 shows the CDF of the SINR versus the SINR threshold of the PPP model and the hexagonal model in the case of penetration loss 30 dB. For a fair comparison, the area of a hexagonal cell is set to be $1/\lambda_s$. As we can see, for the same considered link (backhaul link), the CDF in PPP model is always greater than that of hexagonal model. This is intuitive because there are strong interference generated by close BS in the PPP model. Thus the PPP model gives upper bound results while the hexagonal model gives lower bound results.

Also we compare the CDF of the SINR between the direct link and the backhaul link for a given threshold. The CDF of the SINR on the direct link is always above the CDF of the SINR on the backhaul link. This is because the direct link suffers penetration loss, which is eliminated in relay mode.
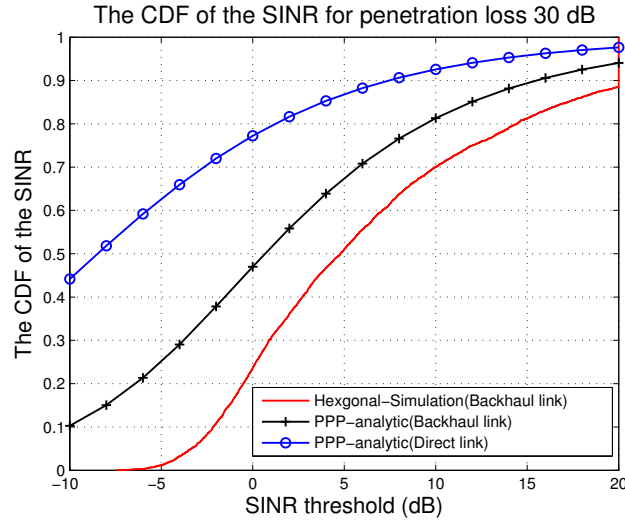
Figure 4.10: The CDF of the SINR vs SINR threshold

4.5.5.2   Average Achievable Rate Comparison

We compare the average achievable rate in the direct mode and the relay mode in terms of the penetration loss. The results are shown in Figure 4.11.

As we can see, with the increase of the penetration loss, the average achievable rate in the direct mode decreases greatly. Signals from the BS are severely attenuated by the penetration loss. The penetration loss does not affect the result of relay mode because it's eliminated. When the penetration loss is very small (10 dB), the average
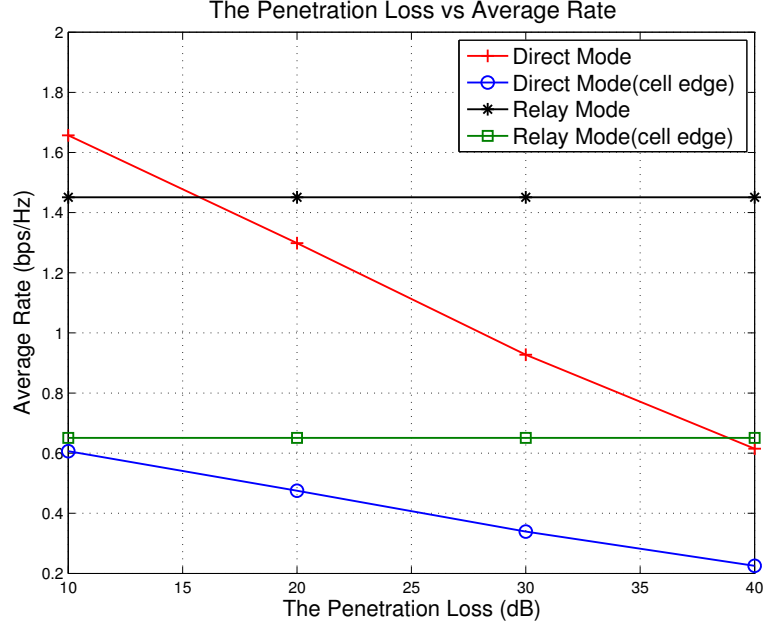
Figure 4.11: Average Achievable Rate vs Penetration Loss

achievable rate in the direct mode is better. This is because the average achievable rate we compute is for a UE distributed in the whole cell area. When UE is close to BS, it's better to remain transmitting on the direct link. The transmission in the relay mode is not efficient due to two phases transmission. Thus we also compare the average achievable rate for cell-edge bus (UE) by adding a minimum distance in the path loss function. The considered vehicular UE is at least 400 m to the BS. In this case we can see that the relay mode could bring considerable data rate gain to a vehicular UE. When penetration loss is 20 dB, mobile relay could bring to +29% data rate gain to a vehicular UE inside the bus.

We consider two relay modes. Both femto-like mode and pure-relay mode have the same average achievable rate, this is because the average achievable rate in relay mode depends on the rate on the backhaul link instead of the access link. The backhaul link is the bottleneck. It's expected that the performance of the backhaul link can be further improved by using more sophisticated receiver on relay node. Furthermore, if we study the system capacity in a multiple users network, femto-like mode should achieve higher system capacity than pure-relay mode since frequency reuse is adopted.

4.6 Summary

In this chapter, we have studied the impact of the interference on the data rate of a vehicular UE. We first consider one mobile relay deployed on a bus in a regular hexagonal network and compute the average data rate provided by this mobile relay based on Monte Carlo simulations. Then considering the limitations of hexagonal networks, we extend our study in a random network and present an analytical model based on the stochastic approach. By applying different parameters into this analytical model, we derive the CDF (Cumulative Distribution Function) of the SINR and the average achievable rate on different links.

According to both simulation and numerical results, we find out that the data rate gain provided by a mobile relay is not guaranteed in all cases. The penetration loss and the distance between the user and the base station are two key factors to decide whether mobile relay could bring data rate gain. Mobile relay can bring data rate gain to the user if the user is not close to the base station. When the user is close to the base station, it is better to switch from a relay mode to direct mode, but this would generate extra signaling cost. Therefore in a real network with several UEs and several mobile relays, whether deploying mobile relay can improve system capacity is still questionable.

Chapter 5

Impact of mobile relays on the cell capacity

5.1 Introduction

In Chapter 4, the impact of the interference on the data rate of a vehicular UE has been analyzed. It's found out that the data rate gain provided by a mobile relay is not guaranteed in all cases, for instance the case when the user is close to the base station. But in a real network, the user can be anywhere in the cell. Can mobile relay bring capacity gain to the system? What's the benefits of deploying mobile relay from the capacity point of view? To answer these questions, in this chapter we study the impact of mobile relays on the cell capacity.

We first consider a hexagonal cellular network with multiple users and multiple relays, and investigate the capacity gain brought by mobile relays deployed in the network. The distribution of users and buses (mobile relays) are modeled by the spatial Poisson distribution. We use equal bit rate scheduling to allocation the resource between users. The overall system performance are evaluated by Monte Carlo simulations.

Then considering the limitations of hexagonal networks, we extend the study to a random cellular network. Based on the analytical model proposed in Chapter 4, we derive the important metrics like the CDF of the SINR and the CDF of the end-to-end rate. The rate of the backhaul link and the rate of the access link are in general correlated when the same spectrum (or frequency) is used on both links, we take this fact into account when deriving the CDF of the end-to-end rate. The interference from the DeNB on the access link sometimes reduces the achievable

data rate. If a specific carrier is used for the access link, this interference is removed and the capacity of the access link can still be very high even with a small amount of bandwidth. We then consider a TDD mode for the access link with a dedicated bandwidth and the classical FDD mode for the direct and the backhaul link with the remaining bandwidth. Our objective is to investigate whether the hybrid TDD/FDD mobile relay mode can achieve higher system capacity FDD mobile relay mode, or in other words if the reduction of the bandwidth on the backhaul link is compensated by a better natural interference management. Furthermore, we evaluate and compare the performance between two relay modes and direct mode using the proposed analytical model. The cell total average rate and the energy efficiency in different modes are evaluated.

5.2 Capacity of an hexagonal network with mobile relays

5.2.1 System Model

5.2.1.1 Spatial Model

In this section we focus on a downlink LTE network with multiple users and multiple relays, as shown in Figure 5.1. We consider three types of nodes existing in the network: mobile relays, ordinary UEs and vehicular UEs. Mobile relays are mounted on public buses. Each mobile relay has an antenna outside the bus for the backhaul link, and an in-vehicle antenna for the access link. Ordinary UEs are outside the bus and always directly connect to the eNodeB. Vehicular UEs are inside the bus.

When mobile relays are deployed, we assume all vehicular UEs are connected to the LTE network through mobile relays. And we assume that ordinary UEs and buses are uniformly distributed in the cell. The locations of mobile relays can be represented by the locations of buses. There are several vehicular UEs in each bus. From the view of the cell, the UEs (ordinary and vehicular) are not uniformly distributed in the cell. The related variables are listed in the Table 5.1.

Based on the spatial Poisson Distribution, the probability to have n_u UEs in area A can be written as:

$$\mathbb{P}(n_u = i) = \frac{(\lambda_u A)^i}{i!} \mathrm{e}^{-\lambda_u A}, i = 0, 1..$$ (5.1)
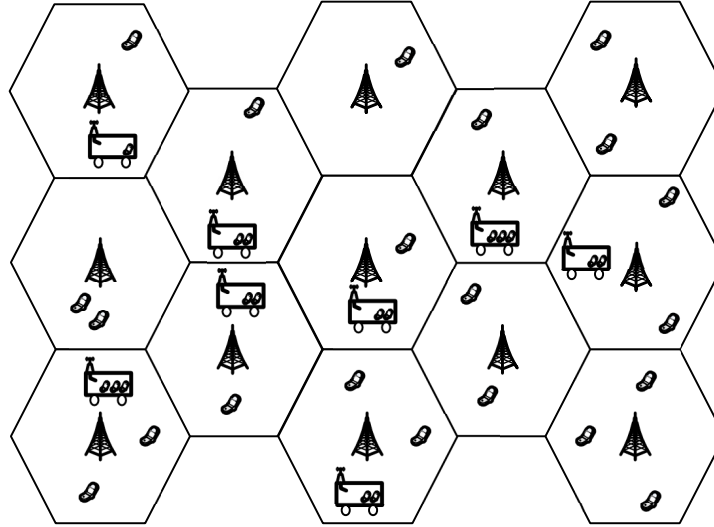
Figure 5.1: A hexagonal network with multiple users and multiple relays

Table 5.1: The table of the Variables for network model

Variable	Define
A	Area of the cell (km^2)
n_u	Total number of UEs in the cell
n_r	Number of buses (mobile relays) in the cell
λ_r	Density of buses in the cell
λ_u	Density of UEs in the cell

Similarly, the probability to have n_r buses (mobile relays) in area A is:

$$\mathbb{P}(n_r = i) = \frac{(\lambda_r A)^i}{i!} \mathrm{e}^{-\lambda_r A}, i = 0, 1..$$ (5.2)

5.2.1.2 Interference Model

In 3GPP specified relay network, the relay utilizes the same frequency band for the access link and the backhaul link, the access link and the backhaul link are separated in time domain. Due to this mechanism, two new types of interferences are brought in the mobile relay scenario. One is Relay-to-Relay interference, the other one is Relay-to-UE interference, as shown in Figure 5.2.
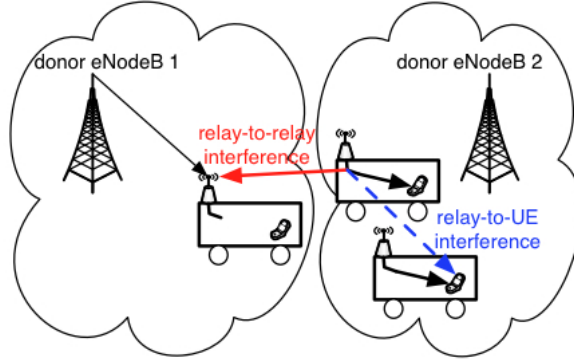
Figure 5.2: Interferences in mobile relay scenario

Relay-to-Relay Interference

Relay-to-Relay interference can occur due to the misalignment of MBSFN subframes, which results in partial overlapping between the reception and the transmission on the backhaul and access links. The reason for such interference is because different DeNBs independently configure the subframes to adapt to different network variations, e.g. cell load or traffic. The Relay-to-Relay interference is shown as solid line in Figure 5.2. In our model, we assume all eNodeBs are synchronized, so this type of interference is not considered.

Relay-to-UE Interference

Another kind of interference is Relay-to-UE interference. When two mobile relays are transmitting to their served vehicular UEs, frequency reuse is applied on the access link. If they are close to each other, which is possible for two buses, the vehicular UEs can be interfered by the neighbor mobile relay. It's shown as dotted line in Figure 5.2. This kind of interference is unique in mobile relay scenario. But since the transmitted power of mobile relay is relatively small, when two mobile relays are far away, this kind of interference is generally small. This interference is considered in our work.

5.2.1.3 Propagation Model

The propagation model is the same as the propagation model in section 4.3.1. The fading effect is not considered.

5.2.1.4 System Mode

Like our previous study, we also compare three modes: direct mode, pure-relay mode and femto-like mode. The direct mode is considered as a baseline mode.

5.2.2 The calculation of SINR

In this section, we compute the SINR of the terminal.

5.2.2.1 SINR in the direct mode

In this mode, the UE connects to the eNodeB directly. We consider outdoor path loss and the penetration loss on the direct link, and the interferences from neighbor eNodeBs. The SINR of a UE in the direct mode is:

$$S^D = \frac{k_2 h y^{-\gamma_1} P_S}{\sum\limits_j P_{S,j} + N_u} \tag{5.3}$$

where P_S is the transmitted power of the serving eNodeB, $P_{S,j}$ is the received power from neighbor eNodeB j, y is the distance between UE and the served eNodeB, $k_2 = 10^{-14.178} \times 10^{-L/10}$, $\gamma_1 = 3.5$, h is the shadowing and N_u is UE's thermal noise.

5.2.2.2 SINR in pure-relay mode and femto-like mode

In relay modes, the backhaul link and the access link are time-division multiplexed, so the interferences are different in the backhaul time slot and in the access time slot. For ordinary UE, the SINR in the backhaul time slot remains the same as the direct mode. For mobile relay, the signal that the mobile relay receives from the DeNB mainly suffers outdoor path loss. The SINR of a mobile relay in the backhaul time slot is:

$$S_r = \frac{k_1 h y^{-\gamma_1} P_S}{\sum\limits_j P_{S,j} + N_r} \tag{5.4}$$

where P_S is the transmitted power of the DeNB, $P_{S,j}$ is the received power from neighbor eNodeB j, y is the distance between relay and donor eNodeB, $k_1 = 10^{-14.178}$, $\gamma_1 = 3.5$ and N_r is mobile relay's thermal noise.

In the access time slot, the signal that a vehicular UE receives mainly suffers in-vehicle path loss, which is assumed be free space propagation. The interferences are from neighbor eNodeBs and other mobile relays. The SINR of a vehicular UE in the pure-relay mode is:

$$S_v = \frac{k_4 y^{-\gamma_2} P_R}{\sum\limits_j P_{S,j} + \sum\limits_k P_{R,k} + N_u} \tag{5.5}$$

where P_R is the transmitted power of mobile relay, $P_{S,j}$ is the received power from neighbor eNodeB j, $P_{R,k}$ is the received power from neighbor mobile relay k, y is the distance between relay indoor antenna and a vehicular UE, $k_4 = 10^{-9.84}$, $\gamma_2 = 2$ and N_u is UE's thermal noise. Note that, the SINR of a vehicular UE in the femto-like mode is basically the same as equation 5.5, except that in the femto-like mode the DeNB is one source of interferences for vehicular UEs. The received power from the DeNB for a vehicular UE should be added as interference in equation 5.5. For ordinary UEs in femto-like mode, in the access time slot mobile relays are one source of interferences. For them the received power from mobile relays should be added as interference in equation 5.3.

5.2.3 Scheduling

We consider equal bit rate scheduling, which means all UEs are served with the same data rate. The served data rate is defined as the unified bit rate per second for each UE, which depends on the number of UEs and channel condition. The data rate on

each link can reflect channel condition, which is calculated by the adjusted Shannon formula and is limited by Modulation Coding Scheme (MCS) [52]. Note that in relay modes the data that mobile relay transmits to vehicular UEs is, at most, the one that the mobile relay receives on the backhaul link. The related variables are listed in the Table in the sequence of alphabet.

Table 5.2: Variables for equal bit scheduling

Variable	Define
n_r	Number of buses (mobile relays) in the cell
n_v^i	Number of UEs inside a bus associated with the mobile relay i
n_o	Number of ordinary UEs in the cell
$\mathcal{R}_{a,i}$	Data rate for vehicular UE i on the access link
$\mathcal{R}_{b,i}$	Data rate for mobile relay i on the backhaul link
$\mathcal{R}_{v,j}$	Data rate for UE j inside the bus in the direct mode
$\mathcal{R}_{o,i}$	Data rate for ordinary UE i in the direct mode
$\mathcal{R}1_{o,i}$	Data rate for ordinary UE i in the backhaul time slot
$\mathcal{R}2_{o,i}$	Data rate for ordinary UE i in the access time slot
$\mathcal{R}_{served}^{D}$	Served date rate for all UEs in direct mode
$\mathcal{R}_{served}^{P}$	Served date rate for all UEs in pure-relay mode
$\mathcal{R}_{served}^{F}$	Served date rate for all UEs in femto-like mode

First we calculate the served data rate in the direct mode. The idea is to calculate how many bits can be transmitted per second for each UE. The inverse of the data rate can be seen as the time to transmit 1 bit. In the direct mode, eNodeB can serve the UEs all the time. So the served data rate in the direct mode $\mathcal{R}_{served}^{D}$ can be written as:

$$\mathcal{R}_{served}^{D} = \frac{1}{\sum\limits_{i=1}^{n_o} \frac{1}{\mathcal{R}_{o,i}} + \sum\limits_{i=1}^{n_r} \sum\limits_{j=1}^{n_v^i} \frac{1}{\mathcal{R}_{v,j}}} \tag{5.6}$$

Then in the pure-relay mode, eNodeB can only serve the UEs in the backhaul time slot, so the served rate in the pure-relay mode $\mathcal{R}_{served}^{P}$ can be written as:

$$\mathcal{R}_{served}^{P} = \frac{1}{\sum\limits_{i=1}^{n_o} \frac{1}{\mathcal{R}1_{o,i}} + \sum\limits_{i=1}^{n_r} \sum\limits_{j=1}^{n_v^i} \left(\frac{1}{\mathcal{R}_{b,i}} + \frac{1}{\mathcal{R}_{a,j}} \right)} \tag{5.7}$$

In the femto-like mode, eNodeB can serve ordinary UEs all the time, so the served rate in the femto-like mode $\mathcal{R}_{served}^{F}$ can be written as:

$$\mathcal{R}_{served}^{F} = \cfrac{1}{\sum\limits_{i=1}^{n_o} \frac{1}{\mathcal{R}1_{o,i}+\mathcal{R}2_{o,i}} + \sum\limits_{i=1}^{n_r} \sum\limits_{j=1}^{n_v^i} \left(\frac{1}{\mathcal{R}_{b,i}} + \frac{1}{\mathcal{R}_{a,j}} \right)} \tag{5.8}$$

5.2.4   Resource Allocation Model

To simplify the resource allocation process, we allocate the resource in the manner of time, as is shown in Figure 5.3. In this model each mobile relay or UE takes the whole system bandwidth, but because of different channel conditions, they consume different time resource.
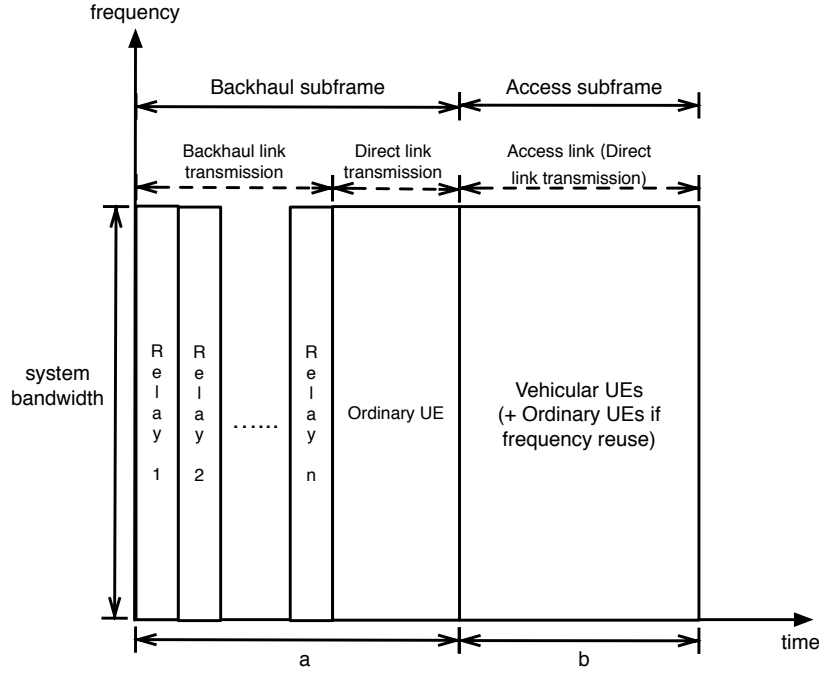
Figure 5.3: Resource allocation in time domain

From the figure, we can see that eNodeB first allocates resources to mobile relays in the backhaul time slot. After that, if there are extra resources, eNodeB can keep allocating resources to ordinary UEs in the backhaul time slot. Then in the access time slot, mobile relays allocate resources to their vehicular UEs. In the femto-like mode the DeNB can allocate resources to unserved ordinary UEs simultaneously in the access time slot. The resource allocated to each node i is calculated according to its channel condition:

$$\delta_{x,i} = \frac{\mathcal{R}_{served}}{\mathcal{R}_{x,i}} \tag{5.9}$$

where $x = o1, o2, b, a$ stands for ordinary UE in the backhaul time slot, ordinary UE in the access time slot, mobile relay and vehicular UE respectively.

5.2.5   Performance evaluation

The system level performance is evaluated in this section. The evaluation is performed by Monte Carlo simulations. The total number of UEs and the number of buses (mobile relays) in the cell in each snapshot is a Poisson random parameter. Mobility and handover are not taken into account. Random shadowing is fixed in each snapshot. The vehicles (per km of road) in France was 37 in 2010 [90]. This data include cars, buses, and freight vehicles. We only consider public buses in mobile relay scenario, the density of buses is set to 4 $per\ km^2$. In the direct mode, all UEs connect directly to the DeNB. In the pure-relay mode and the femto-like mode the distance between mobile relay and a vehicular UE is assumed to be 20 meters (the bus is usually 40 meters long at most), and the transmitted power of mobile relay is set to -10 dBm. The number of backhaul subframes in one LTE radio frame is set to 6. Some main parameters are listed in Table 5.3.

5.2.5.1   The Served Data Rate

First of all, we compare the served data rate in three modes under different ratio of vehicular UEs in the cell. The simulation result is shown in Figure 5.4. As shown in Figure 5.4, two relay modes have higher served data rate, this is because the penetration loss is eliminated in relay modes. With the increase of the proportion of UEs inside the vehicle, more UEs suffer from the penetration loss, which leads to the decrease of the served data rate in the direct mode. In the relay modes with the increase of UEs inside the vehicle, backhaul link increasingly becomes the bottleneck, so the served data rate also decreases.

5.2.5.2   The Penetration Loss

The penetration loss affects the performance significantly. We compare the system capacity in different modes under different penetration loss when the number of vehicular UEs in a bus is fixed to 5. The proportion of vehicular UEs under this

Table 5.3: System Parameters

Parameter	Value
Network parameters	
Number of eNodeBs	19
Radius from the center of the cell	1km
The density of vehicles (per km^2)	4
The density of UEs (per km^2)	50
The number of UEs in a bus	5
System parameters	
Carrier Frequency	2 GHz
System Bandwidth	10 MHz
Bandwidth Efficiency	0.65
SNR Efficiency	0.95
Penetration loss	[10, 30] dB
Outdoor Shadowing	8 dB
In-vehicle Shadowing	4 dB
eNodeB parameters	
Transmit power	46 dBm
Antenna Gain	14 dBi
Mobile Relay parameters	
Transmit power	-10 dBm
Noise Figure	5 dB
User Equipment parameters	
Noise Figure	9 dB
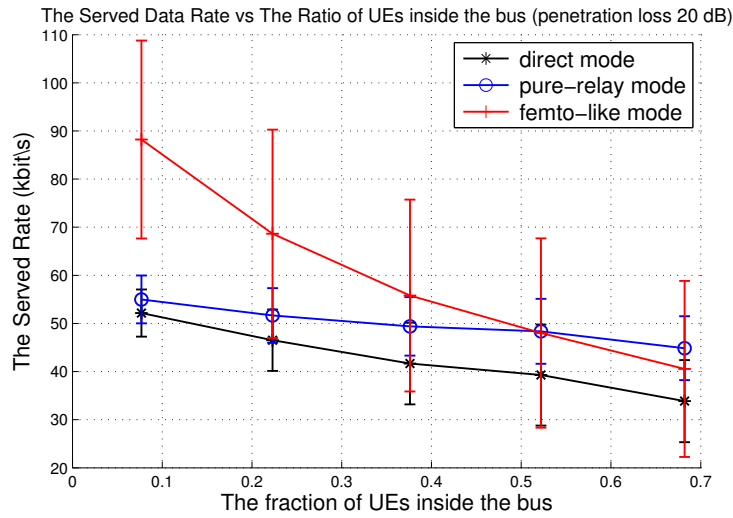
Figure 5.4: the served data rate vs the fraction of vehicular UEs (with 95% confidence interval)

configuration is 40%. The system capacity is the sum of the achievable data rate of all served UEs. The results are shown in Figure 5.5.
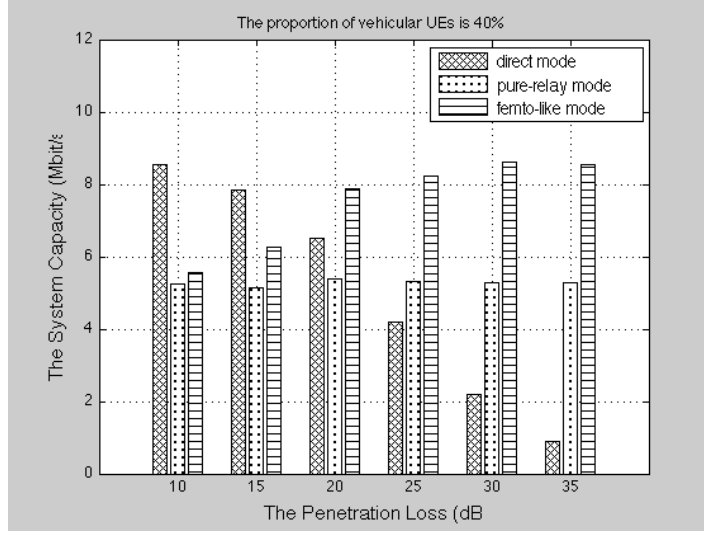
Figure 5.5: System Capacity vs Penetration Loss

From the figure we can see that, the larger the penetration loss is, the higher capacity relay modes could achieve. Thus more capacity gain can be brought by mobile relays. This is because a mobile relay eliminates the effect of the penetration loss. In the direct mode, the penetration loss deteriorates the signal. According to [89], the penetration loss in vehicles is normally between 20 to 30 dB. When penetration loss is 25 dB, the pure-relay mode can bring about +30% capacity gain, the femto-like mode can bring almost +100% capacity gain compared with the direct mode, so capacity gain can be attained by deploying mobile relay in public transportation systems.

Also we can see femto-like mode can achieve higher system capacity than pure-relay mode. This is because frequency reuse is applied in femto-like mode, eNodeB and mobile relay can send data simultaneously, which improves the bandwidth efficiency. In pure-relay mode, the system capacity has very small variations due to simulation noise.

5.3   Random Network Model

From this section, we extend our study to a more realistic random network. We first introduce the general system model in this section.

5.3.1 System Mode

We consider an operator who has 2W bandwidth (e.g. W for downlink and W for uplink) for the network. In this part of the work we focus on the bit rates of mobile users inside or outside the buses for a simple scheduling policy (round robin). As schedulers typically operate on a 10-ms cycle, the speed of terminals or relays has no impact within a scheduling cycle (at 36 km/h, the travelled distance in 10 ms is 10 cm). We thus consider a snapshot of the system with a given distribution of users and buses. In the following, we consider three system modes and analyze their differences.

5.3.1.1 Direct Mode

In direct mode, all types of UEs (ordinary UEs and vehicular UEs) are directly associated with a base station. There are no mobile relays in the network. For vehicular UEs, the signal is deteriorated by the penetration loss. This mode is a baseline mode.

5.3.1.2 FDD Mobile Relay Mode

In FDD mobile relay mode, ordinary UEs are associated with base stations, while vehicular UEs are associated with mobile relays installed on the bus. The backhaul links and the access links are both based on FDD with the same pair of frequency. When a relay receives data from the donor base station, it cannot transmit data to vehicular UEs. Otherwise, it would create self-interference and degrade the reception by the relay. However, when the relay transmits data to vehicular UEs, the donor base station can transmit to ordinary UEs. Full frequency reuse is applied among the direct links and the access links. Base stations and mobile relays transmit to their associated UEs on the same spectrum simultaneously.

The interference on mobile relays comes from neighbor base stations. The interference on vehicular UEs comes from both other relays and all base stations. The interference on ordinary UEs comes from other base stations and all relays, as shown in Fig. 5.6.

5.3.1.3 TDD/FDD Hybrid Mobile Relay Mode

Ordinary UEs and vehicular UEs are associated with base stations and mobile relays respectively. Mobile relays operate in TDD on the access link, while the backhaul
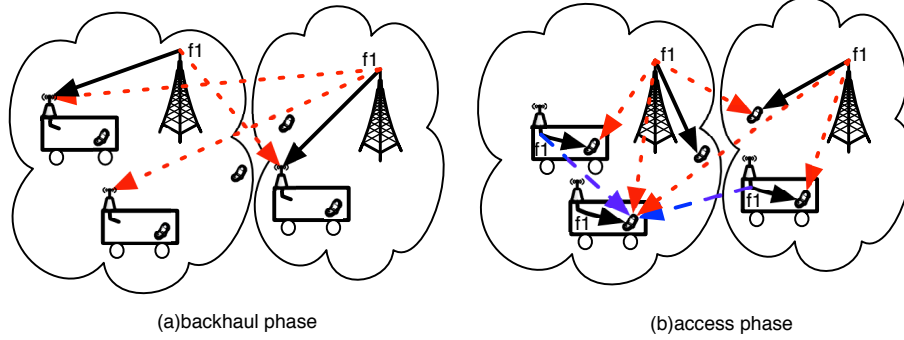
Figure 5.6: Interference illustration in FDD mobile relay mode with frequency reuse (the useful signal is represented in solid line, interference is represented in dashed line)

link remains FDD for downlink and uplink. The access link operates on a small dedicated spectrum separate from system bandwidth W. The backhaul link and the access link can thus operate independently without additional complex mechanisms to avoid self-interference. The separation in the frequency domain depends on a parameter α, which can be adjusted according to requirement. The bandwidth for FDD downlink transmission is thus αW, the dedicated bandwidth for the access link is $(1 - \alpha)2W$. Let ρ be the parameter for downlink/uplink subframe configuration. The available resource for downlink on the access link is $\rho(1 - \alpha)2W$.

The backhaul link and the access link operate on different frequencies, mobile relays can thus receive and transmit data simultaneously, which improves the transmission efficiency compared with FDD mobile relay mode. Furthermore, TDD/FDD hybrid mobile relay mode offers the flexibility to configure channel capacity with respect to asymmetric downlink or uplink traffic on the access link. Since vehicular UEs are relatively static and close to mobile relay, it's easy for them to synchronize with mobile relays.

The interference on vehicular UEs comes from neighbor relays which transmit on the downlink and other vehicular UEs which transmit on the uplink. The interference on ordinary UEs and mobile relays comes from neighbor base stations, as shown in Fig. 5.7. The differences between these modes are shown in Table 5.4.

Table 5.4: The differences between different modes

	Penetration Loss	Interference source on the backhaul link	Interference source on the access link
Direct mode	yes	no backhaul link	no access link
FDD mobile relay mode	eliminated	neighbor BSs	all BSs and neighbor relays
TDD/FDD mobile relay mode	eliminated	neighbor BSs	neighbor relays
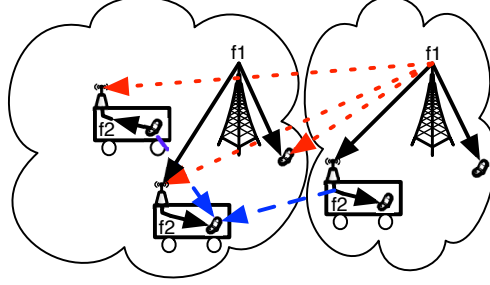
Figure 5.7: Interference illustration in TDD/FDD hybrid mobile relay mode (the useful signal is represented in solid line, interference is represented in dashed line)

5.3.2 Network Model

We only consider transmissions on the downlink. Base stations, buses and ordinary UEs are spatially distributed as homogeneous Poisson Point Process (PPP) Π_s, Π_r and Π_o with respective intensities λ_s, λ_r and λ_o, as shown in Fig. 5.8. Each bus is installed with one mobile relay. There are several vehicular UEs in each bus. Each vehicular UE is always attached to the mobile relay of the bus in which it is located. That relay is called the serving mobile relay. The number of vehicular UEs in each bus is assumed to follow a Poisson distribution with an average of $\overline{n_v}$.
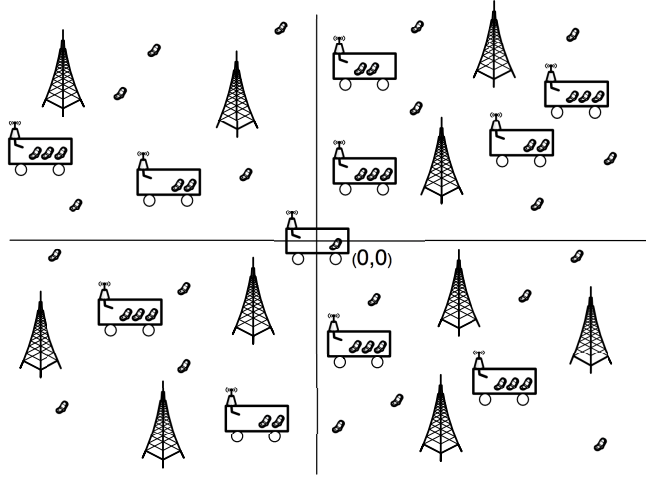
Figure 5.8: Network Model

The distance between vehicular UE and its serving mobile relay is relatively small compared to the distance to the base stations and between the relays. In other words, a bus and all vehicular UEs in the bus can be seen as at the same

98

location. Without loss of generality, we assume that the UE and the mobile relay under consideration are located at the origin. The other relays are distributed as a PPP.

5.3.3 Propagation Model

The propagation loss is modeled with Okumura-Hata formula. Both shadowing and fading are considered. Let y be the distance from a transmitter to a receiver, the received signal power p is:

$$p = rhky^{-\gamma}P = rhy^{-\gamma}\chi \tag{5.10}$$

where r and h are factors that take the fading effect and shadowing into account, k is a propagation factor, γ is the path loss exponent, P is the transmit power, χ is a reference power defined as kP. Variable χ takes both the transmit power and the specific propagation factor on the considered link into account. Note that χ is the power received at distance 1 ($y = 1$) when there is no fading ($r = 1$) and no shadowing ($h = 1$). We assume all base stations have the same transmit power P_S and all mobile relays have the same fixed transmit power P_R.

In the considered network, different links suffer different propagation loss (k, γ), as shown in Fig. 5.9. The direct link between ordinary UE and base station suffers outdoor path loss. The backhaul link also suffers outdoor path loss. The direct link between vehicular UE and base station suffers outdoor path loss and penetration loss. We assume free space propagation without shadowing on the access link between vehicular UE and its serving mobile relay. The received useful signal on the access link when there is no fading is thus constant and denoted by p_0.
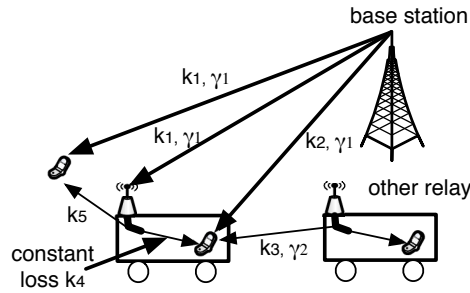
Figure 5.9: Illustration of propagation loss on different links

The fading effect is modeled by an exponential r.v. of mean 1. The shadowing

effect is modeled by a log-normal random variable H. In other words, $10 \log H$ is a Gaussian r.v. with standard deviation σ_s. It has been proved that the effect of shadowing can be equivalently interpreted as a random displacement of the original location [91].

Lemma 1: For a homogeneous PPP $\Phi \in \mathbb{R}^2$ with density λ, if each point $x \in \Phi$ is transformed to $x' \in \mathbb{R}^2$ such that $x' = h^{-\frac{1}{\gamma}}x$, where h are i.i.d (independent and identically distributed), such that $\mathbb{E}h^{\frac{2}{\gamma}} < \infty$, the new point process $\Phi^{(e)} \in \mathbb{R}^2$ defined by the transformed points x' is also a homogeneous PPP with density $\lambda^{(e)} = \lambda \mathbb{E}h^{\frac{2}{\gamma}}$.

The details of the proof can be found in [91]. We use the result of **Lemma 1**, the received power p can be thus written as:

$$p = r y'^{-\gamma} \chi \tag{5.11}$$

where y' is the distance of a point in the new PPP with density $\lambda \mathbb{E}h^{\frac{2}{\gamma}}$. Therefore, base stations, buses and ordinary UEs can be equivalently spatially distributed as PPPs Π'_s, Π'_r and Π'_o with intensities λ'_s, λ'_r and λ'_o, where $\lambda'_i = \lambda_i \mathbb{E}h^{\frac{2}{\gamma}}$, $i = \{s, r, o\}$ and $\gamma = \{\gamma_1, \gamma_2\}$.

5.3.4 Association Policy

We assume that each ordinary UE and mobile relay is associated with the closest base station. Based on that, the association region of each base station is a Voronoi cell. Let s be the distance between ordinary UE/mobile relay and its associated base station. The probability density function (pdf) of s is thus $e^{-\lambda'_s \pi s^2} 2\pi \lambda'_s s$ [10]. For vehicular UE, its serving mobile relay is assumed to be known.

5.3.5 Distribution of UEs in the cell

Denote the area of a single Voronoi cell as $\mathcal{A}$. A simple approximation for the pdf of $\mathcal{A}$ has been proved accurate for practical purposes [92]. The pdf of the area of a single Voronoi cell is given by:

$$f(\mathcal{A}) = \frac{343}{15}\sqrt{\frac{7}{2\pi}}(\mathcal{A}\lambda'_s)^{\frac{5}{2}}\exp(-\frac{7}{2}\mathcal{A}\lambda'_s)\lambda'_s \tag{5.12}$$

Denote the number of ordinary UEs in a cell as n_o, which is a Poisson random variable with mean $\lambda'_o \mathcal{A}$. Conditioned on $\mathcal{A}$, the probability generating function

100

(PGF) of the n_o is given by [92]:

$$G_o(z) = \frac{343}{8}\sqrt{\frac{7}{2}}(\frac{7}{2} - \frac{\lambda'_o}{\lambda'_s}(z-1))^{-\frac{7}{2}} \tag{5.13}$$

The distribution of n_o in a cell is therefore given by the ith derivative of $G_o(z)$ denoted by $G_o^{(i)}(z)$:

$$\mathbb{P}\{n_o = i\} = \frac{G_o^{(i)}(0)}{i!}, i = 0, 1.. \tag{5.14}$$

Denote the number of buses in a cell as n_r, which is also a Poisson random variable with mean $\lambda'_r \mathcal{A}$. Similarly, $\mathbb{P}\{n_r = i\}$ can be obtained by considering $\frac{\lambda'_r}{\lambda'_s}$ in (5.13), which can be given by:

$$\mathbb{P}\{n_r = i\} = \frac{G_r^{(i)}(0)}{i!}, i = 0, 1.. \tag{5.15}$$

where $G_r(z) = \frac{343}{8}\sqrt{\frac{7}{2}}(\frac{7}{2} - \frac{\lambda'_r}{\lambda'_s}(z-1))^{-\frac{7}{2}}$.

Denote the total number of vehicular UEs in a cell as n_{tv}. Denote the number of vehicular UEs in a bus under a certain mobile relay as n_v. Variable n_v follows a Poisson distribution with mean $\overline{n_v}$. Then the total number of vehicular UEs $n_{tv} = \sum_{i=1}^{n_r} n_v^i$, which is the sum of n_r independent poisson distributions. Conditioned on the number of buses n_r, the distribution of n_{tv} in a cell is given by:

$$
\begin{aligned}
\mathbb{P}\{n_{tv} = i\} &= \sum_{j=0}^{\infty} \mathbb{P}\{n_{tv} = i | n_r = j\}\mathbb{P}\{n_r = j\} \\
&= \sum_{j=0}^{\infty} \frac{e^{-j\overline{n_v}}(j\overline{n_v})^i}{i!}\mathbb{P}\{n_r = j\} \\
&= \sum_{j=0}^{\infty} \frac{e^{-j\overline{n_v}}(j\overline{n_v})^i}{i!}\frac{G_r^{(j)}(0)}{j!}
\end{aligned}
\tag{5.16}
$$

Denote the total number of UEs in a cell as n_u. We have $n_u = n_o + n_{tv}$. The distribution of n_u can be obtained by:

$$
\begin{aligned}
\mathbb{P}\{n_u = u\} &= \sum_{i=0}^{\infty} \mathbb{P}\{n_o = i\}\mathbb{P}\{n_{tv} = u - i\} \\
&= \sum_{i=0}^{\infty} \mathbb{P}\{n_o = i\}\sum_{j=0}^{\infty} \frac{e^{-j\overline{n_v}}(j\overline{n_v})^{u-i}}{(u-i)!}\mathbb{P}\{n_r = j\}
\end{aligned}
\tag{5.17}
$$

where $\mathbb{P}\{n_o = i\}$ and $\mathbb{P}\{n_r = j\}$ are respectively given by equation 5.14 and equation 5.15.

5.3.6 Scheduling and Rate

We consider Round Robin scheduling. The bandwidth is equally shared among all users within a cell. For an available bandwidth w, the downlink rate of a typical UE is:

$$\mathcal{R} = \frac{w}{n_u} \log_2(1 + S) \tag{5.18}$$

where S is SINR. Note that n_u and S are in general correlated. For tractability, we assume random variables n_u and S are independent. Such assumption does not compromise the accuracy of the analysis and has been justified by S. Dhillon et al in [93].

5.3.7 Power Consumption Model

Generally, the components that contribute to total power consumption can be separated into two fundamental parts. The first one describes the static power consumption, which includes signal processing overhead, battery backup, cooling power consumption, etc. The second part represents the output power. We use the power consumption model in [94][95] to model the total power consumption. The power consumption of base station and mobile relay can be given by:

$$P_{S\_tot} = P_{S\_0} + \tau_S P_S \tag{5.19}$$

$$P_{R\_tot} = P_{R\_0} + \tau_R P_R \tag{5.20}$$

where the efficiency of the power amplifier for base stations and mobile relays is denoted by $1/\tau_S$, $1/\tau_R$, the transmit power of base stations and mobile relays is denoted by P_S and P_R, the static power consumption for base stations and mobile relays is denoted by P_{S_0} and P_{R_0}, respectively.

5.3.8 Energy Efficiency Function

We define the energy efficiency for mobile relay network as:

$$\eta = \frac{\epsilon}{W(P_{S\_ave} + P_{R\_ave})}(bps/Hz/W) \tag{5.21}$$

where ϵ denotes the cell's total average rate, W is the system bandwidth, P_{S_ave} and P_{R_ave} denote the average power consumption for base station and mobile relays in the cell, respectively.

5.4 Capacity of different spectrum sharing methods

We first derive the CDF of SINR in different modes, as the SINR level at the receiver is a key performance indicator for wireless systems. The CDF of SINR on the backhaul link and the access link are assumed to be independent in this section. Next we turn our attention to the CDF of the rate of a UE. We first compute the rate in direct mode, then the computation of the end-to-end rate for vehicular UE in mobile relay modes is given. Then the energy efficiency expression is given for all modes.

5.4.1 Direct Mode

5.4.1.1 SINR distribution on different links

The derivation of the CDF of SINR in direct mode is similar as the computation made in [10, 70, 71]. For the sake of completeness and clarity, we give the main steps here.

All UEs in this mode are associated with the nearest base station. The interference comes from other base stations. Let S^D be the SINR of a UE in direct mode, which is defined by:

$$S^D = \frac{r_{y_c} \chi y_c^{-\gamma_1}}{N_u + I_{BS}} \tag{5.22}$$

where y_c is the closest distance to the base station, r_{y_c} is fading related to the serving base station, γ_1 is the path loss exponent on the direct link, N_u is the noise power of UE, and $I_{BS} = \sum_{y_i \neq y_c} r_i \chi y_i^{-\gamma_1}$ is the cumulative interference from other base station i.

Conditioned on the event that the distance between the considered UE and the served base station is y_c, the CDF of the SINR on the direct link is:

$$\mathbb{P}(S^D \leq T) = 1 - \mathbb{E}_{y_c}[\mathbb{P}(S^D > T | y_c)] \tag{5.23}$$

where T is denoted as the SINR threshold. Using the fact that $r \sim \exp(1)$, the

conditional probability can be expressed as:

$$\mathbb{P}(S^D > T | y_c) = \mathbb{E}_{I_{BS}}[\mathbb{P}(r_{y_c} \geq \frac{Ty_c^{\gamma_1}(N_u + I_{BS})}{\chi} | y_c, I_{BS})]$$

$$= \mathbb{E}_{I_{BS}}(e^{-\frac{Ty_c^{\gamma_1}(N_u + I_{BS})}{\chi}} | y_c) \qquad (5.24)$$

$$= e^{-\frac{Ty_c^{\gamma_1}N_u}{\chi}} \mathcal{L}_{I_{BS}}(\frac{Ty_c^{\gamma_1}}{\chi})$$

where $\mathcal{L}_{I_{BS}}$ is:

$$\mathcal{L}_{I_{BS}}(u) = \mathbb{E}_{\Pi'_s, r}\left[\exp\left(-u \sum_{y \neq y_c} r_i \chi y_i^{-\gamma_1}\right)\right]$$

$$= \mathbb{E}_{\Pi'_s}\left[\prod_{y_i \neq y_c} \mathbb{E}_r[\exp(-u r_i \chi y_i^{-\gamma_1})]\right] \qquad (5.25)$$

where i refers to neighbor base station i.

Note that the equation 5.24 is different with the equation 4.23 in Chapter 4. This is because the computing here is conditioned on the closest distance while the computing in Chapter 4 is conditioned on the maximum received power.

As $\mathcal{L}_{I_{BS}}$ is expressed as a probability generating functional (PGFL) [96], we have:

$$\mathcal{L}_{I_{BS}}(u) = \exp(-2\pi\lambda'_s \int_{y_c}^{\infty} (1 - \mathbb{E}_r[e^{-u r \chi s^{-\gamma_1}}]) s \, ds)$$

$$= \exp(-2\pi\lambda'_s \int_{y_c}^{\infty} (1 - \frac{1}{1 + u\chi s^{-\gamma_1}}) s \, ds) \qquad (5.26)$$

Note that the integration limits are from y_c to ∞, as the UE is connected to the nearest base station and all the interfering base stations cannot be closer.

The CDF of the SINR averaged over the plane is:

$$\mathbb{P}(S^D \leq T) = 1 - \int_{\mathbb{R}^+} e^{-\frac{Ty_c^{\gamma_1}N_u}{\chi}} \mathcal{L}_I(\frac{Ty_c^{\gamma_1}}{\chi}) f(y_c) \, dy_c \qquad (5.27)$$

where $f(y_c) = e^{-\lambda'_s \pi y_c^2} 2\pi\lambda'_s y_c$.

Therefore, for ordinary UE and vehicular UE, the CDF of the SINR is obtained by applying $\chi_1 = k_1 P_S$ and $\chi_2 = k_2 P_S$ into (5.27) respectively.

5.4.1.2 Distribution of the rate

For total available bandwidth W Hz, the downlink rate in bps of a UE in direct mode is:

$$\mathcal{R}^D = \frac{W}{n_u} \log_2(1 + S^D) \qquad (5.28)$$

where n_u is defined as the number of UEs in one cell as previous. The CDF of the rate $F_{\mathcal{R}^D}$ for a given n_u is thus given by:

$$F_{\mathcal{R}^D}(t) = \mathbb{P}(\mathcal{R}^D \leq t) = \mathbb{P}(S^D \leq 2^{\frac{n_u}{W}t} - 1) \tag{5.29}$$

where the CDF of S^D can be obtained from equation (5.27).

5.4.1.3 Energy efficiency

The number of UEs in one cell n_u is a random variable. For a given number of ordinary UEs $n_o = i$ and vehicular UEs $n_{tv} = j$, the cell's total average rate conditioned on i and j is:

$$\begin{aligned}
\epsilon_D^{i,j} &= \mathbb{E}[\sum_i \mathcal{R}_o^D + \sum_j \mathcal{R}_v^D] = i\mathbb{E}[\mathcal{R}_o^D] + j\mathbb{E}[\mathcal{R}_v^D] \\
&= i\int_0^\infty \mathbb{P}(\mathcal{R}_o^D > x)\mathrm{d}x + j\int_0^\infty \mathbb{P}(\mathcal{R}_v^D > x)\mathrm{d}x
\end{aligned} \tag{5.30}$$

where the CCDF of $\mathcal{R}_o^D$ and $\mathcal{R}_v^D$ can be computed from equation (5.29). By averaging all possible i and j, the cell's average rate in direct mode is:

$$\epsilon_D = \sum_i \sum_j \epsilon_D^{i,j}\mathbb{P}(n_o = i)\mathbb{P}(n_{tv} = j) \tag{5.31}$$

where $\mathbb{P}\{n_o = i\}$, $\mathbb{P}\{n_{tv} = j\}$ can be computed from equation (5.14)(5.16). The cell energy efficiency in direct mode is thus:

$$\eta_D = \frac{\epsilon_D}{WP_{S\_ave}} \tag{5.32}$$

where the average energy consumption of base station $P_{S\_ave} = P_{S\_tot}$.

5.4.2 FDD mobile relay mode

5.4.2.1 SINR distribution on different links

Ordinary UE

In FDD mobile relay mode, the interference for ordinary UE not only comes from neighbor base stations, but also from mobile relays due to frequency reuse. Let S_o^F be the SINR of ordinary UE in this mode, which is defined by:

$$S_o^F = \frac{r_{y_c}\chi_1 y_c^{-\gamma_1}}{N_u + I_{BS} + I_R} \tag{5.33}$$

where the cumulative interference from mobile relays $I_R = \sum r_i \chi_5 z^{-\gamma_2}$ with $\chi_3 = k_5 P_R$. By using similar approach in section 5.4.1.1, the CDF of the SINR for ordinary UE in this mode is:

$$\mathbb{P}(S_o^F \leq T) = 1 - \int_{\mathbb{R}^+} e^{-\frac{T y_c^{\gamma_1} N_u}{\chi_1}} \mathcal{L}_{I_{BS}}\left(\frac{T y_c^{\gamma_1}}{\chi_1}\right) \mathcal{L}_{I_R}\left(\frac{T y_c^{\gamma_1}}{\chi_1}\right) f(y_c) \mathrm{d}y_c \qquad (5.34)$$

where the Laplace transform $\mathcal{L}_{I_R}(u)$ is given by:

$$\mathcal{L}_{I_R}(u) = \mathbb{E}_{\Pi'_r, r}\left[\exp\left(-u \sum r_i \chi_3 z_i^{-\gamma_2}\right)\right] \qquad (5.35)$$

Similarly like equation 5.26, we have:

$$\begin{aligned}
\mathcal{L}_{I_R}(u) &= \exp\left(-2\pi\lambda'_r \int_0^\infty (1 - \mathbb{E}_r[e^{-ur\chi_3 s^{-\gamma_2}}])s\mathrm{d}s\right) \\
&= \exp\left(-2\pi\lambda'_r \int_0^\infty (1 - \frac{1}{1 + u\chi_3 s^{-\gamma_2}})s\mathrm{d}s\right)
\end{aligned} \qquad (5.36)$$

where the integration limits are from 0 to ∞, as all mobile relays are interferers for ordinary UE.

Mobile Relay

Mobile relay is associated with the closest base station like ordinary UEs. Let S_r^F be the CDF of the SINR for mobile relay, which can be obtained by applying $\chi_1 = k_1 P_S$ and the noise power of mobile relay N_r into (5.27):

$$\mathbb{P}(S_r^F \leq T) = 1 - \int_{\mathbb{R}^+} e^{-\frac{T y_c^{\gamma_1} N_r}{\chi_1}} \mathcal{L}_I\left(\frac{T y_c^{\gamma_1}}{\chi_1}\right) f(y_c) \mathrm{d}y_c \qquad (5.37)$$

where $f(y_c) = e^{-\lambda'_s \pi y_c^2} 2\pi\lambda'_s y_c$.

Vehicular UE

For vehicular UE, the interference comes from all base stations (including the base station that serves the relay), and other relays. Let S_v^F be the SINR on the

access link, the CDF of the SINR is defined by:

$$\mathbb{P}(S_v^F \le T) = 1 - \mathbb{P}(\frac{r_0 p_0}{N_u + I_{allBS} + I_R} > T)$$

$$= 1 - \mathbb{E}_{I_{allBS}, I_R}\Big[\mathbb{P}(r_0 \ge \frac{T(N_u + I_{allBS} + I_R)}{p_0} | I_{allBS}, I_R)\Big] \qquad (5.38)$$

$$= 1 - \exp\left(-\frac{TN_u}{p_0}\right)\mathcal{L}_{I_{allBS}}\left(\frac{T}{p_0}\right)\mathcal{L}_{I_R}\left(\frac{T}{p_0}\right)$$

where $I_{allBS} = \sum r_i \chi_2 y_i^{-\gamma_1}$. The Laplace transform $\mathcal{L}_{I_{allBS}}(u)$ can be computed by using (5.26), but the integration limits are from 0 to ∞, as the donor base station is also one source of interference. The Laplace transform $\mathcal{L}_{I_R}(u)$ is computed by using (5.36) with $\chi_4 = k_4 P_R$ instead of χ_3. Hence, we have:

$$\mathcal{L}_{I_{allBS}}(u) = \exp(-2\pi\lambda_s' \int_0^\infty (1 - \frac{1}{1 + u\chi_2 s^{-\gamma_1}})s ds) \qquad (5.39)$$

$$\mathcal{L}_{I_R}(u) = \exp(-2\pi\lambda_r' \int_0^\infty (1 - \frac{1}{1 + u\chi_4 s^{-\gamma_2}})s ds) \qquad (5.40)$$

5.4.2.2   Distribution of the rate

In FDD mobile relay mode, the resource of the base station is shared between ordinary UEs and mobile relays. Mobile relay first receives data from base station, then mobile relay transmits to vehicular UEs. The resource of a mobile relay is shared among n_v UEs that are associated with it.

Ordinary UE

Denote the rate of an ordinary UE in this mode as $\mathcal{R}_o^F$, denote the CDF of the rate as $F_{\mathcal{R}_o^F}(t)$. Similarly, $F_{\mathcal{R}_o^F}(t)$ can be obtained by using equation (5.29).

Vehicular UE

Assume the backhaul link and access link are equally separated in the time domain. The downlink end-to-end rate in bps of vehicular UE is:

$$\mathcal{R}_v^F = \frac{1}{2}\min\{\frac{W}{n_u}\log_2(1 + S_r^F), \frac{W}{n_v}\log_2(1 + S_v^F)\} \qquad (5.41)$$

107

where n_v is the number of vehicular UE associated with a certain mobile relay. The 1/2 factor is due to the two phases operation of the relay transmission. The backhaul and access links are both interfered by neighbor base stations, there is a dependency between two links. To precisely capture this fact, we first compute the CCDF (Complementary Cumulative Distribution Function) of $\mathcal{R}_v^F$ conditioned on the closest base station y_c that the mobile relay is associated to, which is given by:

$$
\begin{aligned}
&\mathbb{P}(\mathcal{R}_v^F > t|y_c) \\
&= \mathbb{P}(\frac{1}{2}\min\{\frac{W}{n_u}\log_2(1+S_r^F), \frac{W}{n_v}\log_2(1+S_v^F)\} > t|y_c) \\
&= \mathbb{P}(S_r^F > 2^{2tn_u/W} - 1, S_v^F > 2^{2tn_v/W} - 1|y_c) \\
&= \mathbb{P}(\frac{r_1\chi_1 y_c^{-\gamma_1}}{N_r+I_{BS}} > g_1(t), \frac{r_0 p_0}{N_u+I_R+I_{allBS}} > g_2(t)|y_c)
\end{aligned}
\tag{5.42}
$$

where $g_1(t) = 2^{2tn_u/W} - 1$ and $g_2(t) = 2^{2tn_v/W} - 1$. The interference from all base stations on the access link can be seen as the interference from other base stations on the backhaul link plus the interference from donor base station, with additional penetration loss $L = \frac{k_2}{k_1}$, which means $I_{allBS} = L(I_{BS} + r_{y_c}\chi_1 y_c^{-\gamma_1})$. The equation 5.42 can be written as:

$$
\begin{aligned}
&\mathbb{P}(\mathcal{R}_v^F > t|y_c) \\
&= \mathbb{P}(r_1 > \frac{g_1(t)(N_r + I_{BS})}{\chi_1 y_c^{-\gamma_1}}, r_0 > \frac{g_2(t)(N_u + I_R + L(I_{BS} + r_{y_c}\chi_1 y_c^{-\gamma_1}))}{p_0}|y_c)
\end{aligned}
\tag{5.43}
$$

Let $f_{I_{BS}}$ denote the pdf of I_{BS}, f_{I_R} denote the pdf of I_R. Using the fact $r_i \sim \exp(1)$, $i = \{0, 1, y_c\}$, the conditional CCDF of $\mathcal{R}_v^F$ can be expressed as:

$$
\begin{aligned}
&\mathbb{P}(\mathcal{R}_v^F > t|y_c) \\
&= \mathbb{E}[e^{-\frac{g_1(t)(N_r+I_{BS})}{\chi_1 y_c^{-\gamma_1}}}, e^{-\frac{g_2(t)(N_u+I_R+L(I_{BS}+r_{y_c}\chi_1 y_c^{-\gamma_1}))}{p_0}}|y_c, I_{BS}, I_R, r_{y_c})]
\end{aligned}
\tag{5.44}
$$

which can be further computed by using triple points. Let x denote I_{BS}, let y denote

r, let z denote the pdf of I_R. Then we have:

$$\mathbb{P}(\mathcal{R}_v^F > t | y_c) = \int_{x=0}^{\infty} f_{I_{BS}}(x) \exp\left[-\frac{g_1(t)(N_r + x)}{\chi_1 y_c^{-\gamma_1}}\right] \int_{y=0}^{\infty} e^{-y} \int_{z=0}^{\infty} f_{I_R}(z)$$

$$\times \exp\left[-\frac{g_2(t)(N_u + z + L(x + y\chi_1 y_c^{-\gamma_1}))}{p_0}\right] dz dy dx$$

$$= \exp\left[-\frac{g_1(t)N_r}{\chi_1 y_c^{-\gamma_1}} - \frac{g_2(t)N_u}{p_0}\right] \mathcal{L}_{I_{BS}}\left(\frac{g_1(t)}{\chi_1 y_c^{-\gamma_1}} + \frac{g_2(t)L}{p_0}\right) \times \mathcal{L}_{I_R}\left(\frac{g_2(t)}{p_0}\right) \frac{1}{1 + \frac{L\chi_1 y_c^{-\gamma_1}}{p_0}}$$

$$(5.45)$$

By averaging all y_c, the CDF of the end-to-end rate of vehicular UE in FDD mobile relay mode is:

$$F_{\mathcal{R}_v^F}(t) = 1 - \int_{\mathbb{R}+} \mathbb{P}(\mathcal{R}_v^F \geq t | y_c) 2\pi \lambda_s' y_c e^{-\lambda_s' \pi y_c^2} dy_c \qquad (5.46)$$

5.4.2.3 Energy efficiency

In FDD mobile relay mode, the end-to-end rate of an vehicular UE $\mathcal{R}_v^F$ depends on the number of vehicular UE associated to a certain mobile relay $n_v = k$. For a given number of ordinary UE i, vehicular UE j and k, the conditional cell's total average rate is given by:

$$\epsilon_F^{i,j,k} = \mathbb{E}\left[\sum_i \mathcal{R}_o^F + \sum_{j,k} \mathcal{R}_v^F\right] \qquad (5.47)$$

where the CCDF of $\mathcal{R}_o^F$ and $\mathcal{R}_v^F$ can be computed from section 5.4.2.2. By averaging all i, j, k, the cell's average rate is:

$$\epsilon_F = \sum_i \sum_{j,k} \epsilon_F^{i,j,k} \mathbb{P}(n_o = i) \mathbb{P}(n_{tv} = j, n_v = k) \qquad (5.48)$$

where the joint probability $\mathbb{P}(n_{tv} = j, n_v = k)$ can be easily obtained since the distribution of the rest vehicular UE $j - k$ is still a sum of independent Poisson distributions. Then since mobile relays only transmit in the access phase in this mode, the average power consumption of mobile relay in the cell is:

$$P_{R\_ave}^F = \sum_i i(P_{R\_0} + \frac{1}{2}\tau_r P_R) \mathbb{P}\{n_r = i\} \qquad (5.49)$$

The cell energy efficiency in this mode is thus:

$$\eta_F = \frac{\epsilon_F}{W(P_{S\_ave} + P_{R\_ave}^F)} \qquad (5.50)$$

109

where the average energy consumption of base station $P_{S\_ave} = P_{S\_tot}$.

5.4.3 TDD/FDD hybrid mobile relay mode

5.4.3.1 SINR distribution on different links

Ordinary UE

The CDF of the SINR for ordinary UE in this mode S_o^T is the same as the case in direct mode.

Mobile Relay

The CDF of the SINR for mobile relay in this mode S_r^T is the same as the case in FDD mobile relay mode.

Vehicular UE

In this mode mobile relay operates in TDD on the access link. Each mobile relay is an independent TDD system. The interferences come from either neighbor relays which are transmitting on the downlink or vehicular UEs which are transmitting on the uplink. The interference signals suffer from path loss and two times penetration loss. For vehicular UE, the distance to the serving mobile relay is relative small compared with the distance to other mobile relays or other vehicular UEs, the interference from other vehicular UEs on the uplink can be approximately equal to the interference from other relays. So the interferences on the access link in this mode are assumed to come from all neighbor relays.

Let S_v^T be the SINR on the access link, the CDF of S_v^T is thus defined by:

$$
\begin{aligned}
\mathbb{P}(S_v^T \leq T) &= 1 - \mathbb{P}(\frac{r_0 p_0}{N_u + I_R} > T) \\
&= 1 - \mathbb{E}_{I_R}\big[\mathbb{P}(r_0 \geq \frac{T(N_u + I_R)}{p_0}|I_R)\big] \\
&= 1 - \exp\left(-\frac{T N_u}{p_0}\right)\mathcal{L}_{I_R}(\frac{T}{p_0})
\end{aligned}
\tag{5.51}
$$

where $I_R = \sum r\chi_4 z^{-\gamma_2}$ with $\chi_4 = k_4 P_R$. The Laplace transform $\mathcal{L}_{I_R}(u)$ is computed by using (5.36):

$$
\mathcal{L}_{I_R}(u) = \exp(-2\pi\lambda'_r \int_0^\infty (1 - \frac{1}{1 + u\chi_4 s^{-\gamma_2}})s ds)
\tag{5.52}
$$

5.4.3.2 Distribution of the rate

Ordinary UE

In TDD/FDD hybrid mobile relay mode, notice that the available bandwidth for ordinary UE is αW. Similarly like the computing in section 5.4.1.2, the downlink rate in bps of an ordinary UE can be obtained.

Vehicular UE

In TDD/FDD hybrid mobile relay mode, the backhaul link and the access link operates independently at the same time. The downlink end-to-end rate in bps of an vehicular UE is:

$$\mathcal{R}_v^T = \min\{\frac{\alpha W}{n_u}\log_2(1+S_r^T), \rho\frac{2W(1-\alpha)}{n_v}\log_2(1+S_v^T)\} \tag{5.53}$$

where ρ is the downlink/uplink configuration on the access link. The CCDF of $\mathcal{R}_v^T$ is given by:

$$
\begin{aligned}
\mathbb{P}(\mathcal{R}_v^T > t) &= \mathbb{P}(\min\{\frac{\alpha W}{n_u}\log_2(1+S_r^T), \rho\frac{2W(1-\alpha)}{n_v}\log_2(1+S_v^T)\}>t) \\
&= \mathbb{P}(\frac{\alpha W}{n_u}\log_2(1+S_r^T)>t)\mathbb{P}(\frac{\rho 2W(1-\alpha)}{n_v}\log_2(1+S_v^T)>t) \\
&= \mathbb{P}(S_r^T > 2^{\frac{n_u t}{\alpha W}} - 1)\mathbb{P}(S_v^T > 2^{\frac{n_v t}{\rho 2W(1-\alpha)}} - 1)
\end{aligned} \tag{5.54}
$$

where the CCDF of S_r^T and S_v^T can be computed as the discussions in section 5.4.3.

5.4.3.3 Energy efficiency

Based on the CCDF of $\mathcal{R}_o^T$ and $\mathcal{R}_v^T$ which can be computed in section 5.4.3.2, the cell's average rate in TDD/FDD hybrid mobile relay mode is:

$$\epsilon_T = \sum_i \sum_{j,k} \epsilon_T^{i,j,k}\mathbb{P}(n_o = i)\mathbb{P}(n_{tv} = j, n_v = k) \tag{5.55}$$

In this mode, mobile relays can receive and transmit simultaneously. The average power consumption of mobile relay in the cell is:

$$P_{R\_ave}^T = \sum_i i(P_{R\_0} + \tau_R P_R)\mathbb{P}\{n_r = i\} \tag{5.56}$$

The cell energy efficiency in TDD/FDD hybrid mobile relay mode is thus:

$$\eta_T = \frac{\epsilon_T}{W(P_{S\_ave} + P_{R\_ave}^T)} \tag{5.57}$$

where the average energy consumption of base station $P_{S\_ave} = P_{S\_tot}$.

5.4.4　Performance and Discussion

The results are presented in this section. This evaluation depends on many variables, different cases are studied where some parameters vary, while the remaining ones, unless otherwise stated, are equal to their default values, summarized in Table 5.5. The path loss exponent γ_1, γ_2 are set to be 4, where simplification of calculations is possible. The power model parameters are obtained from [94]. Considering the bus is normally no longer than 20 meters, the distance between a vehicular UE and its serving mobile relay is set to be 20 meters, the transmit power of mobile relay is set to be 0 dBm [88]. In TDD/FDD hybrid mobile relay mode, the access link operates in TDD, downlink/uplink configuration ρ is set to be 0.5, half of the resource is allocated to downlink transmission on the access link.

5.4.4.1　The CDF of SINR in direct mode

Firstly, we compare analytical results with Monte-Carlo simulations. The main objective is to assess the validation of our proposed model. The CDF of the SINR of an ordinary UE and a vehicular UE in direct mode are displayed in Fig. 5.10, which shows that the simulation results of the PPP model are well consistent with the analytical results. We also compare the analytical results with the simulation results of the hexagonal model. For a fair comparison, the area of a hexagonal cell is set to be $1/\lambda_s$. As we can see, the CDF of the analytical model are always higher than that of the hexagonal model. This is because in the PPP model there are strong interference generated by nearby base stations. Thus the PPP model gives pessimistic results compared with the results of the hexagonal model.

Also we can see for a given SINR threshold, vehicular UEs always have higher outage probability than ordinary UEs. This is because they suffer penetration loss, which deteriorates the signal and cannot be neglected.

Table 5.5: Model Parameters

Total system bandwidth	$W = 10$ MHz
Base station intensity	$\lambda_s = 1$ BS $/km^2$
Bus intensity	$\lambda_r = 5$ buses $/km^2$
Ordinary UE intensity	$\lambda_o = 20$ UEs $/km^2$
Average number of UEs in a bus	$\overline{n_v} = 4$
Base station transmit power	$P_S = 36$ dBm
Base station static power consumption	$P_{S\_0} = 130$ W
Base station power slope	$\tau_S = 4.7$
Mobile relay transmit power	$P_R = 0$ dBm
Mobile relay static power consumption	$P_{R\_0} = 4.8$ W
Mobile relay power slope	$\tau_R = 8.0$
Bus penetration loss	$L = 20$ dB
Propagation factor for ordinary UE/mobile relay	$k_1 = 10^{-14.2}$
Propagation factor for vehicular UE	$k_2 = 10^{-14.2-L/10}$
Path loss exponent	$\gamma_1 = \gamma_2 = 4$
Shadowing	$\sigma_s = 6$ dB
Noise power spectral density	-174 dBm/Hz
Mobile relay noise figure	5 dB
UE noise figure	9 dB
Distance between mobile relay and vehicular UE	20 m
Frequency division parameter in TDD/FDD mode	$\alpha = 0.9$
Downlink/uplink configuration in TDD/FDD mode	$\rho = 0.5$

5.4.4.2 Data rates of ordinary UEs

The CDF of the rate of an ordinary UE is illustrated in Fig. 5.11. As we can see, ordinary UEs have the same CDF of rate in direct mode and FDD mobile relay mode. It means that the interferences depend on neighbor base stations. The interferences from mobile relays in FDD mobile relay mode are negligible due to small transmit power of mobile relay and large penetration loss (20 dB in this plot).

We also study the impact of frequency division parameter α on ordinary UEs in TDD/FDD hybrid mobile relay mode. With the decrease of α, more bandwidth is dedicated to the access link, less bandwidth is available for ordinary UEs, the CDF of the rate thus becomes higher. There exists a tradeoff between the rate of ordinary UEs and the dedicated bandwidth of the access link. Considering vehicular UEs and the serving mobile relay are relatively close, the access link can have a good channel condition, it's expected that a small dedicated bandwidth (large α) is enough to guarantee the high speed transmission on the access link. The CDF of the end-to-end rate of a vehicular UE is analyzed next.
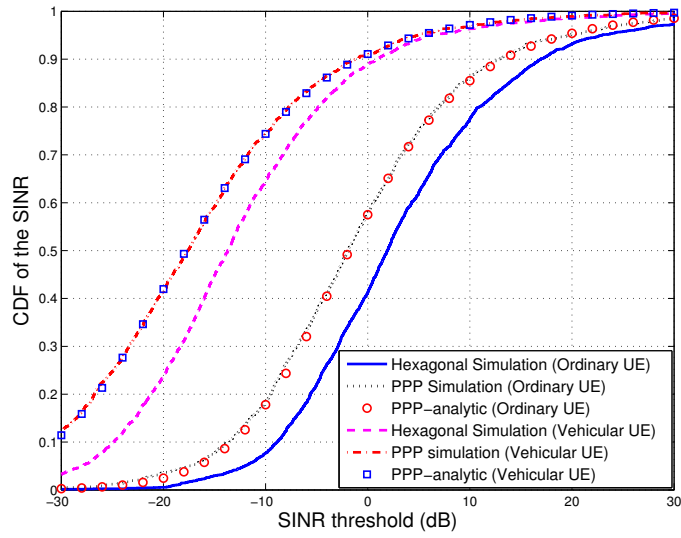
Figure 5.10: CDF of SINR in direct mode
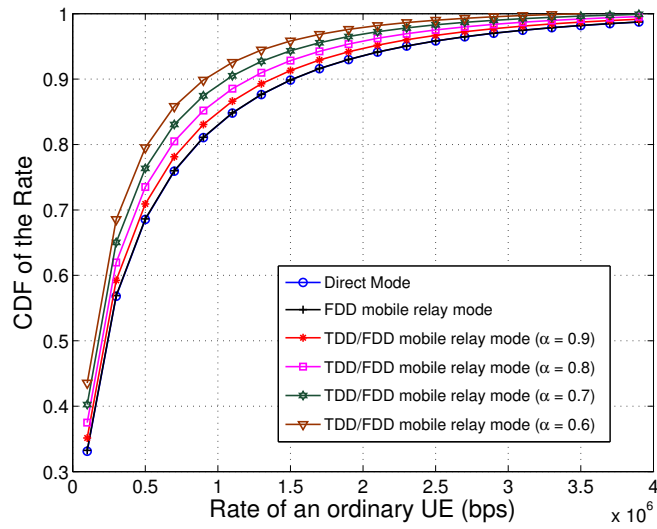
Figure 5.11: CDF of the rate of an ordinary UE

5.4.4.3 End-to-end data rates of vehicular UEs

The CDF of the end-to-end rate of a vehicular UE is illustrated in Fig. 5.12. As we can see, with the increase of penetration loss, the end-to-end rate of a vehicular UE in direct mode becomes significantly worse. If penetration loss is large, the mobile relay modes can both have better rate. But if penetration loss is small, for example $L = 10$ dB, FDD mobile relay mode cannot always bring data rate gain to vehicular UEs due to two phases operation of the relay transmission. The backhaul link and the access link cannot operate simultaneously in this mode.
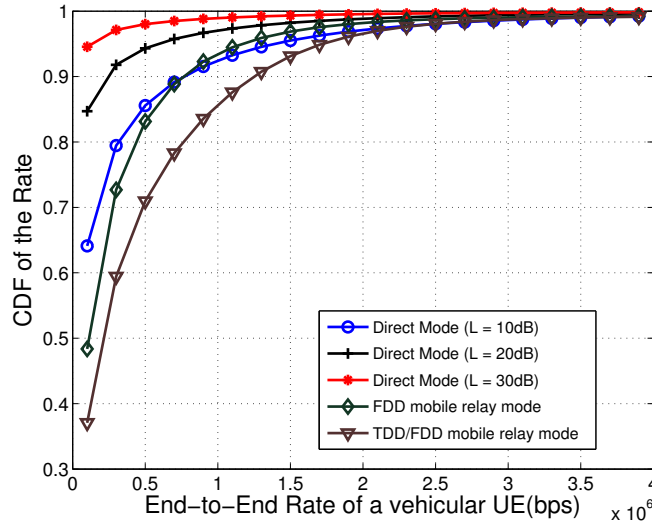
Figure 5.12: CDF of the end-to-end rate of a vehicular UE

Large α is used in this plot. When $\alpha = 0.9$, TDD/FDD hybrid mobile relay mode can achieve the best rate for vehicular UEs. This is because the backhaul link and the access link can operate simultaneously in this mode, the data can be transmitted to vehicular UEs all the time. Considering the impact of α on ordinary UEs as discussed before, parameter α is set to be 0.9 in default. Finding optimal α under certain parameters is out the scope of this paper.

5.4.4.4 Impact of the Penetration Loss

The penetration loss between outdoor and in-vehicle makes the signal severely attenuated. To study the impact of the penetration loss, the cell total average rate in direct mode under different penetration losses is illustrated in Fig. 5.13. It can be seen that with the increase of the ratio of vehicular UEs in the cell, the cell total

average rate in direct mode decreases, this is because more and more vehicular UEs suffer penetration loss.
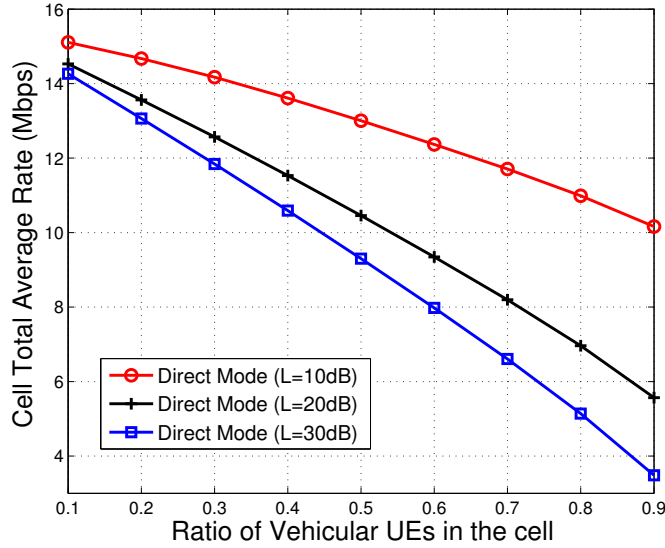
Figure 5.13: Cell total average rate for different penetration losses

5.4.4.5 The Cell Total Average Rate

We consider a given total number of UEs and different proportions of vehicular UEs. The total intensity of UEs is constant or in other words $\lambda_t = \lambda_o + \lambda_r * \overline{n_v}$ is constant. We make the ratio of vehicular UEs $\upsilon = \frac{\lambda_r * \overline{n_v}}{\lambda_t}$ vary from 0.1 to 0.9. There are two cases. In case 1, we consider that the average number of UEs in a bus $\overline{n_v}$ is fixed and make υ vary (hence, λ_o and λ_r are variables). In case 2, we consider that the intensity of buses λ_r is fixed and make υ vary (hence, λ_o and $\overline{n_v}$ are variables). In both cases, we consider the same density of UEs but different distribution patterns of vehicular UEs. The cell total average rate under different modes against the ratio of vehicular UEs is illustrated in Fig. 5.14.

As we can see, with the increase of the ratio of vehicular UEs in the cell, both FDD mobile relay mode and TDD/FDD hybrid mobile relay modes perform better than direct mode. For instance, when the ratio of vehicular UEs is 0.4, FDD mobile relay mode and TDD/FDD hybrid mobile relay mode can respectively achieve about +16.3% and +29.1% cell rate gain compared to direct mode. Also the cell total average rate in FDD mobile relay mode decreases with the increase of vehicular UEs
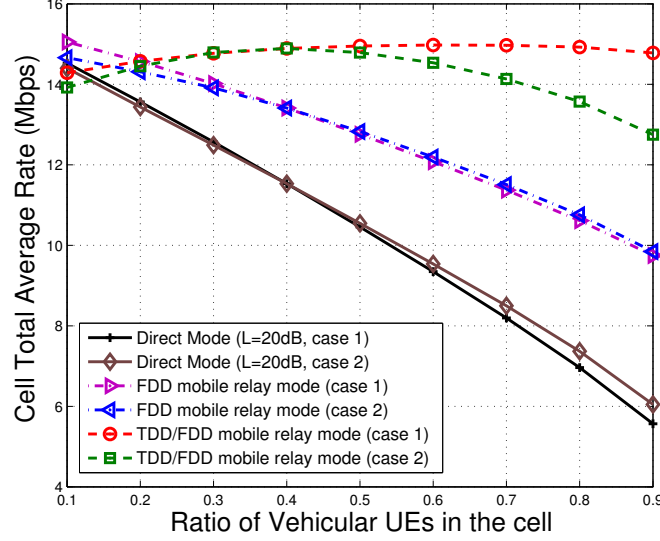
Figure 5.14: Cell total average rate against the ratio of vehicular UEs

in the cell while the cell total average rate in TDD/FDD hybrid mobile relay mode is rather stable. This is because more UEs are served through two phase transmission in time where only half of the time is fully effective in FDD mobile relay mode.

In addition, of the three modes the TDD/FDD hybrid mobile relay mode has the best performance when the ratio of vehicular UEs is larger than 0.1. This is because although ordinary UEs have lower rates in this mode, the end-to-end rate gain of vehicular UEs can compensate the rate loss of ordinary UEs. From the capacity point of view, the cell can thus achieve higher total cell rate. But when the cell has far more ordinary UEs than vehicular UEs, the rate loss of ordinary UEs in TDD/FDD hybrid mobile relay mode cannot be compensated by the rate gain of vehicular UEs. This is why the cell total average rate of TDD/FDD hybrid mobile relay mode is worst when the ratio of vehicular UEs is 0.1. It's not worth using a dedicated bandwidth for the access link when there are very little vehicular UEs in the cell. Furthermore, it's very interesting to see that the cell average rate does not make much difference between case 1 and case 2 in direct mode and FDD mobile relay mode, but the cell average rate in case 2 of TDD/FDD hybrid mobile relay mode decreases when the ratio of vehicular UEs increases. This is because in case 2, there are more and more vehicular UEs in a bus, so the access link becomes a bottle neck if the dedicated bandwidth for the access link remains the same.

5.4.4.6 Energy Efficiency

Fig. 5.15 presents the energy efficiency against the ratio of vehicular UEs in the cell. Since the distribution patterns of vehicular UEs mainly affect TDD/FDD hybrid mobile relay mode, only the results of TDD/FDD hybrid mobile relay mode are shown in two cases. When penetration loss is high, mobile relay modes can achieve better energy efficiency compared with direct mode because the data rate gain brought about by mobile relay exceeds the extra power consumption of mobile relays. For instance, when $L = 20$ dB and the ratio of vehicular UEs is 0.5, FDD mobile relay mode and TDD/FDD hybrid mobile relay mode can respectively achieve +5.7% and +24.2% energy efficiency gain compared with direct mode. But when penetration loss is small ($L = 10$ dB) and the ratio of vehicular UEs is smaller than 0.5, direct mode is better from the energy efficiency point of view. In this case the data rate gain brought by mobile relay is cancelled out by the extra power consumption of mobile relays.
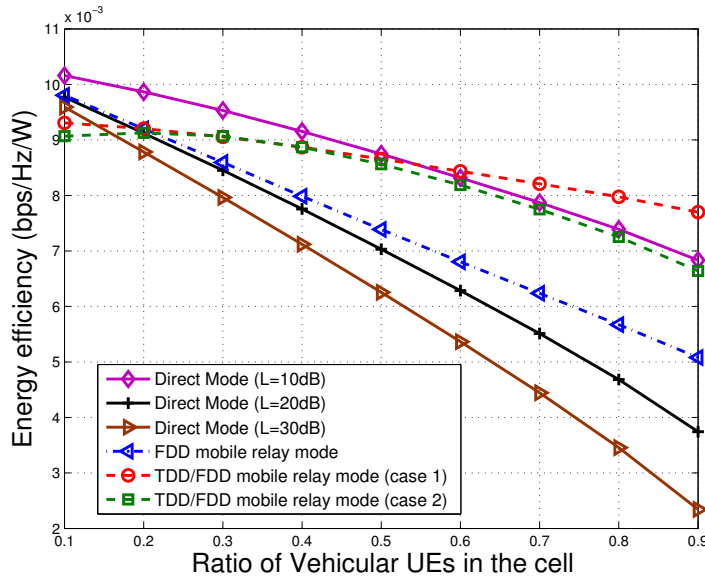
Figure 5.15: Energy efficiency against the ratio of vehicular UEs

5.5   Summary

In this chapter, we have studied the cell capacity that mobile relay could bring into a public transportation system. First we consider a traditional hexagonal network

and use the spatial Poisson distribution to model the distribution of terminals and buses (mobile relays) in the cell. Through Monte Carlo simulations we compare the performance of direct mode, pure-relay mode and femto-like mode. Then we extend the study in a more realistic random network. We provide a general analytical model using the stochastic geometry. Important metrics like the CDF of the SINR and the CDF of the end-to-end rate are derived. Moreover, motivated by the fact that a vehicular UE is static relative to its serving mobile relay and close to it in this specific scenario, we propose a TDD/FDD hybrid mode which is suitable for mobile relay scenario. Then based on the analytical model, we evaluate the cell total average rate and energy efficiency. It was found that the penetration loss is a factor that determines how much gain mobile relay can bring. When the penetration loss is large and a relatively large amount of vehicular UEs in the cell, it's better to deploy mobile relay in the cell in order to provide satisfactory service to vehicular UEs.

Chapter 6

Conclusions and Future Work

In this chapter, we summarize our major contributions and discuss future research directions.

6.1 Major Contributions

This work aims investigating the fundamental benefits of deploying mobile relay in a LTE cellular network. The study has been done from two aspects: mobility management study and performance study. Specifically, the main contributions can be summarized as follows.

- Improvement of mobility procedures for mobile relays in LTE networks

  In mobility management study, we first gave a state of the art about mobility management study of mobile relays. Then we studied different signaling procedures when the mobile relay is embedded in a public transport vehicle. We proposed to keep the same protocol stack that was defined for fixed relay and to extend it to mobile relays. The concept of global tunnel, which gathers several tunnels and is compatible with the GTP protocol, was proposed to optimize the handover procedure of mobile relay nodes. Without adding any protocol in the stack, it was possible to group several handovers while keeping the possibility of managing the tunnel of each UE individually. The results showed that the proposed solution dramatically reduces the number of signaling messages that each network node should process can be dramatically reduced when global tunnels are combined with a specific tracking area and when S1 tunnels are kept alive for inactive vehicular UEs. The proposed

solution introduced can be easily applied to any transport systems: metros, tramways and trains.

- Impact of the interference on the data rate of one vehicular UE

  We first analyzed and calculated the data rate gain of a UE provided by a mobile relay deployed in a hexagonal cellular network. We considered a network with one UE and one mobile relay. The analysis was based on the Shannon formula modified for LTE. We considered the case when the UE directly connects to the base station and compared with the case when the UE is served by a mobile relay. Through Monte Carlo simulations, the data rate under different cases were obtained, and the effect of penetration loss on the data rate was studied.

  Then, we extended the study to a random cellular network and computed some important metrics, such as the Cumulative Distribution Function (CDF) of the SINR and the average achievable rate on both the backhaul link and the access link. The computing was based on stochastic geometry approach, which can capture the irregularity and randomness of a realistic network. Both log-normal shadowing and Rayleigh fading were considered.

  According to both simulation and numerical results, we fount out that the data rate gain provided by a mobile relay is not guaranteed in all cases. The penetration loss and the distance between the user and the base station are two key factors to decide whether mobile relay could bring data rate gain. When the vehicular user is not close to the base station, mobile relay can bring data rate gain to the user. When the user is close to the base station, the data rate gain is not guaranteed.

- Impact of mobile relays on the cell capacity

  We first investigated the capacity gain brought by mobile relays deployed in a hexagonal cellular network. We considered a network with multi-users and multi-relays. The distribution of terminals and mobile relays were modeled by the spatial Poisson distribution. Equal bit rate scheduling was used. Two relay modes: pure-relay mode and femto-like mode were proposed and compared. The system performance was evaluated by Monte Carlo simulations.

  Then, we extended the study to a random cellular network. A general analytical model for mobile relay scenario was proposed using stochastic geometry. Important metrics like the CDF of the SINR and the CDF of the end-to-end

rate were derived. The rate of the backhaul link and the rate of the access link are in general correlated when the same spectrum (or frequency) is used on both links, we took this fact into account when deriving the CDF of the end-to-end rate. Furthermore, we proposed a TDD/FDD (Time Division Duplexing/Frequency Division Duplexing) hybrid mobile relay mode, motivated by the fact that a vehicular UE is static relative to its serving mobile relay and close to it in this specific scenario, which leads to a relatively good channel condition on the access link. A small bandwidth was dedicated to the access link. The backhaul link and the access link can thus operate independently without additional complex mechanisms to avoid self-interference. In addition, we evaluated and compared the performance between two relay modes and direct mode using the proposed analytical model. The cell total average rate and the energy efficiency in different modes were obtained.

We found out that the penetration loss is a major factor that determines how much capacity gain mobile relay can bring. When the penetration loss is large and a relatively large amount of vehicular UEs in the cell, deploying mobile relay in the cell can improve the cell capacity. Numerical results showed that when the ratio of vehicular UEs in the cell is 0.4 and the penetration loss is 20 dB, FDD mobile relay mode and TDD/FDD hybrid mobile relay mode can achieve +16.3%, +29.1% cell rate gain respectively compared with the direct mode.

6.2 Future Work

This work mainly focuses on the fundamental benefits of deploying mobile relay in a LTE cellular network. There are several research directions in which the work can be extended.

6.2.1 The mobility of mobile relay

We did not consider the mobility of bus mounted with mobile relays when evaluating the performance of mobile relay network. However, with the movement of public transportation, this moving network also comes with challenging problems in terms of mobility management. To study how mobility affects the system performance and handover rate, it would be interesting to have a theoretical analysis using the

stochastic geometry approach.

6.2.2   Prediction of moving directions

Another interesting idea is to predict the moving directions of public transportations deployed with mobile relays. Public transportations usually move along a fixed route track, it means that it is possible to predict the moving direction of mobile relays. For instance, deploy two RNs on each side of the bus or train. We can obtain 2 measurement samples at the same time and predict the moving directions with measurement samples. By doing this, it is able to shorten the reporting period and perform some handover procedures in advance.

6.2.3   The Doppler Frequency Shift

It has been found out that mobile relay can bring considerable gains in low mobility scenario, such as public buses. But in high speed scenario, such as high speed trains, the Doppler frequency shift can not be neglected. Hence, to guarantee the performance of mobile relays in such kinds of scenarios, developing advanced methods to compensate the Doppler effect is required.

6.2.4   Full duplex mobile relay

Currently, the 5th generation (5G) network has become a keyword among researchers and engineers in the communication society. As a candidate of 5G technologies, full duplex has been received great attention and discussed a lot. Full duplex wireless system can maximally achieve doubled spectral efficiency by transmitting and receiving signals at the same time and frequency. Due to advances in both radio and digital processing, full duplex can now be implemented at reasonable cost and without complex radio hardware.

In our work it is found out that when the penetration loss is small, mobile relay mode can not bring data rate gain to vehicular UEs due to two phases operation of the relay transmission where only half of the time is fully effective. In our work we considered half duplex relay node, hence the backhaul link and the access link cannot operate simultaneously. So enabling full duplex technique on mobile relay node might be an promising idea, as it can bring data rate gains as long as the penetration loss exists.

6.2.5 Ginibre Point Process

As a powerful mathematical tool, the Poisson Point Process (PPP) has been widely applied to model the randomness of wireless networks. However, the base stations can be very close in a PPP deployed network, as their positions are uncorrelated with each other. As a result, the PPP model generates more interference than that of a real network and provides a pessimistic result. To have a more accurate analysis of wireless networks, it would be interesting to consider the spatial correlations between base stations and model the network with some repulsive Point Processes, such as Ginibre Point Process (GPP).

Appendix A

Analyse de performances des relais mobiles dans un réseau LTE

A.1 Contexte de la thèse

Notre travail a été effectué au sein du projet SYSTUF (SYStème Telecom pour les Transports Urbains du Futur). Ce projet constitue une réponse à l'appel Systèmes de transport intelligent du programme Investissements d'avenir - Fonds national pour la société numérique. Il traite de la recherche et du développement dans les technologies, les produits et services liés aux systèmes de transport intelligents innovants et se concentre sur les tramways et les métros. Les principaux partenaires du projet sont Alcatel-Lucent, IFSTTAR, ALSTOM, Eurecom, RATP, Mitsubishi Electric R & D Centre Europe, Télécom Bretagne et SIMPLUSE. Le projet s'étale de 2012 à 2016.

Le projet vise à démontrer la faisabilité d'utiliser une technologie de communication unique basée sur la technologie LTE (évolution à long term) à la fois pour les opérateurs de transport et pour les passagers afin de répondre aux exigences de qualité de service, tant pour le technique (contrôle, de commande, vidéosurveillance, etc.) que le trafic des utilisateurs (Web, vidéo, etc.). Le trafic technique peut être critique (contrôle-commande) ou non essentiel tandis que le trafic utilisateur est toujours non vital. Le projet vise également à permettre le développement de services innovants qui contribuent à la mobilité transparente et répondent à la demande croissante de "mobilité intelligente et respectueuse de l'environnement".

Notre travail dans le projet est d'étudier la façon de répondre aux exigences du trafic utilisateur pour les passagers. Nous nous concentrons donc notre étude sur les relais mobiles.

A.2   Les Contributions

Nous considérons des relais mobiles qui sont installés dans les transports publics. Comme le véhicule se déplace, le relais mobile se déplace en même temps que les UE dans le véhicule. Les terminaux se connectent au réseau de communication via le relais mobile qui a une antenne à l'intérieur du véhicule. D'autre part, le relais mobile communique avec l'eNB donneur (DeNB) par l'intermédiaire de l'antenne extérieure du relais mobile. En utilisant deux antennes distinctes, on peut éliminer la perte de pénétration entre l'extérieur et le véhicule. De plus, le relais mobile peut créer sa propre cellule à l'intérieur d'un véhicule : la gestion de mobilité du groupe d'UE véhicules desservis par le même relais mobile peut être optimisée.

Cependant, il y a aussi des défis à relever en utilisant des relais mobiles. Quel gain peut être atteint par des relais mobiles dans un réseau LTE ? Comment faire pour effectuer un transfert inter-cellulaire groupé en utilisant des relais mobiles dans l'architecture du système LTE actuelle? Quels sont les avantages fondamentaux du déploiement de relais mobile sur les véhicules de transport en commun? Répondre à ces questions requiert une étude approfondie.

Dans cette thèse, nous considérons le scénario où les relais mobiles sont déployés dans les bus et étudions les avantages fondamentaux du déploiement de relais mobile dans un réseau cellulaire LTE. Dans la thèse, nous prenons l'exemple des autobus pour des raisons de simplicité. Cependant, l'analyse peut être étendue à d'autres systèmes de transport comme les métros, les tramways et les trains. Les contributions de notre travail de thèse peuvent se résumer en trois parties : amélioration des procédures de mobilité, calcul du gain sur le débit individuel apporté par un relais, étude du gain de capacité pour une cellule avec plusieurs relais.

A.2.1   Amélioration des procé dures de mobilité pour les re-lais mobiles dans les ré seaux LTE

Nous étudions d'abord les différentes procédures de signalisation lorsque le relais mobile est intégré dans un véhicule de transport public. Nous proposons de garder

la même pile de protocole qui a été définie pour le relais fixe, et de l'étendre à des relais mobiles. Nous proposons le concept de tunnel global pour optimiser la procédure de transfert intercellulaire de noeuds relais mobiles.

L'idée principal est de rassembler plusieurs tunnels dans le même tunnel global et d'utiliser ce tunnel global pour transporter le trafic de données pour tous les terminaux dans le même véhicule et desservis par conséquent par le même relais mobile. Le tunnel global utilise le protocole GTP-U (GPRS Tunnelling Protocol in the User Plane). Conformément à la spécification, l'en-tête GTP-U comprend un champ d'extension (E). Nous proposons d'utiliser cette option pour transporter un deuxième TEID dans l'extension qui identifie le tunnel spécifique à un UE. Le TEID qui est dans la tête standard identifie le tunnel global. L'en-tête GTP-U étendu est représenté sur la Figure A.1.

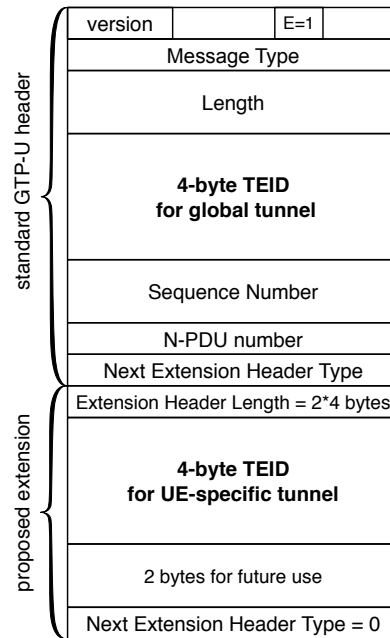Figure A.1: Format de l'en-tête GTP-U pour un tunnel global

A.2.1.1 Global X2 Tunnel

Nous proposons de mettre en place un tunnel global entre la source DeNB et la cible DeNB pour la transmission de données de terminaux embarqués pendant le transfert, comme le montre la Figure A.2. Tous les terminaux embarqués qui étaient connectés au relais mobile avant le transfert inter-cellulaire voient leurs données transmises

sur le chemin suivant: relais mobile-cible DeNB-source DeNB-SGW. Mais pour les terminaux qui se connectent via le relais mobile après le transfert inter-cellulaire, un chemin direct est établi entre la cible DeNB et SGW (UE). Pour un UE donné, son ancre de mobilité est le DeNB auquel il est connecté au moment il s'attache au relais mobile. Le tunnel X2 global est maintenu aussi longtemps que cela est nécessaire. Il est libéré dès que tous les UE qui l'utilisent quittent le véhicule.
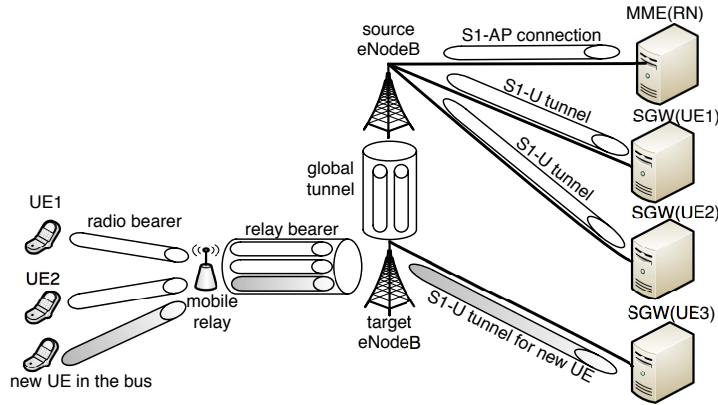
Figure A.2: Le tunnel X2 global après un transfert inter-cellulaire de relais mobile

A.2.1.2 Résultats

En mode relais mobile, nous considérons deux cas: le mode R1 pour lequel la même zone de suivi (TAI, Tracking Area Identiy) est affectée au DeNB et au relais et le mode R2 avec une zone de suivi spécifique au relais. Les résultats sont présentés sur la Figure A.3. Lorsque le nombre d'UE dans un bus augmente, le nombre de messages de signalisation augmente également dans tous les modes. Le mode R1 ne réduit pas les messages de signalisation par rapport au mode direct. En effet, le transfert intercellulaire est peu fréquent si le bus se déplace relativement lentement, l'avantage d'un transfert intercellulaire groupé n'est pas conséquent. Cependant, en mode R2, le nombre de messages de signalisation est réduit d'environ 85% par rapport à mode direct quand il y a 20 UEs en moyenne dans un bus. Cette partie du travail a été présentée à la conférence internationale PIMRC 2015 [21].

130
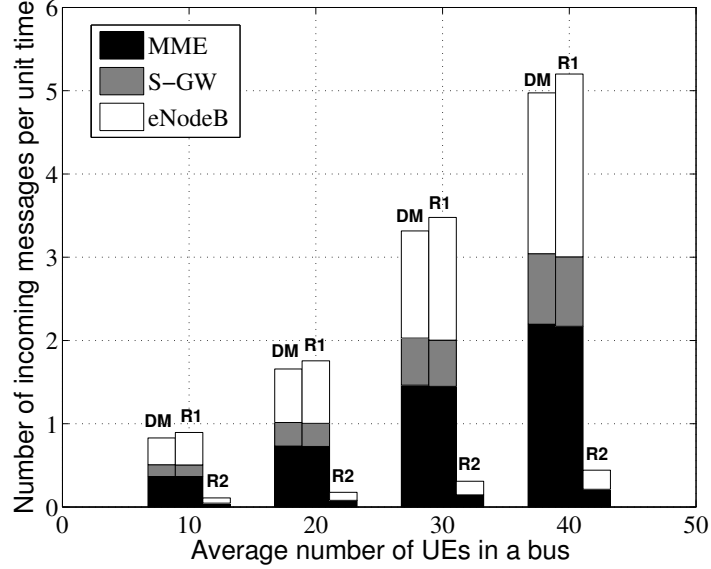
Figure A.3: Coût de signalisation en fonction du nombre moyen d'UEs dans un bus

A.2.2 L'impact de l'interférence sur le taux de l'un des véhicules UE de données

Dans l'étude de la performance, nous avons d'abord analysé et calculé le gain de débit fourni par un relais mobile déployé dans un réseau cellulaire hexagonal. Nous considérons un réseau avec un seul UE et un seul relais mobile. Nous considérons le cas où l'UE est directement relié à une station de base et nous comparons avec le cas où un UE est servi par un relais mobile. Grâce à des simulations de Monte Carlo, nous comparons le débit de données réalisable pour un UE à des distances différentes dans le mode direct et dans le mode relais. Les résultats sont présentés dans la Figure A.4. Cette partie du travail a été publiée dans la conférence internationale WPMC 2013 [22].

De la Figure A.4, nous pouvons voir que, lorsque l'UE est situé à proximité de l'eNB serveur, le mode direct fonctionne mieux. Ceci est parce qu'il y a deux liaisons de transmission distinctes et successives dans les modes relais. Lorsque la distance entre l'UE et l'eNB augmente, le débit de données commence à diminuer. En raison de la perte de la pénétration, le signal dans le mode direct se détériore plus rapidement que celle dans les modes de relais. Aussi, nous constatons que lorsque l'UE est proche de l'eNodeB, l'interférence engendrée par le donneur eNodeB
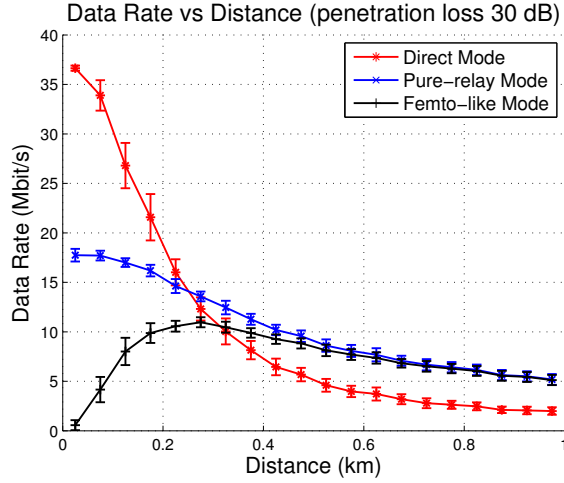
Figure A.4: Débit réalisable (avec un intervalle de confiance de 95%)

diminue le débit de données de manière significative.

Ensuite, nous étendons l'étude à un réseau cellulaire aléatoire et calculons certains indicateurs importants, tels que la fonction de répartition (CDF, Cumulative Distribution Function) du rapport signal sur interférence et bruit et le débit moyen à la fois sur la liaison de raccordement (backhaul) et le lien d'accès. Le calcul est basé sur la géométrie stochastique, qui peut capturer l'irrégularité et le caractère aléatoire d'un réseau réaliste. Cette partie du travail a été publiée dans Globecom 2014 [23].

A.2.3 Impact de relais mobiles sur la capacité de la cellule

Nous étudions le gain de capacité apporté par les relais mobiles déployés dans un réseau cellulaire hexagonal avec des plusieurs terminaux et plusieurs relais. Deux modes: le mode pur-relais et le mode femto sont proposés et comparés. La performance est évaluée par simulation de Monte Carlo. Cette partie du travail a été publiée à la conférence internationale CCNC 2014 [24].

Ensuite, nous étendons l'étude à un réseau cellulaire aléatoire. Un modèle analytique général pour le scénario de relais mobile est proposé en utilisant la géométrie stochastique. Des indicateurs importants comme la CDF du SINR et la CDF du débit de bout en bout sont calculés. Le débit de la liaison de raccordement et le débit de la liaison d'accès sont en général corrélés lorsque le même spectre (ou fréquence) est utilisé sur les deux liens, nous prenons en compte ce fait lors du calcul de la CDF

du débit de bout en bout. En outre, nous proposons un mode TDD / FDD combiné (Time Division Duplex / Frequency Division Duplex). Nous sommes motivés par le fait qu'un UE embarqué est statique par rapport à son relais mobile serveur et près de lui, ce qui conduit à une condition de canal relativement bonne sur le lien d'accès. Une faible bande passante est dédiée à la liaison d'accès. La liaison de raccordement et le lien d'accès peuvent donc fonctionner indépendamment sans mécanismes complexes supplémentaires pour éviter l'interférence. De plus, nous évaluons et comparons les performances des deux modes (relais et direct) en utilisant le modèle analytique proposé. L'algorithme d'ordonnancement des ressources entre les utilisateurs au sein d'une cellule est de type "tour de rôle" (Round-Robin). Le débit et l'efficacité énergétique moyenne totale sont évalués dans différents modes.

A.2.3.1   Résultats

Nous considérons un nombre total d'UEs donné et différentes proportions d'UEs embarqués. Le rapport des UEs embarqués varient de 0.1 à 0.9. Nous considérons la même densité d'UE mais différents modèles de distribution d'UEs embarqués. Dans le cas 1, nous considérons que le nombre moyen d'UE dans un bus est fixe et faisons varier l'intensité de bus. Dans le cas 2, nous considérons que la densité des bus est fixe et faisons varier le nombre moyen d'UE dans un bus. Les résultats sont présentés sur la Figure A.5.

Lorsque la proportion d'UEs embarqués dans la cellule augmente, le mode relais FDD et le mode relais TDD/FDD hybride offrent de meilleures performances que le mode direct. Par exemple, lorsque le rapport d'UE embarqués est de 0.4, le mode relais FDD et le mode TDD/FDD hybride peuvent apporter respectivement un gain sur le débit d'environ +16.3% et +29.1% par rapport au mode direct. De plus, le débit moyen global de la cellule du mode relais FDD diminue avec l'augmentation des UEs dans la cellule tandis que le débit moyen total dans le mode de relais mobile TDD/FDD hybride est assez stable. Ceci s'explique parce que, dans le mode relais FDD, une phase de transmission se fait à faible débit lorsque le nombre de terminaux embarqués est important.

En outre, des trois modes, le mode relais TDD/FDD hybride a les meilleures performances lorsque le taux d'UE embarqués est supérieur à 0.1. Ceci est parce que même si les UE ordinaires ont des débits inférieurs dans ce mode, le gain en débit de bout en bout pour les UE embarqués compense la perte en débit des UE ordinaires. Du point de vue de la capacité, la cellule peut donc atteindre une capacité plus élevée.
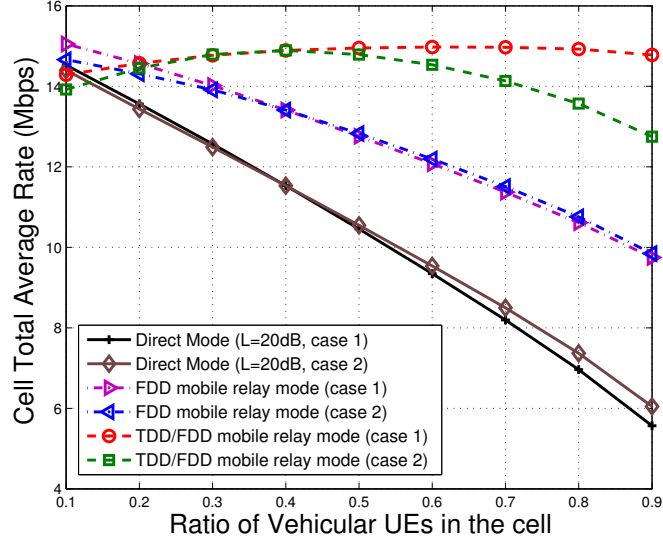
Figure A.5: Cellule taux moyen totale contre le rapport d'UE véhiculaires

Mais lorsque la cellule a beaucoup plus d'UEs ordinaires que d'UE embarqués, la perte de débit des UE ordinaires ne peut pas être compensée par le gain de débit des UE véhiculaires. Ceci est la raison pour laquelle le débit moyen total de la cellule du mode relais mobile TDD/FDD hybride est pire lorsque le rapport d'UE véhicules est de 0.1. Cela ne se produit pas en utilisant une bande passante dédiée pour le lien d'accès quand il y a très peu de véhicules UEs dans la cellule.

Appendix B

Computation of Rennes Bus parameters

In this Appendix, we explain how we set the values of some parameters in Table 3.1. We compute the average dwell time of a UE in a bus and the average speed of a bus based on real statistics in Rennes, France. We obtained a survey data collected in March 2009 from the company Star, a local transport company. The data has collected many statistics how citizens in Rennes utilized bus line 3, such as the number of passengers go on and go off each stop for each race of bus line 3, a very main bus line in Rennes, for two whole days.

From the data, we can get how many stops a passengers has stayed on the bus. The total running time of line 3 is 36 minutes, there are 30 bus stops in all, which are strict, so the average running time between two stops is 1.2 minutes. Then we compute the average number of stops that one passenger has dwelled on the bus, combined with the average running between two stops, we get the average dwell time of a UE in a bus as 600s.

Then we estimate the length of the route of bus line 3 from google maps, the length of the route is around 9km. Considering the running time is 36 minutes, the average speed is 15 km/h without counting the parking time at each stop. We also find a statistic on the wikiterritorial [97], it's said the speed of a bus in urban area is normally 14.4 km/h (4 m/s), so we set the average speed of a bus as 4 m/s.

As for the cell radius, we obtained it from Cartoradio on Rennes and set it as 700 meters [98].

As for the rest of the parameters (average number of UEs in a bus, probability of

UE-triggered service request, etc.), we set default values for them and study their impact in the section of numerical results.

List of Publications

Peer-reviewed International Conferences

1. Yangyang Chen and Lagrange Xavier, "Downlink data rate gain provided by a mobile relay for LTE-advanced," In 2013 16th International Symposium on Wireless Personal Multimedia Communications (WPMC), pp.1-5, Atlantic City, USA, 24-27 June 2013.

2. Yangyang Chen and Xavier Lagrange, "Downlink capacity gain analysis of mobile relay in lte-advanced network," In 2014 IEEE 11th Consumer Communications and Networking Conference (CCNC), pages 544-550, Las Vegas, USA, January 2014.

3. Yangyang Chen, Philippe Martins, Laurent Decreusefond, Xavier Lagrange, and Feng Yan, "Stochastic analysis of a cellular network with mobile relays," In GLOBECOM 2014 : IEEE Global communications conference, Austin, USA, December 2014.

4. Yangyang Chen and Xavier Lagrange, "Analysis and improvement of mobility procedures for mobile relays in lte networks," In proceedings of IEEE 26th Annual International Symposium on Personal, Indoor, and Mobile Radio Communications (PIMRC), pages 1-6, Hongkong China, August 30 - September 2, 2015.

References

[1] Cisco. *Cisco visual networking index: Global mobile data traffic forecast update, 2013–2018*. San Jose, CA, USA, white paper edition, February 2014.

[2] Stefanis Sesia, Issam Toufik, and Matthew Baker. *LTE – The UMTS Long Term Evolution, From Theory to Practice*. Wiley, 2009.

[3] Erik Dahlman, Stefan Parkvall, and Johan Skold. *4G LTE/LTE-Advanced for Mobile Broadband*. Elsevier, 2011.

[4] Xavier Lagrange. Lte-4g. telecom-bretagne, 2010.

[5] Xavier Lagrange. Lte relays and overview of systuf project. telecom-bretagne, 2013.

[6] 3GPP Technical Specification 36.300. Evolved Universal Terrestrial Radio Access (E-UTRA) and Evolved Universal Terrestrial Radio Access Network (E-UTRAN); Overall description; Stage 2 (Release 10), January 2015.

[7] 3GPP Technical Report 36.806. Evolved Universal Terrestrial Radio Access (E-UTRA); Relay architectures for E-UTRA (LTE-Advanced), April 2010.

[8] Aleksandar Damnjanovic, Juan Montojo, Yongbin Wei, Tingfang Ji, Tao Luo, Madhavan Vajapeyam, Taesang Yooosok Song, and Durga Malladi. A survey on 3gpp heterogeneous networks. *IEEE Wireless Communications*, 18(3):10–21, June 2011.

[9] A. Ghosh, N. Mangalvedhe, R. Ratasuk, B. Mondal, M. Cudak, E. Visotsky, T.A. Thomas, J.G. Andrews, P. Xia, H.S. Jo, H.S. Dhillon, and T.D. Novlan. Heterogeneous cellular networks: From theory to practice. *IEEE Communications Magazine*, 50(6):54–64, June 2012.

[10] J.G. Andrews, F. Baccelli, and R.K. Ganti. A tractable approach to coverage and rate in cellular networks. *IEEE Transactions on Communications*, 59(11): 3122–3134, November 2011.

[11] V. Chandrasekhar, J.G. Andrews, and Alan Gatherer. Femtocell networks: a survey. *IEEE Communications Magazine*, 46(9):59–67, September 2008.

[12] C Hoymann, Wanshi Chen, J. Montojo, A. Golitschek, C. Koutsimanis, and Xiaodong Shen. Relaying operation in 3gpp lte: challenges and solutions. *IEEE Communications Magazine*, 50(2):156–162, February 2012.

[13] Harri Holma and Antti Toskala, editors. *LTE Advanced: 3GPP Solution for IMT-Advanced*. Wiley, 2012.

[14] Liu Liu, Cheng Tao, Jiahui Qiu, Houjin Chen, Li Yu, Weihui Dong, and Yao Yuan. Position-based modeling for wireless channel on high-speed railway under a viaduct at 2.35 ghz. *IEEE Journal on Selected Areas in Communications*, 30 (4):834–845, 2012.

[15] Xiangqian Zhu, Shanzhi Chen, Haijing Hu, Xin Su, and Yan Shi. Tdd-based mobile communication solutions for high-speed railway scenarios. *IEEE Wireless Communications*, 20(6):22–29, December 2013.

[16] Hans-Peter Mayer Peter Fertl Petar Popovski, Volker Braun. Scenarios, requirements and KPIs for 5G mobile and wireless system. Technical report, May 2013.

[17] Lin Chen, Ying Huang, Feng Xie, Yin Gao, Li Chu, Haigang He, Yunfeng Li, Feng Liang, and Yifei Yuan. Mobile relay in lte-advanced systems. *IEEE Communications Magazine*, 51(11):144–151, November 2013. ISSN 0163-6804. doi: 10.1109/MCOM.2013.6658666.

[18] Yutao Sui, Jaakko Vihriala, Agisilaos Papadogiannis, Mikael Sternad, Wei Yang, and Tommy Svensson. Moving cells: A promising solution to boost performance for vehicular users. *IEEE Communications Magazine*, 51(6):62–68, June 2013.

[19] 3GPP Technical Report 36.836. Evolved Universal Terrestrial Radio Access (E-UTRA); Study on mobile relay (Release 12), June 2014.

[20] 3GPP. Overview of 3gpp release 12, September 2012.

[21] Yangyang CHEN and Xavier Lagrange. Analysis and improvement of mobility procedures for mobile relays in lte networks. In *In proceedings of IEEE PIMRC 2015*, pages 1–6, 2015.

[22] Yangyang CHEN and Xavier Lagrange. Downlink data rate gain provided by a mobile relay for lte-advanced. In *2013 16th International Symposium on Wireless Personal Multimedia Communications (WPMC)*, pages 1–5, June 2013.

[23] Yangyang Chen, Philippe Martins, Laurent Decreusefond, Xavier Lagrange, and Feng Yan. Stochastic analysis of a cellular network with mobile relays. In *GLOBECOM 2014 : IEEE Global communications conference*, 2014.

[24] Yangyang CHEN and Xavier Lagrange. Downlink capacity gain analysis of mobile relay in lte-advanced network. In *2014 IEEE 11th Consumer Communications and Networking Conference (CCNC)*, pages 544–550, January 2014.

[25] 3GPP Technical Specification 29.060. General Packet Radio Service (GPRS); GPRS Tunnelling Protocol (GTP) across the Gn and Gp interface (Release 12), July 2015.

[26] 3GPP Technical Specification 36.413. Evolved Universal Terrestrial Radio Access Network (E-UTRAN); S1 Application Protocol (S1AP), September 2014.

[27] Mattia Minelli, Maode Ma, Marceau Coupechoux, Jean-Marc Kelif, Marc Sigelle, and Philippe Godlewski. Optimal relay placement in cellular networks. *IEEE Transactions on Wireless Communications*, 13(2):998–1009, February 2014.

[28] 3GPP. Further advancements for e-utra physical layer aspects, March 2010.

[29] Mohammad N. Patwary, Predrag B. Rapajic, and Ian Oppermann. Capacity and coverage increase with repeaters in umts urban cellular mobile communication environment. *IEEE Transactions on Communications*, 53(10):1620–1624, October 2015.

[30] IEEE 802.11WG. Wireless LAN Medium Access Control (MAC) and Physical Layer (PHY) Specifications. Amendment 8: Medium Access Control (MAC) Quality of Service Enhancements, November 2005.

[31] Marco Domenico Aime, Giorgio Calandriello, and Antonio Lioy. Dependability in wireless networks: Can we rely on wifi? *IEEE Security Privacy*, 5(1):23–29, January 2007.

[32] Sheen Wern-Ho, Shiang-Jiun Lin, and Chia-Chi Huang. Downlink optimization and performance of relay-assisted cellular networks in multicell environments. *IEEE Transactions on Vehicular Technology*, 59(5):2529–2542, June 2010.

[33] Wei Hong, Jing Han, and Haiming Wang. Full uplink performance evaluation of fdd/tdd lte-advanced networks with type-1 relays. In *2011 IEEE Vehicular Technology Conference (VTC Fall)*, pages 1–5, Sept 2011.

[34] V. Aggarwal, A. Bennatan, and A.R. Calderbank. On maximizing coverage in gaussian relay channels. *IEEE Transactions on Information Theory*, 55(6): 2518–2536, June 2009.

[35] Wei Zhang and Khaled Letaief. Full-rate distributed space-time codes for cooperative communications. *IEEE Transactions on Wireless Communications*, 7(7):2446–2451, July 2008.

[36] M. Salem, A. Adinoyi, M. Rahman, H. Yanikomeroglu, D. Falconer, Young-Doo Kim, Eungsun Kim, and Yoon-Chae Cheong. An overview of radio resource management in relay-enhanced ofdma-based networks. *IEEE Communications Surveys Tutorials*, 12(3):422–438, Third 2010.

[37] Ju Honghao, Liang Ben, Li Jiandong, and Yang Xiaoniu. Dynamic joint resource optimization for lte-advanced relay networks. *IEEE Transactions on Wireless Communications*, 12(11):5668–5678, November 2013.

[38] Yao Hua, Qian Zhang, and Zhisheng Niu. Resource allocation in multi-cell ofdma-based relay networks. In *INFOCOM, 2010 Proceedings IEEE*, pages 1–9, March 2010.

[39] M.O. Hasna and M.-S. Alouini. Optimal power allocation for relayed transmissions over rayleigh-fading channels. *IEEE Transactions on Wireless Communications*, 3(6):1999–2004, November 2004.

[40] Qian Li, R.Q. Hu, Geng Wu, and Yi Qian. On the optimal mobile association in heterogeneous wireless relay networks. In *INFOCOM, 2012 Proceedings IEEE*, pages 1359–1367, March 2012.

[41] Andrey Krendzel. Lte-a mobile relay handling: Architecture aspects. In *Proceedings of the 2013 19th European Wireless Conference (EW)*, pages 1–6, April 2013.

[42] Meng-Shiuan Pan, Tzu-Ming Lin, and Wen-Tsuen Chen. An enhanced handover scheme for mobile relays in lte-a high-speed rail networks. *IEEE Transactions on Vehicular Technology*, PP(99):1, 2014.

[43] Qing Huang, Jianmei Zhou, Cheng Tao, Su Yi, and Ming Lei. Mobile relay based fast handover scheme in high-speed mobile environment. In *IEEE Vehicular Technology Conference (VTC Fall)*, pages 1–6, September 2012.

[44] Hongxia Zhao, Rongsheng Huang, Jietao Zhang, and Yuguang Fang. Handoff for wireless networks with mobile relay stations. In *2011 IEEE Wireless Communications and Networking Conference (WCNC)*, pages 826–831, March 2011.

[45] R. Balakrishnan, X. Yang, M. Venkatachalam, and Ian F. Akyildiz. Mobile relay and group mobility for 4g wimax networks. In *2011 IEEE Wireless Communications and Networking Conference (WCNC)*, pages 1224–1229, March 2011.

[46] Yutao Sui, Zhe Ren, Wanlu Sun, Svensson Tommy, and Peter Fertl. Performance study of fixed and moving relays for vehicular users with multi-cell handover under co-channel interference. In *2013 International Conference on Connected Vehicles and Expo (ICCVE)*, pages 514–520, Dec 2013.

[47] Qi Liao, Federico Penna, Slawomir Stanczak, Zhe Ren, and Peter Fertl. Context-aware handover optimization for relay-aided vehicular terminals. In *2013 IEEE 14th Workshop on Signal Processing Advances in Wireless Communications (SPAWC)*, pages 555–559, June 2013.

[48] Christian Pietsch, Stefan Brueck, Michael Farber, Thiago Moraes, Mourad Khanfouci, Jaakko Vihriala, M. Danish Nisar, Eiko Seidel, Tommy Svensson, Agisilaos Papadogiannis, Yutao Sui, and Mikael Sternad. Moving Relays and Mobility aspects. Technical report, Artist4G deliverable, May 2012.

[49] 3GPP Technical Specification 29.281. Universal Mobile Telecommunications System (UMTS); LTE; General Packet Radio System (GPRS) Tunnelling Protocol User Plane (GTPv1-U) (Release 12), January 2015.

[50] R. Thomas, H. Gilbert, and G. Mazziotto. Influence of the moving of the mobile stations on the performance of a radio mobile cellular network. *Proceedings of the Nordic Seminar on Digital Land Mobile Radio Communications*, 1988.

[51] Timothy X Brown and Seshadri Mohan. Mobility management for personal communications systems. *IEEE Transactions on Vehicular Technology*, 46(2): 269–278, May 1997.

[52] P. Mogensen, Wei Na, I.Z. Kovacs, F. Frederiksen, A. Pokhariyal, K.I. Pedersen, T. Kolding, K. Hugl, and M. Kuusela. Lte capacity compared to the shannon bound. In *IEEE 65th Vehicular Technology Conference, 2007. VTC2007-Spring.*, pages 1234–1238, April 2007.

[53] Wenyu Li, Chao Zhang, Xiaoyu Duan, Shucong Jia, Yu Liu, and Lin Zhang. Performance evaluation and analysis on group mobility of mobile relay for lte advanced system. In *2012 IEEE Vehicular Technology Conference (VTC Fall)*, pages 1–5, Sept 2012.

[54] R. Atat, E. Yaacoub, M. Alouini, and A. Abu-Dayya. Heterogeneous lte/802.11a mobile relays for data rate enhancement and energy-efficiency in high speed trains. In *2012 IEEE Globecom Workshops (GC Wkshps)*, pages 421–425, Dec 2012.

[55] Vinh Van Phan, K. Horneman, Ling Yu, and J. Vihriala. Providing enhanced cellular coverage in public transportation with smart relay systems. In *2010 IEEE Vehicular Networking Conference (VNC)*, pages 301–308, Dec 2010.

[56] S. Scott, J. Leinonen, P. Pirinen, J. Vihriala, Vinh Van Phan, and M. Latva-Aho. A cooperative moving relay node system deployment in a high speed train. In *2013 IEEE 77th Vehicular Technology Conference (VTC Spring)*, pages 1–5, June 2013.

[57] Lihua Yang, Guangliang Ren, and Zhiliang Qiu. A novel doppler frequency offset estimation method for dvb-t system in hst environment. *IEEE Transactions on Broadcasting*, 58(1):139–143, March 2012.

[58] Yaoqing Yang, Pingyi Fan, and Yongming Huang. Doppler frequency offsets estimation and diversity reception scheme of high speed railway with multiple antennas on separated carriages. In *2012 International Conference on Wireless Communications Signal Processing (WCSP)*, pages 1–6, Oct 2012.

[59] Huang Lin, Daqing Gu, Wenbo Wang, and Hongwen Yang. Capacity analysis of dedicated fixed and mobile relay in lte-advanced cellular networks. In *Communications Technology and Applications, 2009. ICCTA '09. IEEE International Conference on*, pages 354–359, Oct 2009. doi: 10.1109/ICCOMTA.2009.5349178.

[60] Y. Sui, A. Papadogiannis, and T. Svensson. The potential of moving relays - a performance analysis. In *2012 IEEE 75th Vehicular Technology Conference (VTC Spring)*, pages 1–5, May 2012. doi: 10.1109/VETECS.2012.6240247.

[61] Yutao Sui, A. Papadogiannis, Wei Yang, and T. Svensson. The energy efficiency potential of moving and fixed relays for vehicular users. In *Vehicular Technology Conference (VTC Fall), 2013 IEEE 78th*, pages 1–7, Sept 2013. doi: 10.1109/VTCFall.2013.6692436.

[62] Yutao Sui, Papadogiannis Agisilaos, Wei Yang, and Svensson Tommy. Performance comparison of fixed and moving relays under co-channel interference. In *2012 IEEE Globecom Workshops (GC Wkshps)*, pages 574–579, Dec 2012.

[63] Joonas Kokkoniemi, Juha Ylitalo, Petri Luoto, Simon Scott, Jouko Leinonen, and Matti Latva-aho. Performance evaluation of vehicular lte mobile relay nodes. In *2013 IEEE 24th International Symposium on Personal Indoor and Mobile Radio Communications (PIMRC)*, pages 1972–1976, September 2013.

[64] Michael Grieger and Gerhard Fettweis. Field trial results on uplink joint detection for moving relays. In *2012 IEEE 8th International Conference on Wireless and Mobile Computing, Networking and Communications (WiMob)*, pages 586–592, Oct 2012.

[65] Sui Yutao, Guvenc Ismail, and Svensson Tommy. Interference management for moving networks in ultra-dense urban scenarios. *EURASIP Journal on Wireless Communications and Networking*, 2015(1):1–32, 2015.

[66] Mikael Sternad, Michael Grieger, Rikke Apelfrojd, Tommy Svensson, Daniel Aronsson, and Ana Belen Martinez. Using "predictor antennas" for long-range prediction of fast fading for moving relays. In *2012 IEEE Wireless Communications and Networking Conference Workshops (WCNCW)*, pages 253–257, April 2012.

[67] Ahmad Alsharoa, Hakim Ghazzai, Elias Yaacoub, and Mohamed-Slim Alouini. Energy-efficient two-hop lte resource allocation in high speed trains with moving relays. In *2014 12th International Symposium on Modeling and Optimization in Mobile, Ad Hoc, and Wireless Networks (WiOpt)*, pages 528–533, May 2014.

[68] Dinh-Thuy Phan-Huy, Mikael Sternad, and Svensson Tommy. Adaptive large miso downlink with predictor antenna array for very fast moving vehicles. In *2013 International Conference on Connected Vehicles and Expo (ICCVE)*, pages 331–336, Dec 2013.

[69] Dinh-Thuy Phan-Huy, M. Sternad, and T. Svensson. Making 5g adaptive antennas work for very fast moving vehicles. *IEEE Intelligent Transportation Systems Magazine*, 7(2):71–84, Summer 2015.

[70] M. Haenggi, J.G. Andrews, F. Baccelli, O. Dousse, and M. Franceschetti. Stochastic geometry and random graphs for the analysis and design of wireless networks. *IEEE Journal on Selected Areas in Communications*, 27(7): 1029–1046, September 2009.

[71] Baccelli, François and Blaszczyszyn, Bartlomiej. *Stochastic Geometry and Wireless Networks, Volume I - Theory*. Foundations and Trends in Networking Vol. 3: No 3-4, pp 249-449. NoW Publishers, 2009.

[72] T. T. Vu, L. Decreusefond, and P. Martins. An analytical model for evaluating outage and handover probability of cellular wireless networks. In *2012 15th International Symposium on Wireless Personal Multimedia Communications (WPMC)*, pages 643–647, Sept 2012.

[73] Dimitrios Tsilimantos, Jean-Marie Gorce, and Eitan Altman. Stochastic analysis of energy savings with sleep mode in ofdma wireless networks. In *2013 Proceedings IEEE INFOCOM*, pages 1097–1105, April 2013.

[74] Namyoon Lee, Xingqin Lin, J.G. Andrews, and R.W. Heath. Power control for d2d underlaid cellular networks: Modeling, algorithms, and analysis. *IEEE Journal on Selected Areas in Communications*, 33(1):1–13, Jan 2015.

[75] H.S. Dhillon, R.K. Ganti, F. Baccelli, and J.G. Andrews. Modeling and analysis of k-tier downlink heterogeneous cellular networks. *IEEE Journal on Selected Areas in Communications*, 30(3):550–560, April 2012.

[76] H.S. Dhillon and J.G. Andrews. Downlink rate distribution in heterogeneous cellular networks under generalized cell selection. *IEEE Wireless Communications Letters*, 3(1):42–45, February 2014.

[77] K. Abboud and Weihua Zhuang. Stochastic analysis of a single-hop communication link in vehicular ad hoc networks. *IEEE Transactions on Intelligent Transportation Systems*, 15(5):2297–2307, Oct 2014.

[78] Eitan Altman Manjesh Kumar Hanawal and Francois Baccelli. Stochastic geometry based medium access games in wireless ad hoc networks. *IEEE Journal on Selected Areas in Communications*, 30(11):2146–2157, December 2012.

[79] Hesham ElSawy, Ekram Hossain, and Martin Haenggi. Stochastic geometry for modeling, analysis, and design of multi-tier and cognitive cellular wireless networks: A survey. *IEEE Communications Surveys Tutorials*, 15(3):996–1019, Third 2013.

[80] Na Deng, Sihai Zhang, Wuyang Zhou, and Jinkang Zhu. A stochastic geometry approach to energy efficiency in relay-assisted cellular networks. In *IEEE Global Communications Conference (GLOBECOM)*, pages 3484–3489, December 2012.

[81] Huan Yu, Yunzhou Li, Marios Kountouris, Xibin Xu, and Jing Wang. Energy efficiency analysis of relay-assisted cellular networks. *EURASIP Journal on Advances in Signal Processing*, 2014:32, 2014.

[82] Huan Yu, Yunzhou Li, Marios Kountouris, Xibin Xu, and Jing Wang. Energy efficiency analysis of relay-assisted cellular networks using stochastic geometry. In *2014 12th International Symposium on Modeling and Optimization in Mobile, Ad Hoc, and Wireless Networks (WiOpt)*, pages 667–671, May 2014.

[83] Zhiwei Zhang, Yunzhou Li, Kaizhi Huang, and Chen Liang. Energy efficiency analysis of energy harvesting relay-aided cooperative networks. In *2015 13th International Symposium on Modeling and Optimization in Mobile, Ad Hoc, and Wireless Networks (WiOpt)*, pages 1–7, May 2015.

[84] Xavier Lagrange, Philippe Godlewski, and SamiTabbane. *Réseaux GSM*. Editions Hermès Science, (5ème édition) edition, 2000.

[85] Holger Claussen. Performance of macro- and co-channel femtocells in a hierarchical cell structure. In *in IEEE 18th International Symposium on Personal,*

Indoor and Mobile Radio Communications, 2007. PIMRC 2007., pages 1–5, Sept 2007.

[86] 3GPP Technical Specification 36.213. Evolved Universal Terrestrial Radio Access (E-UTRA); Physical layer procedures, September 2009.

[87] M Gudmundson. Correlation model for shadow fading in mobile radio systems. *Electronics Letters*, 27(23):2145–2146, Nov 1991.

[88] H. Claussen, L. T W Ho, and L.G. Samuel. Self-optimization of coverage for femtocell deployments. In *Wireless Telecommunications Symposium, 2008. WTS 2008*, pages 278–285, April 2008.

[89] Harri Holma and Antti Toskala. *LTE for UMTS - Evolution to LTE-Advanced*. Wiley, March 2011.

[90] The World Bank. Vehicles (per km of road), 2013. URL http://data.worldbank.org/indicator/IS.VEH.ROAD.K1.

[91] H.S. Dhillon and J.G. Andrews. Downlink rate distribution in heterogeneous cellular networks under generalized cell selection. *IEEE Wireless Communications Letters*, 3(1):42 – 45, February 2014.

[92] J.-S. Ferenc and Z. Neda. On the size distribution of poisson-voronoi cells. *Physica A-Statistical Mechanics And Its Applications*, 385(2):518–526, 2007.

[93] S. Singh, H.S. Dhillon, and J.G. Andrews. Offloading in heterogeneous networks: Modeling, analysis, and design insights. *IEEE Transactions on Wireless Communications*, 12(5):2484–2497, May 2013.

[94] G. Auer, V. Giannini, C. Desset, I Godor, P. Skillermark, M. Olsson, M.A Imran, D. Sabella, M.J. Gonzalez, O. Blume, and A Fehske. How much energy is needed to run a wireless network? *IEEE Wireless Communications*, 18(5): 40–49, October 2011.

[95] AJ. Fehske, F. Richter, and G.P. Fettweis. Energy efficiency improvements through micro sites in cellular mobile radio networks. In *IEEE GLOBECOM Workshops*, pages 1–5, November 2009.

[96] Dietrich Stoyan, Wilfrid S. Kendall, and Joseph Mecke. *Stochastic geometry and its applications*. Wiley, 2nd edition edition, 1996.

[97] URL http://www.wikiterritorial.cnfpt.fr/xwiki/wiki/
econnaissances/view/Mots-Cles/Vitessecommerciale.

[98] URL www.cartoradio.fr.

Résumé

Le nombre d'utilisateurs des services de haut débit sans fil est en forte augmentation au cours des années 2010 avec l'introduction des téléphones intelligents, ordinateurs tablettes et autres nouveaux appareils mobiles.

Cependant, la qualité de service dans les transports publics est loin d'être satisfaisante. Traditionnellement, les terminaux à l'intérieur des transports publics se connectent à des stations de base macro-cellulaires via des liaisons sans fil, dans lesquelles la perte apportée par la traversée des ondes à travers les fenêtres atténue fortement le niveau du signal et diminue le débit de données réalisable. En outre, en cas de changement de cellule, plusieurs terminaux effectuent des transferts inter-cellulaires simultanément, ce qui provoque un accroissement brusque de signalisation et peut conduire à un engorgement.

Pour offrir des services de haute qualité aux clients des transports, un relais est monté dans un véhicule avec une antenne externe pour avoir un bon bilan de liaison avec la station de base et une antenne dans le bus pour fournir un bilan de liaison optimal avec les terminaux. Cette thèse étudie le déploiement de relais mobile en réseau LTE à partir de deux aspects: gestion de la mobilité et analyse de performance. Nous étudions d'abord les différentes procédures de signalisation quand un relais mobile est intégré dans un véhicule de transport public. Nous proposons de garder la pile de protocole qui a été définie pour le relais fixe par les instances de normalisation et de l'étendre à des relais mobiles. Nous définissons le concept de tunnel global, qui regroupe plusieurs tunnels, pour réduire la signalisation en cas de transfert intercellulaire de noeuds relais mobiles.

Dans l'étude de performances, nous analysons les différents types d'interférences. Deux nouveaux types d'interférences (interférences relais à relais et relais à terminal) sont identifiés. Nous étudions le gain de débit de données fourni par un relais mobile déployé dans un réseau hexagonal avec des simulations de Monte Carlo et dans un réseau aléatoire en utilisant la géométrie stochastique. Nous étudions alors le gain de capacité apporté par les relais mobiles avec plusieurs utilisateurs et plusieurs relais. Des indicateurs importants comme la répartition du rapport signal sur interférence et bruit et celle du débit de bout en bout sont calculés. En outre, nous proposons de combiner les modes duplex en temps et en fréquence, motivés par le fait qu'un terminal embarqué est statique par rapport à son relais mobile de service et proche de lui, ce qui conduit à un excellent bilan de liaison et rend intéressant un duplexage temporel. En outre, nous évaluons et comparons les performances des différents modes de fonctionnement en utilisant le modèle analytique proposé.

Mots-clés : Réseaux mobiles de 4ème génération, Relais Mobile, Gestion de la Mobilité, Géométrie Stochastique, analyse de performance

Abstract

Currently, the number of users using wireless broadband services is rising greatly with the introduction of smart phones, tablet computers and other new mobile devices.

However, the service quality in public transportation vehicles is far from satisfactory. Public transportations are usually well shielded with coated windows, which leads to a rather high penetration loss between outdoor and in-vehicle. Traditionally, the UEs inside the public transportations connect to the macro base stations via wireless links, in which the penetration loss severely attenuates the signal quality and decreases the achievable data rate. Furthermore, during the handover procedure, a large group of UEs perform handover simultaneously, which causes signaling congestion.

To offer high-quality services to vehicular UEs, a relay is mounted in a vehicle with an external antenna to have a good link budget with the eNodeB and an antenna in the bus to provide an optimal link budget with vehicular UEs. This thesis investigates the deployment of mobile relay in LTE network from two aspects: mobility management and performance. We first study the different signaling procedures when a mobile relay is embedded in a public transport vehicle. We propose to keep the protocol stack that was defined for fixed relay and to extend it to mobile relays. The concept of global tunnel, which gathers several tunnels, is proposed to optimize the handover procedure of mobile relay nodes.

In the performance study, we analyze the different interference cases. Two new types of interferences, Relay-to-Relay interference and Relay-to-UE interference are identified. We study the data rate gain of a UE provided by a mobile relay deployed in a hexagonal network with Monte Carlo simulation and in a random network by using stochastic geometry. We then investigate the capacity gain brought by mobile relays with multiple users and multiple relays. Important metrics like the CDF of the SINR and the CDF of the end-to-end rate are derived. Furthermore, we propose a TDD/FDD hybrid mobile relay mode, motivated by the fact that a vehicular UE is static relative to its serving mobile relay and close to it, which leads to a relatively good channel condition on the access link. In addition, we evaluate and compare the performance of different system modes using the proposed analytical model.

Keywords : Mobility Management, Data Rate Gain, Capacity Gain, Stochastic Geometry, Mobile Relay, LTE, Performance Analysis